

**Laboratory Study of Polychlorinated Biphenyl (PCB)  
Contamination and Mitigation in Buildings**

***Part 2. Transport from Primary Sources to Building Materials and Settled Dust***

Zhishi Guo, Xiaoyu Liu, Kenneth A. Krebs, and Dale J. Greenwell

U.S. Environmental Protection Agency

Office of Research and Development

National Risk Management Research Laboratory

Air Pollution Prevention and Control Division

Research Triangle Park, NC 27711

and

Nancy F. Roache, Rayford A. Stinson, Joshua A. Nardin, and Robert H. Pope

ARCADIS U.S. Inc.

Durham, NC 27709

U.S. Environmental Protection Agency

Office of Research and Development

National Risk Management Research Laboratory

Cincinnati, OH 45268

## **NOTICE**

This document has been reviewed internally and externally in accordance with the U.S. Environmental Protection Agency policy and approved for publication. Mention of trade names or commercial products does not constitute endorsement or recommendation for use.

## Executive Summary

### E.1. Background

This is the second report in the series entitled *Laboratory Study of Polychlorinated Biphenyl (PCB) Contamination and Mitigation in Buildings*, published by EPA's National Risk Management Research Laboratory. This report focuses on PCB transport from primary sources to building materials and settled dust in PCB-contaminated buildings. Building materials, furniture, and other indoor environmental constituents (such as settled dust) can "pick up" PCBs through exposure to contaminated air or through direct contact with primary sources of PCBs. The adsorbed PCBs can be re-emitted into the air when the primary sources are removed or severely diminished. Thus, these contaminated materials are often referred to as reversible or re-emitting sinks because both sorption and desorption are involved. In the PCB literature, however, they are often referred to as "secondary sources". In this report, the term "PCB sink" was used although other terms, especially "secondary source", were also cited occasionally.

Many researchers and others have recognized the presence and importance of PCB sinks in PCB-contaminated buildings, but very little information is available about the related transport processes and the re-emission characteristics. Because they are numerous, mitigating the PCB sinks as secondary sources has enormous environmental and economic implications. Better understanding of PCB sinks is important to decision makers, environmental engineers, and researchers who are concerned with risk assessment and risk management for PCB contamination.

### E.2. Objectives

In this study, we attempted to fill some of the data gaps associated with the characterization of PCB sinks in contaminated buildings. The specific objectives were: (1) to conduct laboratory experiments to study the transport of PCBs through material/air partitioning (i.e., from the air to interior surfaces and settled dust) and through material/source partitioning (i.e., from primary sources to settled dust); (2) to identify mathematical tools that can be used to rank the strengths of PCB sinks and to predict their behavior; and (3) to estimate the key parameters required as inputs to the mathematical tools, such as sorption capacity, partition coefficients, and diffusion coefficients.

### E.3. Methods

#### E.3.1 Testing of Building Materials

The sorption of airborne PCBs by building materials and their subsequent re-emission were investigated using two 53-L environmental chambers connected in series (Figure E.1). A field caulk sample was sliced into small pieces and placed in the source chamber to serve as a stable source of PCBs. The test materials, made as small "buttons" (Figure E.2), were placed in the test chamber. During the test, the PCB concentrations in the outlet air of the test chamber were monitored, and the buttons were removed from the test chamber at different times to determine their PCB content. The data were used to calculate the concentrations of the adsorbed PCBs (i.e., sorption concentration) and to estimate the partition and diffusion coefficients.

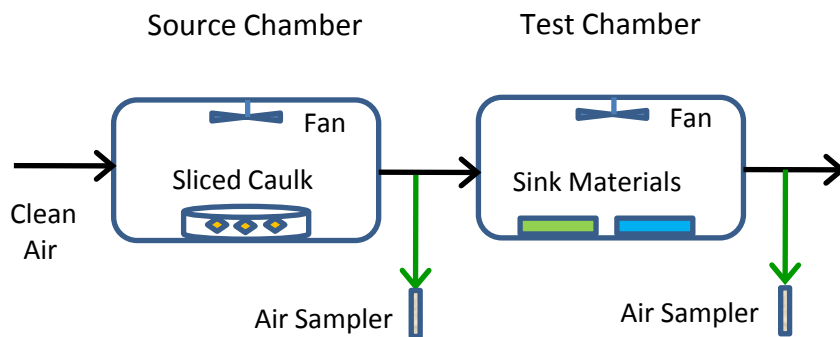


**Figure E.1.** Schematic of the chamber system for testing sink materials



**Figure E.2.** Sink material buttons that were placed in the test chamber

To determine the re-emissions from the PCB sinks, one test was conducted with four pieces of concrete panels that had dimensions of 15 cm × 15 cm × 0.8 cm. After a 167-hour dosing period, the PCB source was shut off, and the test chamber was flushed with clean air for 140 hours. The concentrations of PCB in the air were monitored throughout the test.

### *E.3.2 Testing of Settled Dust*

Indoor dust is an important sink for PCBs. Two types of dust were tested in a 30-m<sup>3</sup> stainless steel chamber. Two types of panels were prepared, i.e., PCB-containing panels and PCB-free panels. The dust was weighed and spread on the panels as evenly as possible. Then the panels were placed on the floor of the chamber (Figure E.3). During the test, panels were removed from the chamber at different times, and the dust was collected to determine its PCB content. The dust samples collected from the PCB panels were used to evaluate the PCB migration from the source to the dust through direct contact; the dust samples collected from the PCB-free panels were used to evaluate the sorption of PCBs through the dust/air partition.

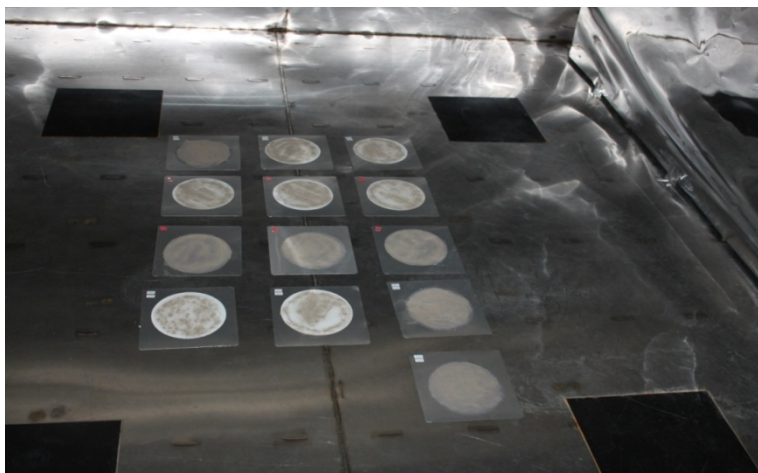


**Figure E.3. Test panels that were loaded with house dust and Arizona Test Dust and placed in the 30-m<sup>3</sup> chamber**

### *E.3.3 Testing of Sorption by the Walls of the Test Chamber*

The interior walls of a test chamber may adsorb some of the PCBs from the air inside the chamber. When a PCB source is tested, such sorption may reduce the PCB concentration in the outlet air, causing underestimation of the emission rate. The two types of chambers that were previously used by the authors to test PCB emissions from caulk and light ballasts were evaluated to determine their sink effects. Wipe samples were taken from the walls of the 44-mL microchambers immediately after an emission test and used to estimate the amount of PCBs adsorbed. The 53-L chambers, which were used to determine the PCB emissions from the light ballasts, were tested using the two-chamber system, described in Section E3.1, above. The sorption by the walls of the chamber was evaluated by comparing the PCB concentrations in the inlet and outlet air samples.

## **E.4. Findings**

### *E.4.1 Building Materials as PCB Sinks*

When the test specimens were exposed to PCB-contaminated air, the PCB content of the specimens increased over time (Figure E.4). The normalized sorption concentrations, i.e., the amount of PCB adsorbed by the sink material per unit surface area divided by the time-averaged air concentration, varied significantly from material to material. Figure E.5 compares the experimentally determined normalized sorption concentrations for 20 materials. A material with a greater normalized sorption concentration tends to adsorb more PCBs from the air.

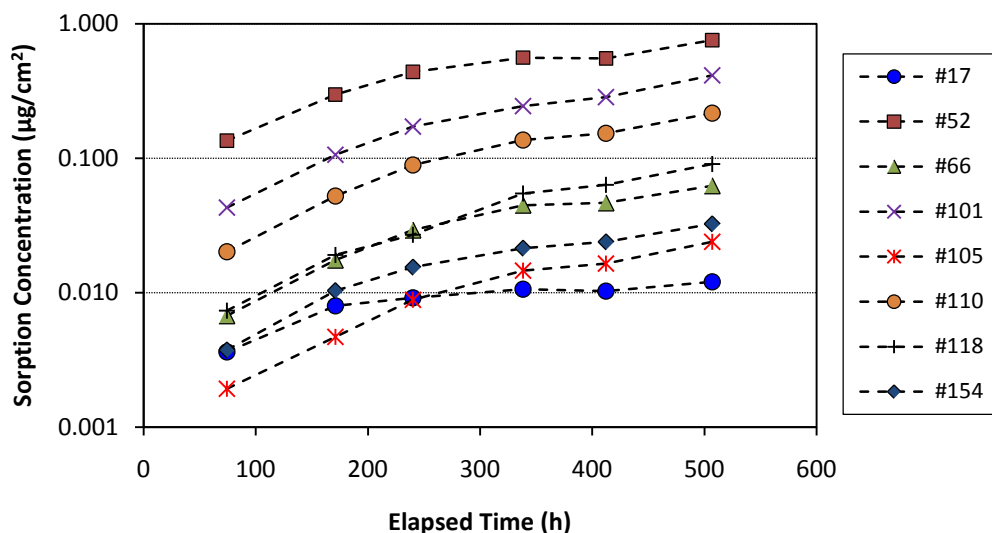


**Figure E.4. Sorption concentrations for concrete as a function of time (The legend shows the congener IDs).**

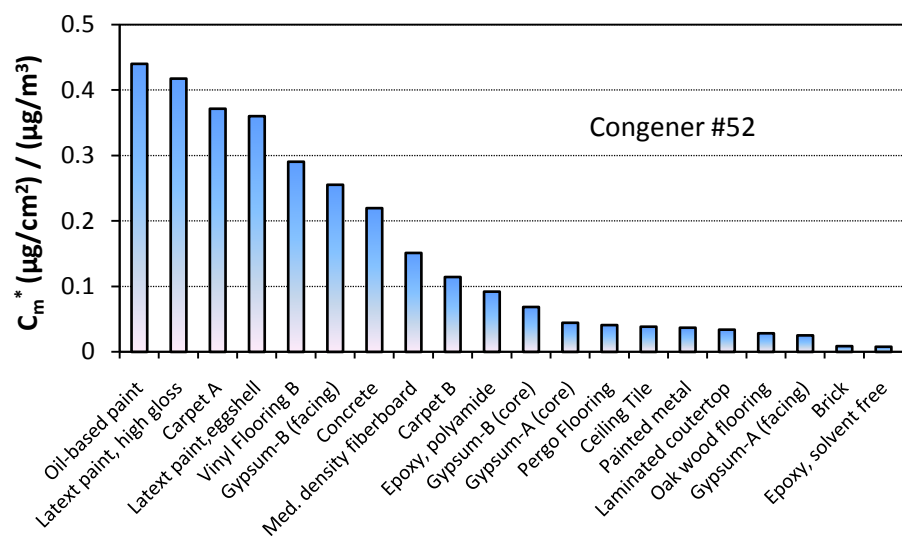


**Figure E.5. Normalized sorption concentrations ( $C_m^*$ ) for congener #52 for 20 materials (exposure time was either 240 or 269 hours)**

For a given sink material, the levels of the sorption differed from congener to congener. In general, congeners with lower vapor pressures were sorbed in larger quantities. Figure E.6 shows the normalized sorption rate (i.e., the normalized sorption concentration divided by the exposure time) for concrete for four congeners. The vapor pressure is  $1.50 \times 10^{-4}$  torr for congener #52,  $2.99 \times 10^{-5}$  torr for congener #101,  $1.68 \times 10^{-5}$  torr for congener #110, and  $8.42 \times 10^{-6}$  torr for congener #118.

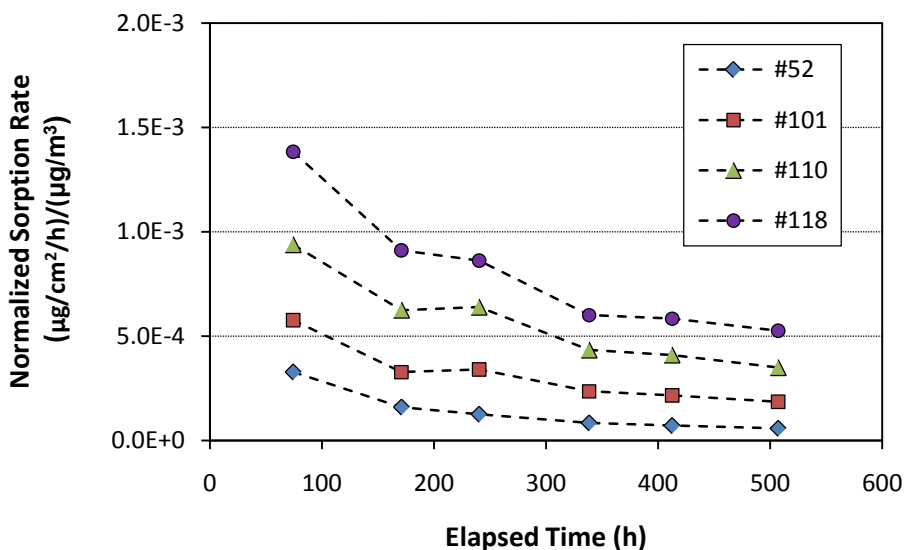


**Figure E.6. Normalized sorption rates for concrete as a function of time for four congeners**

Several mass transfer models are available for describing the sink behaviors, and most of them require the material/air partition coefficient and diffusion coefficient for the solid material. Rough estimates of these two parameters were obtained by applying a sink model to the data acquired from the chamber studies. (See Figure E.4, above.) To rank different sink materials, a new parameter, referred to as the sink sorption index (SSI), was introduced. The definition of SSI is similar to the definition of pH, meaning that materials with smaller SSI values are stronger PCB sinks. Among the materials tested, a petroleum-based paint, a latex paint, and a certain type of carpet were among the strongest sinks. Solvent-free epoxy coating, certain types of flooring materials, and brick were among the weakest sinks.

The rough estimates of the partition and diffusion coefficients made it possible to predict the accumulation of PCBs in the sink materials using the existing mass transfer models. For demonstration purposes, the accumulations of congeners #118 and #156, two dioxin-like PCBs, in concrete within a 1-cm-deep layer were estimated by assuming the following exposure conditions: (1) the average air concentration was  $0.05 \mu\text{g}/\text{m}^3$  for #118 and  $0.01 \mu\text{g}/\text{m}^3$  for #156, and (2) the exposure duration was 40 years. The predicted congener concentrations, converted to mass units, are presented in Figure E.7.

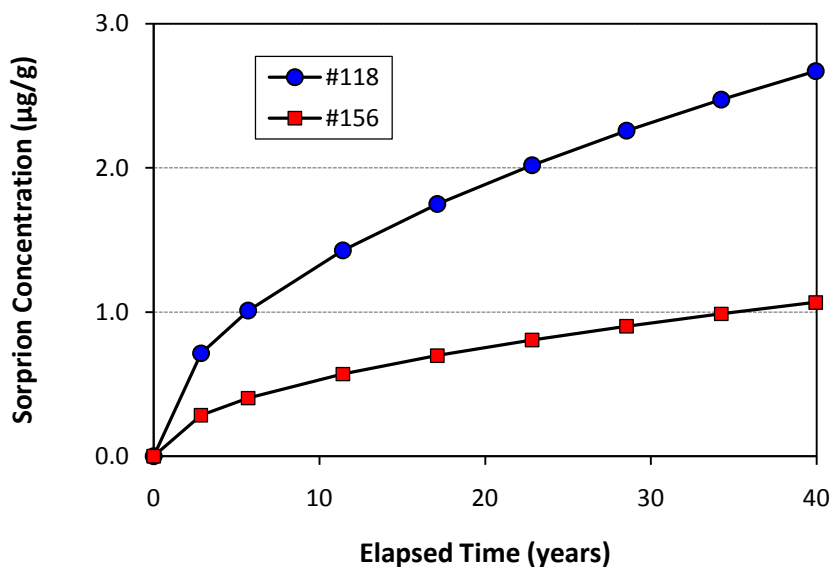


**Figure E.7. Predicted sorption concentrations for concrete (1-cm thick) for congeners #118 and #156**

The desorption test with concrete panels showed that re-emission is a slow process (Figure E.8), suggesting that PCB sinks can release PCBs into the air for a prolonged period of time after the primary sources have been removed from a building and, thus, hinder the remediation efforts.

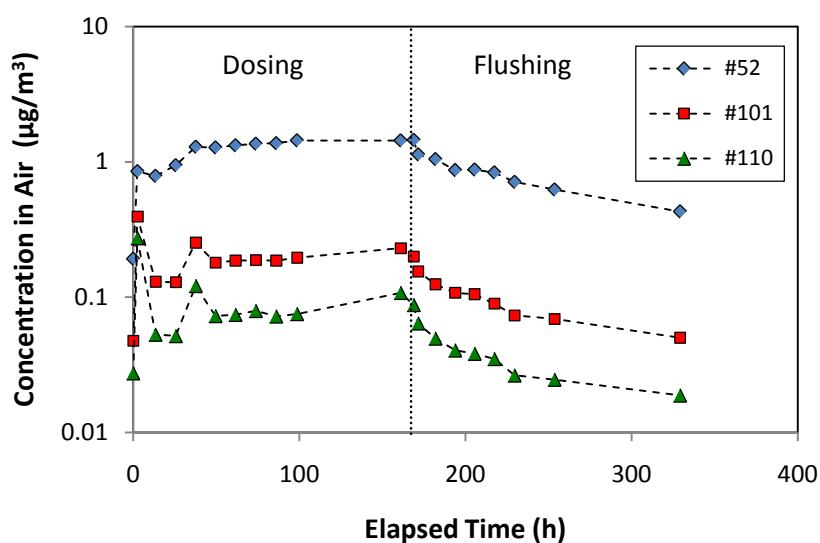


**Figure E.8. Air concentration profiles in a desorption test with concrete panels**  
(Tested at 23 °C and 1 air change per hour)



#### E.4.2 Settled Dust as a PCB Sink

Like other sink materials, settled dust can adsorb PCBs from air. The sorption concentration was dependent on the congener concentration in the air and favored less volatile congeners. Figure E.9 shows the experimentally determined sorption concentrations for four congeners, among which congener #52 had the highest concentration in the chamber air. However, congener #52 had the lowest normalized sorption concentration (i.e., sorption concentration divided by the air concentration) among the four congeners because of its high volatility (Figure E.10).

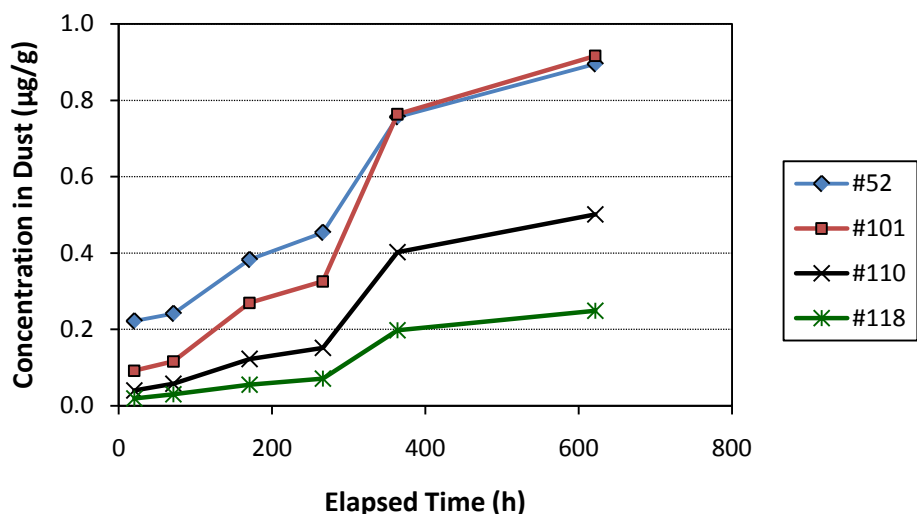


Figure E.9. Experimentally determined sorption concentrations in settled house dust due to dust/air partitioning

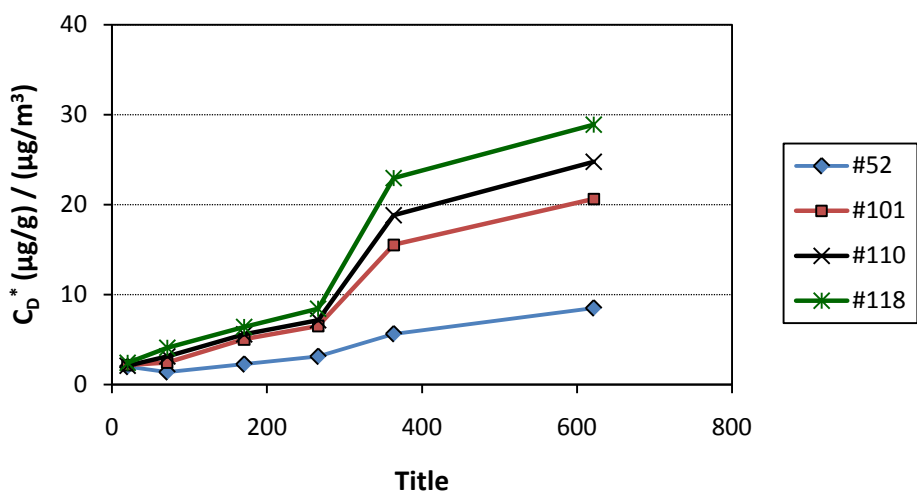
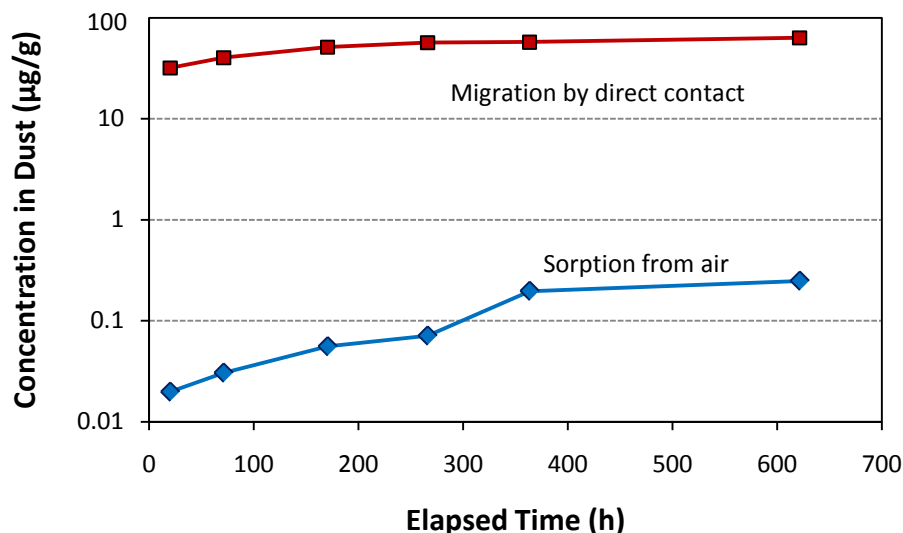
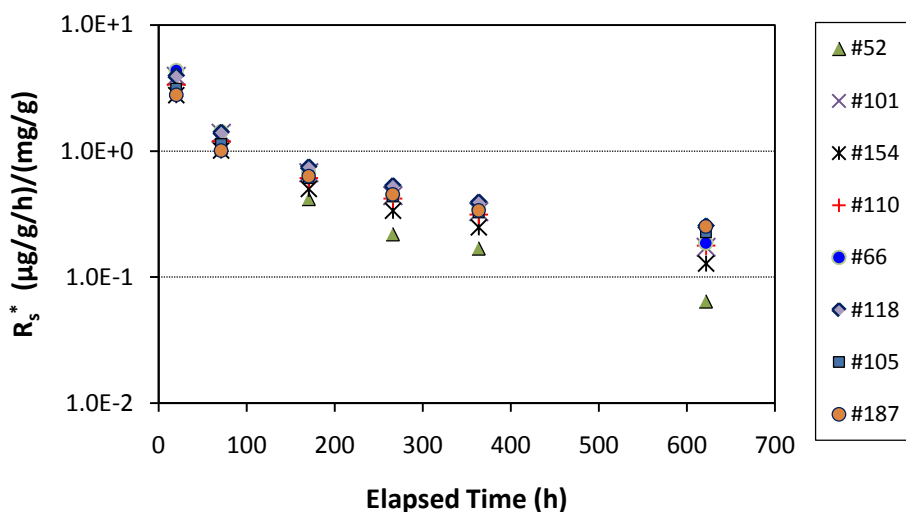


Figure E.10. Normalized sorption concentrations ( $C_D^*$ ) for four congeners in settled house dust

When the house dust was in direct contact with a primary source, PCBs migrated into the dust at a much faster rate than the PCB transfer rate due to the dust/air partition (Figure E.11). Unlike the dust/air partition, the dust/source partition was not significantly affected by the volatility of the congener. Figure E.12 compares the normalized migration rates (i.e., the migration rates divided by the PCB content in the source) for eight congeners.



**Figure E.11. Accumulation of congener #118 in house dust — comparison of two transfer mechanisms**



**Figure E.12. Normalized migration rates ( $R_s^*$ ) as a function of time for house dust in direct contact with the PCB source**

#### *E.4.3 Sorption by the Walls of the Chamber*

Sorption of PCBs by the walls of the 44-mL microchambers was minimal during the emissions tests for caulk samples, whereas the 53-L chamber showed strong sorption because of its much larger area of interior surfaces. For congener #18, the most predominant congener in Aroclor 1242, the sorption by the walls was estimated to cause more than 30% underestimation of PCB emission rates. Measures that may help reduce the sink effect during the emissions testing include using smaller chambers, constructing the chamber walls with materials that are weak sinks for PCBs (such as polytetrafluoroethylene), or coating the chamber walls with PCB-resisting materials.

### **E.5 Study Limitations**

This study marks the beginning of filling the data gaps associated with PCB sinks in PCB-contaminated buildings. The results of the study should help decision makers, environmental engineers, researchers, and the general public to better understand the effects of PCB sinks on PCB contamination and the remediation of these secondary sources. However, this study was necessarily limited in scope, and, thus, could not provide answers for all the important questions. Specific research limitations include the following:

- This study was limited to laboratory testing only. The results are yet to be tested in the field.
- Only a few tests were conducted with a limited number of test specimens.
- It was not feasible to investigate all transport mechanisms in a single study.
- The values of the material/air partition coefficient and the solid-phase diffusion coefficient that we reported were just rough estimates. The average relative standard deviations for the two parameters were 35% and 72%, respectively.

# TABLE OF CONTENTS

<b>Executive Summary</b>	<b>ii</b>
<b>Acronyms and Abbreviations</b>	<b>xxi</b>
<b>1. Introduction</b>	<b>1</b>
1.1 Background	1
1.2 Goals and Objectives	2
1.3 About This Report	2
<b>2. Theoretical Background</b>	<b>3</b>
2.1 Transfer Mechanisms	3
2.2 Material/Air Partition	4
2.2.1 Sorption Capacity	4
2.2.2 Degree of Sorption Saturation (DSS)	6
2.2.3 Dynamic Sink Models	8
2.3 Material/Material Partitioning	9
<b>3. Experimental Considerations</b>	<b>11</b>
3.1 Methods for Testing Building Materials	11
3.1.1 Conventional Chamber Method	11
3.1.2 Microbalance Method	11
3.1.3 Other Sink Test Methods	13
3.1.4 Test Method Used in This Study	13
3.2 Methods for Testing Settled Dust	14
3.2.1 Existing Methods	14
3.2.2 Test Method Used in This Study	15
<b>4. Experimental Methods</b>	<b>16</b>
4.1 Testing of Building Materials	16
4.1.1 Test Specimens	16
4.1.2 Test Facility	17
4.1.3 Test Procedure	18
4.1.3.1 Sink Tests and PCB Source	18
4.1.3.2 Procedure for Sink Tests S-1, S-2, and S-3	19
4.1.3.3 Procedure for Sink Test S-4 with Concrete	23
4.1.3.4 Chamber Air Sampling	24
4.2 Testing of Settled Dust	24
4.2.1 Test Specimens	24
4.2.2 Test Facility	29
4.2.3 Test Procedure	31

4.2.3.1	Preparation of Test Panels	31
4.2.3.2	Loading Dust to Test Panels	32
4.2.3.3	Chamber Testing	33
4.2.3.4	Collecting Dust from Test Panels	34
4.3	Testing of PCB Sorption by the Walls of the Test Chambers	36
4.3.1	Background and Significance	36
4.3.2	Procedure for Testing the 44-mL Microchambers	37
4.3.3	Procedure for Testing of the 53-Liter Environmental Chamber	37
4.4	Sample Extraction and Analysis	38
4.4.1	Target Congeners	38
4.4.2	Extraction of Solid Samples	39
4.4.3	Extraction of Air Samples	39
4.4.4	Sample Analysis	39
<b>5.</b>	<b>Quality Assurance and Quality Control</b>	<b>40</b>
5.1	GC/MS Instrument Calibration	40
5.2	Detection Limits	40
5.3	Environmental Parameters	45
5.4	Quality Control Samples	45
5.5	Recovery Check Standards	50
5.6	Precision for Chamber Tests	50
5.6.1	Congener Concentrations in Building Materials	50
5.6.2	Congener Concentrations in Settled Dust	53
<b>6.</b>	<b>Results</b>	<b>54</b>
6.1	Terminology and Definitions	54
6.1.1	Terminology for Material/Air Partitioning	54
6.1.2	Terminology for Dust/Air and Dust/Source Partitioning	55
6.2	PCB Transfer from Air to Interior Surface Materials	56
6.2.1	Test Summary	56
6.2.2	General Sorption Patterns	57
6.2.2.1	Sorption Concentrations	57
6.2.2.2	Normalized Sorption Concentrations	57
6.2.2.3	Sorption Rate	65
6.2.2.4	Normalized Sorption Rate	65
6.2.3	General Re-emission Patterns	68
6.2.4	Estimation of Partition and Diffusion Coefficients	70
6.3	PCB Transfer to Settled Dust	76
6.3.1	Test Summary	76

6.3.2	PCB Transport to Dust Due to Dust/Air Partition	77
6.3.2.1	Sorption Concentrations	77
6.3.2.2	Normalized Sorption Concentrations	79
6.3.2.3	Sorption Rates	81
6.3.2.4	Normalized Sorption Rates	82
6.3.2.5	Congener Patterns	84
6.3.3	PCB Transfer Due to Dust/Source Partitioning	85
6.3.3.1	General Patterns	85
6.3.3.2	Migration Concentrations	87
6.3.3.3	Normalized Migration Concentrations	87
6.3.3.4	Migration Rates	88
6.3.3.5	Normalized Migration Rates	88
6.3.3.6	Congener Patterns in Dust in Direct Contact with the Source	91
6.3.4	Effect of Dust Loading	92
6.3.5	Effect of Surface Material on Dust/Source Partitioning	93
6.3.6	Comparison of Two Types of Dust	94
6.4	PCB Sorption in Test Chambers	95
6.4.1	Sorption by the Walls of the 44-mL Micro Chamber	95
6.4.2	Sorption by the Walls of the 53-L Chamber	97
<b>7.</b>	<b>Discussion</b>	<b>101</b>
7.1	The General Behavior of PCB Sinks	101
7.2	The Significance of PCB Sinks as Secondary Sources	101
7.3	Comparison of Different Sink Materials	101
7.4	Ranking Building Materials as PCB Sinks	102
7.5	Similarity of Congener Patterns between the Primary Sources and PCB Sinks	103
7.6	Effects of Temperature and Relative Humidity on Sorption by Sink Materials	105
7.7	Predicting Congener Concentrations in the Sink Material	105
7.8	Using the Dynamic Sink Models	107
7.8.1	Predicting the Concentrations in Air after Removal of the Primary Source	107
7.8.2	Predicting the PCB Distribution in the Sink Material	108
7.9	Rough Estimation of the Material/Source Partition Coefficients for House Dust	109
7.10	Study Limitations	109
<b>8.</b>	<b>Conclusions</b>	<b>111</b>
	<b>Acknowledgments</b>	<b>113</b>
	<b>References</b>	<b>114</b>
	<b>Appendix A. Characterization of the Caulk Sample Used as the PCB Source for the Sink Tests</b>	<b>120</b>

<b>Appendix B. Sample Dimensions and Weights in Sink Tests S-2, S-3, and S-4</b>	<b>122</b>
<b>Appendix C. Method for Rough Estimation of the Partition and Diffusion Coefficients for Building Materials</b>	<b>124</b>
<b>Appendix D. Congener Patterns in Primary Sources and Sink Materials</b>	<b>129</b>
<b>Appendix E. Effects of Temperature and Relative Humidity on Sink Behavior</b>	<b>136</b>
<b>Appendix F. Predicting Sorption Concentrations for Sink Materials</b>	<b>139</b>

## List of Tables

Table 2.1.	Possible mechanisms for the transfer of pollutants from sources to sink materials under different conditions	3
Table 2.2.	Rough estimates of partition coefficients for congeners #18, #52, #110, and #187	5
Table 3.1.	Comparison of key features for the three sink test methods	14
Table 4.1.	Sink materials tested	16
Table 4.2.	Test materials and sample preparation methods	19
Table 4.3.	Sample sets of each material collected at specified sampling points	21
Table 4.4.	Selected properties of the two dust samples that were tested	29
Table 4.5.	List of target congeners and their selected properties	38
Table 5.1.	GC/MS calibration for PCB congeners from Aroclor 1254	41
Table 5.2.	GC/MS calibration for PCB congeners from Aroclors 1242 and 1248	42
Table 5.3.	IAP results for each calibration	43
Table 5.4.	Instrument detection limits (IDLs) for PCB congeners on GC/MS (ng/mL)	44
Table 5.5.	Method detection limits (MDLs) of the sonication extraction method for PCB congeners on GC/MS	45
Table 5.6.	Concentration of PCBs ( $\mu\text{g}/\text{m}^3$ ) in the chamber background	47
Table 5.7.	Summary of duplicate samples for tests	48
Table 5.8.	Concentration of PCBs in the field blank samples (ng/PUF sample)	48
Table 5.9.	Average recoveries of DCCs for dust tests in the 30- $\text{m}^3$ chamber	49
Table 5.10.	Average recoveries of DCCs for the sink tests in the 53-L chamber	50
Table 5.11.	Precision of duplicate measurements for sorption concentrations for oil-based paint in Test S-2	51
Table 5.12.	Precision of duplicate measurements for sorption concentrations for concrete sample in Test S-2	51
Table 5.13.	Precision of duplicate measurements for sorption concentrations for brick sample in Test S-3	52
Table 5.14.	Precision of PCB sorption concentrations as determined by replicate measurements	53
Table 6.1.	Terminology used for PCB transport to building materials	54
Table 6.2.	Terminology used for PCB transport to settled dust	55
Table 6.3.	Environmental conditions (mean $\pm$ SD) for small chamber sink tests	57
Table 6.4.	Congeners re-emitted from concrete panels during the 160-hour purging period	69
Table 6.5.	Rough estimates of partition and diffusion coefficients for 20 materials based on data from Tests S-2 and S-3	73
Table 6.6.	Summary of chamber tests for settled dust	77
Table 6.7.	Comparison of the normalized migration rates for dust samples in direct contact with the source from three chamber tests	90



Table 6.8.	Effect of dust loading on the PCB transport due to dust/air partitioning	92
Table 6.9.	Effect of dust loading on the PCB transport due to dust/source partitioning	93
Table 6.10.	Amounts of PCB congeners adsorbed by the walls of the microchamber as determined by wipe sampling (units: $\mu\text{g}$ )	96
Table 6.11.	Amounts of PCB congeners adsorbed by the walls of the microchamber after the tests as a fraction of the total emissions	97
Table 6.12.	Measured congener concentrations at the air inlet and outlet and percent sorption by the empty 53-L chamber	98
Table 6.13.	Estimated congener sorption by the 53-L chamber for the three most predominant congeners in the emissions of Aroclor 1242	99
Table 7.1.	Parameters used to model the congener patterns in concrete and brick as PCB sinks	104
Table 7.2.	Input parameters for predicting the re-emission of congener #52 from concrete walls after the primary source is removed	108
Table 7.3.	Roughly estimated dust/source partition coefficients for the house dust collected from PCB-containing primer panels	109

## List of Figures

Figure 2.1.	Sorption capacities for congeners #18, #52, #110, and #187 as a function of their concentrations in air (using rough estimates of the partition coefficients)	5
Figure 3.1.	Schematic of the conventional chamber method for testing sink materials	12
Figure 3.2.	Typical experimental output of the conventional sink test method (The source is shut off after 50 hours elapse)	12
Figure 3.3.	Typical experimental output from a sink test with the microbalance method	13
Figure 3.4.	Schematic of the test chamber used by Schripp et al. (2010) for dust/air partitioning experiments	15
Figure 4.1.	Picture of source chamber (top) and test chamber (bottom)	17
Figure 4.2.	Schematic of the air flow between chambers showing the PUF sampling locations	18
Figure 4.3.	Field caulk source containing Aroclor 1254	19
Figure 4.4.	Stage with 12 pin mounts for Test S-3	21
Figure 4.5.	Twelve support blocks with sink materials for Test S-2	22
Figure 4.6.	Twelve support blocks with sink materials for Test S-3	22
Figure 4.7.	Concrete panel placement in Test S-4	23
Figure 4.8.	The cage that held the concrete buttons	23
Figure 4.9.	Optical microscopic image for the house dust that was tested	25
Figure 4.10.	Scanning electron microscope images of individual house dust particles (The scale is 1 $\mu\text{m}$ )	26
Figure 4.11.	Optical microscopic image of Arizona Test Dust	27
Figure 4.12.	Scanning electron microscope images of individual ATD particles (The scale is 1 $\mu\text{m}$ )	28
Figure 4.13.	Two-Compartment Chamber System (The compartment on the left was used for this study)	30
Figure 4.14.	Schematic of the Two-Compartment Chamber System	30
Figure 4.15.	Aluminum sheet covered by white shipping label with a 21-cm circle cutout	32
Figure 4.16.	Loading dust to test panels (from left to right: before loading the dust, with the painted area covered by the sieve, and after loading the dust)	33
Figure 4.17.	Test panels placed on the chamber floor	34
Figure 4.18.	Securing the scintillation vial with a centrifuge tube holder	35
Figure 4.19.	Test panel folded into a U shape	35
Figure 4.20.	Test panel after folding and tapping. The dust formed a line along the bottom of the folded panel	36
Figure 4.21.	Dust being transferred to the scintillation vial	36
Figure 4.22.	Markes Microchamber/Thermal Extractor ( $\mu\text{-CTE}$ )	37
Figure 6.1.	Sorption concentrations for the oil-based paint applied on gypsum board in Test S-2 (top: normal scale; bottom: semi-log scale)	58

Figure 6.2.	Sorption concentrations for concrete in Test S-3 (top: normal scale; bottom: semi-log scale)	59
Figure 6.3.	Sorption concentrations for congener #52 for 10 materials in Test S-2	60
Figure 6.4.	Sorption concentrations for congener #52 for 11 materials in Test S-3	60
Figure 6.5.	Concentrations of PCB congeners in the air inside the test chamber for Test S-2 (top: normal scale; bottom: semi-log scale)	61
Figure 6.6.	Concentrations of PCB congeners in the air inside the test chamber for Test S-3 (top: normal scale; bottom: semi-log scale)	62
Figure 6.7.	Normalized sorption concentrations ( $C_m^*$ ) for the oil-based paint applied on gypsum board in Test S-2	63
Figure 6.8.	Normalized sorption concentrations ( $C_m^*$ ) for concrete in Test S-3	63
Figure 6.9.	Normalized sorption concentrations ( $C_m^*$ ) for congener #52 for the materials in Test S-2 ( $t = 269$ h) and Test S-3 ( $t = 240$ h)	64
Figure 6.10.	Normalized sorption concentrations ( $C_m^*$ ) for congener #110 for the materials in Test S-2 ( $t = 269$ h) and Test S-3 ( $t = 240$ h)	64
Figure 6.11.	Normalized sorption concentrations ( $C_m^*$ ) for Aroclor 1254 for the materials in Test S-2 ( $t = 269$ h) and Test S-3 ( $t = 240$ h)	65
Figure 6.12.	Sorption rate as a function of time for gypsum board paper in Test S-3	66
Figure 6.13.	Sorption rate as a function of time for brick in Test S-3	66
Figure 6.14.	Sorption rate as a function of time for concrete in Test S-3	67
Figure 6.15.	Normalized sorption rates for four congeners in concrete (Test S-3)	67
Figure 6.16.	Air concentration profiles in Test S-4 for concrete panels	68
Figure 6.17.	Percent re-emissions from concrete as a function of vapor pressure of the congeners	70
Figure 6.18.	Amounts of PCB congeners adsorbed by concrete, $M(t)$ , and the goodness of fit for estimating the partition and diffusion coefficients (data from Test S-3)	75
Figure 6.19.	Amounts of PCB congeners adsorbed by the core of a GREENGUARD-certified gypsum board, $M(t)$ , and the goodness of fit for estimating the partition and diffusion coefficients (data from Test S-3)	75
Figure 6.20.	Amounts of PCB congeners adsorbed by laminated flooring, $M(t)$ , and the goodness of fit for estimating the partition and diffusion coefficients (data from Test S-2)	76
Figure 6.21.	Amounts of PCB congeners adsorbed by oak flooring, $M(t)$ , and the goodness of fit for estimating the partition and diffusion coefficients (data from Test S-2)	76
Figure 6.22.	Experimentally determined sorption concentrations in settled house dust due to dust/air partitioning in Test D-2	78
Figure 6.23.	Concentrations of four congeners in the air inside the chamber in Test D-2. The decrease in these concentrations was caused mainly by the removal of PCB source panels.	78
Figure 6.24.	Sorption concentrations for congeners #15, #17, #18, and #22 in Test D-4.	79
Figure 6.25.	Concentrations of congeners #15, #17, #18, and #22 in chamber air (Test D-4)	79

Figure 6.26.	Concentration profile for congener #52 in Test D-2 created by the third-degree Lagrange interpolation (LG-3)	80
Figure 6.27.	Normalized sorption concentrations ( $C_D^*$ ) for four congeners in Test D-2	81
Figure 6.28.	Normalized sorption concentrations ( $C_D^*$ ) for four congeners in Test D-4	81
Figure 6.29.	Sorption rates for congeners #52, #101, #110, and #118 due to dust/air partitioning in Test D-2	82
Figure 6.30.	Sorption rates for congeners #15, #17, #18, and #22 due to dust/air partitioning in Test D-4	82
Figure 6.31.	Normalized sorption rates for four congeners due to dust/air partitioning (Test D-2)	83
Figure 6.32.	Normalized sorption rate ( $R_D^*$ ) as a function of vapor pressure (Test D-2; exposure time = 622 h)	84
Figure 6.33.	Normalized sorption rate ( $R_D^*$ ) for four congeners in Aroclor 1242 (Test D-4)	84
Figure 6.34.	Comparison of the congener patterns between the dust collected from PCB-free panels and the source (Test D-2; exposure time = 622 hours)	85
Figure 6.35.	Comparison of PCB accumulations in settled dust for congener #52 in Test D-2	85
Figure 6.36.	Comparison of PCB accumulations in settled dust for congener #101 in Test D-2	86
Figure 6.37.	Comparison of PCB accumulations in settled dust for congener #118 in Test D-2	86
Figure 6.38.	Migration concentrations in dust due to direct contact with the source (Test D-2)	87
Figure 6.39.	Normalized migration concentrations ( $C_s^*$ ) for dust in direct contact with the source (Test D-2; congener #77 was not detected in the air)	87
Figure 6.40.	Time-averaged migration rates ( $R_s$ ) for house dust in direct contact with the source (Test D-2)	88
Figure 6.41.	Normalized migration rates ( $R_s^*$ ) as a function of time for dust in direct contact with the source (Test D-2; congener #77 was not detected in the air)	89
Figure 6.42.	Normalized migration rate ( $R_s^*$ ) for dust/source partition as a function of vapor pressure (Test D-1; $t = 335$ h)	91
Figure 6.43.	Comparison of congener patterns between the source and the dust in direct contact with the source (Test D-2; $t = 622$ h)	91
Figure 6.44.	Comparison of congener patterns between the dust collected from PCB-free panels and the dust collected from the PCB panels (Test D-2; $t = 622$ h)	92
Figure 6.45.	Normalized migration concentration ( $C_s^*$ ) for dust in direct contact with PCB-containing primer and caulk panels in Test D-3 (The error bars represent $\pm 1$ SD; $n = 3$ for each data point)	93
Figure 6.46.	Comparison of sorption concentrations between the house dust and Arizona Test Dust ( $t = 335$ hours)	94
Figure 6.47.	Comparison of migration concentrations between the house dust and Arizona Test Dust ( $t = 335$ hours)	95
Figure 6.48.	Sorption by the walls of the microchamber as a function of vapor pressure of congeners	97
Figure 6.49.	Experimental results and exponential fit for sorption of PCB congeners by the interior walls of the 53-L chamber as a function of vapor pressure (error bar = $\pm 1$ SD)	99

Figure 7.1.	Correlation between SSI and experimentally determined normalized sorption concentrations ( $C_m^*$ ) for congener #52 ( $t = 269$ h for data from Test S-2 and $t = 240$ h for data from Test S-3)	103
Figure 7.2.	Comparison of congener patterns of the primary source (caulk) and the PCB sink (concrete)	104
Figure 7.3.	Comparison of congener patterns of the primary source (caulk) and the PCB sink (brick)	105
Figure 7.4.	Predicted DSS for congeners #118 and #156 in concrete	106
Figure 7.5.	Predicted concentrations for congeners #118 and #156 in concrete.	107
Figure 7.6.	Re-emission of congener #52 from concrete walls after the primary source was removed at 40 years elapse	108

## Acronyms and Abbreviations

ACH	Air changes per hour
ASHRAE	American Society of Heating, Refrigeration and Air-conditioning Engineers
ASTM	American Society for Testing and Materials
ATD	Arizona Test Dust
BET	Brunauer-Emmett-Teller
cfm	Cubic feet per minute
DCC	Daily calibration check
DEHP	Di (2-ethylhexyl) phthalate
DnBP	Di- <i>n</i> -butyl phthalate
DQI	Data quality indicator
DSS	Degree of sorption saturation, also SSD (sorption saturation degree) in the literature
EH&E	Environmental Health & Engineering, Inc.
FLEC	Field and Laboratory Emission Cell
GC/MS	Gas chromatography/mass spectrometry
IAP	Internal audit program
IDL	Instrument detection limit
LC(s)	Laboratory control(s)
NERL	National Exposure Research Laboratory
PCB(s)	Polychlorinated biphenyl(s)
ppm	Parts per million
PQL	Practical quantification limit
PTFE	Polytetrafluoroethylene
PUF	Polyurethane foam
QSAR	Quantitative structure-activity relationship
RCS	Recovery check standard
RH	Relative humidity
RRF	Relative response factor
RSD	Relative standard deviation
RTD	Resistance temperature detector
SD	Standard deviation

SSI	Sink sorption index
TSCA	Toxic Substance Control Act
TCC	Two-Compartment Chamber (System)
TMX	1,2,3,5-Tetrachloro-4,6-dimethylbenzene
ULPA	Ultra-low particulate air (filter)
VOC(s)	Volatile organic compound(s)

# 1. Introduction

## 1.1 Background

The phenomenon of polychlorinated biphenyls (PCBs) transport from primary sources to building materials and other indoor constituents in PCB contaminated buildings is well known but poorly understood. It is generally agreed that PCB sinks, often referred to as secondary sources in the literature, can cause elevated concentrations of PCBs in indoor air after the primary sources have been removed (U.S. EPA, 2010), thereby hindering the mitigation effort. Mitigating large quantities of contaminated building materials by decontamination, encapsulation, and removal has enormous environmental and economic implications. Therefore, understanding the process of PCB transport and the behavior of PCB sinks is critical to exposure assessment and risk management for PCBs in buildings.

There are no strict scientific definitions for primary sources and sinks for PCBs in buildings. In this study, a primary source is defined as an indoor constituent (e.g., building material, furniture, or light fixture) that contained PCBs when it was brought into the building. Most frequently mentioned primary sources are PCB-containing caulking materials and sealants and PCB-containing light ballasts. A PCB sink is an indoor constituent that did not contain PCBs initially but later “picked up” PCBs as a result of exposure to contaminated indoor air or as a result of direct contact with a primary source. PCB sinks are also referred to as secondary sources, reversible sinks, or re-emitting sinks. In this report, the term “PCB sink” is used in most places although other terms are also used occasionally. The term “secondary source” is used when citing the literature. Conventionally, contaminated indoor air is not considered a PCB sink.

Field measurements have demonstrated that PCB sinks are widespread in PCB-contaminated buildings. A study by Weis et al. (2003) identified 16 “secondary sources” in four heavily contaminated schools in Germany, where the air concentrations of PCBs ranged from 7.4 to 39  $\mu\text{g}/\text{m}^3$ . The PCB content of those secondary sources ranged from 360 to 7600 mg/kg. Several studies (Köppl and Piloty, 1993; Bent et al., 2000; Kohler, et al., 2005) noticed the potential contribution of secondary sources to the PCB concentrations in indoor air. A recent literature review of mitigation methods for PCBs in buildings (EH&E, 2012) identified over a dozen likely secondary sources in contaminated buildings. Gabrio et al. (2000) noticed the similarity in congener patterns between the primary and secondary sources. Overall, information related to secondary sources of PCBs in buildings is scarce in the literature. There is little or no information on the transport process between primary and secondary sources of PCBs.

Dust is an important sink for indoor air pollutants. Dust differs from other sink materials in many ways. For instance, dust is very small in size, has a much greater surface area-to-volume ratio, can settle on source or non-source surfaces, and can be re-suspended, allowing it to contribute to inhalation exposure. Elevated PCB concentrations in indoor dust have been reported by many researchers worldwide (Vorhees et al., 1999; Wilson et al., 2001; Coghlan et al., 2002; Weis et al., 2003; Herrick et al., 2004; Tan et al., 2007; Hwang et al., 2008; Rudel et al., 2008; Hover et al., 2009; Franzblau et al., 2009; Harrad et al., 2010; Roosens et al., 2010; Tue et al., 2010). The reported PCB content in dust varied greatly, from <1 to 890  $\mu\text{g}/\text{g}$ . Vorhees et al. (1999) noticed that the fine fractions (<150  $\mu\text{m}$ ) of the dust samples were likely to contain higher concentrations of PCBs than the coarse fractions. Some mitigation processes, such as using sand blasting to remove PCB paint, may create PCB-containing dust (Hellman et al., 2008).



## **1.2 Goals and Objectives**

The study conducted was designed to establish a general understanding of the transport of PCBs from primary sources to PCB sinks in buildings. The specific objectives were (1) to conduct laboratory experiments to study the transport of PCBs from air to interior surface materials, from air to settled dust, and from sources to settled dust; (2) to identify potentially useful mathematical tools for predicting the behavior of PCB sinks in PCB-contaminated buildings; and (3) to estimate the key parameters, such as sorption capacity, partition coefficients, and diffusion coefficients, required by the tools. This study supports risk management decision-making and exposure assessment for PCBs in buildings.

## **1.3 About This Report**

This is the second report in the publication series entitled *Laboratory Study of Polychlorinated Biphenyl (PCB) Contamination and Mitigation in Buildings*, produced by EPA's Office of Research and Development (ORD), National Risk Management Research Laboratory. The first report (Guo et al., 2011) was a characterization of primary sources with focus on PCB-containing caulking materials and light ballasts. This second report summarizes the research results for PCB transport from primary sources to PCB sinks, including interior surface materials and settled dust. This study was limited to a laboratory investigation, and it complements and supplements an ongoing field study in school buildings conducted by the ORD's National Exposure Research Laboratory (NERL, 2010).

## 2. Theoretical Background

Sorption of airborne pollutants by interior surface materials in buildings and the subsequent re-emissions of the pollutants from these materials, which is often referred to as the “sink effect”, has been a topic of active research for over two decades. As a result, much has been learned and many models have been developed, some of which can be used to study the PCB transport from primary sources to PCB sinks.

### 2.1 Transfer Mechanisms

Three mass transfer mechanisms that are responsible for pollutant transport from indoor sources to building materials and dust have been identified:

- Solid material/air partitioning including dust/air partitioning (e.g., Little and Hodgson, 1996; Schwarzenbach et al., 2003; Kuusisto et al., 2007; Weschler and Nazaroff, 2008)
- Solid material/solid material partitioning (Kumar and Little, 2003; Webster et al., 2009)
- Particle formation due to weathering of the source or mechanical forces such as abrasion applied to the source (Webster et al., 2009).

Depending on the types of sink materials and exposure conditions, different mechanisms may apply (Table 2.1).

**Table 2.1. Possible mechanisms for the transfer of pollutants from sources to sink materials under different conditions**

Indoor Media	Exposure conditions	Mechanisms <sup>[a]</sup>		
		MA	MM	PF <sup>[b]</sup>
Building materials and furniture	Surfaces exposed to indoor air	√		
	In direct contact with a source		√	
Dust	Settled on source surfaces	√	√	√
	Settled on nonsource surfaces	√		√
	Suspended in air	√		√

<sup>[a]</sup> MA = material/air partitioning; MM = material/material partitioning; PF = particle formation due to source weathering or abrasion.

<sup>[b]</sup> Mainly for floor dust; sandblasting of PCB-containing surfaces may create PCB dust in air.

## 2.2 Material/Air Partition

### 2.2.1 Sorption Capacity

Sorption capacity determines the upper bound of the amount of pollutant that the sink material can take up from the air. Sorption capacity can be calculated in different ways (Deng et al., 2010). In this study, sorption capacity is estimated from the material/air partition coefficient (Equation 2.1):

$$K_{ma} = \frac{C_{m\infty}}{C_a} \quad (2.1)$$

where  $K_{ma}$  = material/air partition coefficient (dimensionless)

$C_a$  = pollutant concentration in room air ( $\mu\text{g}/\text{m}^3$ )

$C_{m\infty}$  = sorption capacity (i.e., pollutant concentration in the material in equilibrium with  $C_a$ ) ( $\mu\text{g}/\text{m}^3$ )

According to Equation 2.1, the content of a pollutant in the sink material will eventually approach  $C_{m\infty} = K_{ma} C_a$  if the concentration of the pollutant in room air is constant, and if the exposure duration is sufficiently long. Conventionally, the pollutant concentration in the solid material is expressed in mass units such as ( $\mu\text{g}/\text{g}$ ). Then, Equation 2.1 becomes:

$$K_{ma} = \frac{10^6 d x}{C_a} \quad (2.2)$$

or,

$$x = 10^{-6} \frac{K_{ma} C_a}{d} \quad (2.3)$$

where  $x$  = sorption capacity expressed in mass/mass units ( $\mu\text{g}/\text{g}$ )

$d$  = density of the solid material ( $\text{g}/\text{cm}^3$ )

At present, no solid/air partition coefficients for PCB congeners and common building materials have been determined experimentally. For demonstration purposes, an empirical model (Equation 2.4) proposed by Guo (2002) can be used to obtain a rough estimate of the partition coefficients for congeners and materials:

$$\ln K_{ma} = 8.78 - 0.785 \ln P \quad (2.4)$$

where  $P$  = vapor pressure of the chemical (torr)

As an example, the calculated partition coefficients for four congeners are presented in Table 2.2. Figure 2.1 shows the relationship between the concentration in air ( $C_a$ ) and the sorption capacity of the sink material expressed in  $\mu\text{g}/\text{g}$ , assuming the density of the material is  $1.5 \text{ g}/\text{cm}^3$  (The reader can select other density

values). Figure 2.1 can be used to determine the sorption capacities at different air concentrations. For example, if the air concentration is  $0.1 \mu\text{g}/\text{m}^3$  for each congener, the sorption capacities for congeners #18, #52, #110, and #187 are 0.14, 0.44, 2.4, and  $10 \mu\text{g}/\text{g}$ , respectively.

Note that the partition coefficients for common building materials for PCB congeners are currently not available, and that the values calculated from Equation 2.4 should be used with caution because it is an empirical, general-purpose model which does not differentiate between different materials.

**Table 2.2. Rough estimates of partition coefficients for congeners #18, #52, #110, and #187**

Congener ID	Number of chlorines	P <sup>[a]</sup> (torr)	K <sub>ma</sub> <sup>[b]</sup> (dimensionless)
#18	3	$6.38 \times 10^{-4}$	$2.09 \times 10^6$
#52	4	$1.50 \times 10^{-4}$	$6.54 \times 10^6$
#110	5	$1.68 \times 10^{-5}$	$3.64 \times 10^7$
#187	7	$2.79 \times 10^{-6}$	$1.49 \times 10^8$

<sup>[a]</sup> Vapor pressure, from Fischer et al. (1992) (method B).

<sup>[b]</sup> From Equation 2.4.

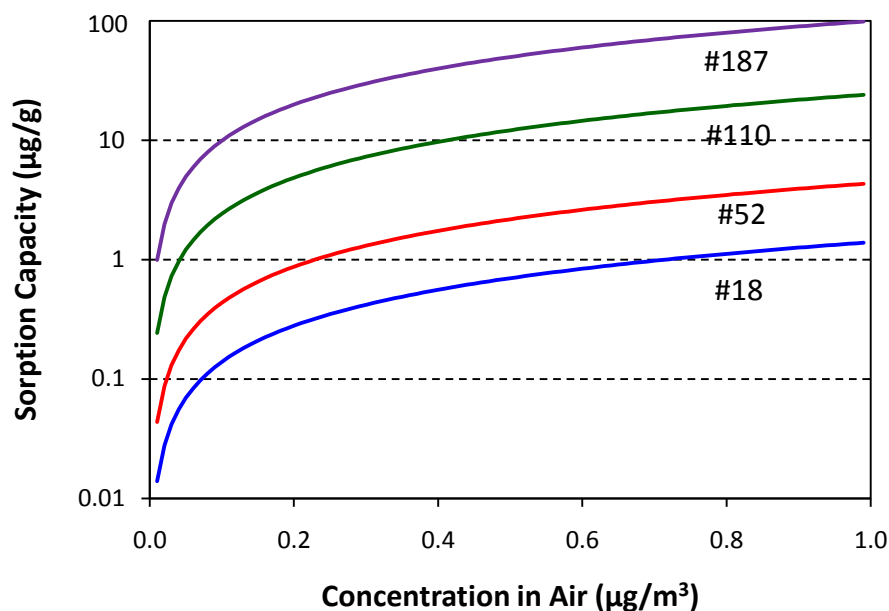


**Figure 2.1. Sorption capacities for congeners #18, #52, #110, and #187 as a function of their concentrations in air (using rough estimates of the partition coefficients)**

The following observations can be made from Equations 2.1 and 2.4 and Figure 2.1:

- The sorption is not unlimited. The upper bound is determined by the material/air partition coefficient and the concentration in room air.
- For a given PCB congener and a given sink material, the sorption capacity is proportional to the congener concentration in room air.
- If two congeners have the same concentrations in air, the sink material has a greater tendency to take up the less volatile congener. In other words, the sorption favors the less volatile congener.

However, the transport of PCBs from primary sources to PCB sinks involves two steps, i.e., emissions from the primary source and sorption by the sink material. Although the sorption favors the less volatile congeners, the emissions from the primary source favor the more volatile congeners (Guo et al., 2011). The combination of these two opposite effects often results in a congener pattern for the PCB sink that is similar, but not identical, to the congener pattern for the primary source. More discussion of this topic is given in Section 7.3.

### 2.2.2 Degree of Sorption Saturation (DSS)

As described above, sorption capacity defines the upper bound of the sorption. Sorption capacity does not provide any indication of the amount of time it takes to approach saturation or whether the sink material is saturated. A useful parameter for addressing these questions is the degree of sorption saturation (DSS), also known in the literature as sorption saturation degree (SSD) (Deng et al., 2010). DSS is defined as:

$$DSS = \frac{M(t)}{M_{\infty}} = \frac{M(t)}{C_{m\infty} A \delta} \quad (2.5)$$

where  $M(t)$  = amount of pollutant that has entered the sink material at time  $t$  ( $\mu\text{g}$ )

$M_{\infty}$  = maximum amount of pollutant the sink material can adsorb at a given air concentration ( $\mu\text{g}$ )

$C_{m\infty}$  = sorption capacity ( $\mu\text{g}/\text{m}^3$ )

$A$  = surface area of the sink material ( $\text{m}^2$ )

$\delta$  = thickness of the sink material (m)

Several models are available for predicting the DSS. The model derived by Crank (Crank, 1975; also in Little and Hodgson, 1996) is shown as Equation 2.6:

$$DSS = \frac{M(t)}{M_{\infty}} = 1 - \sum_{n=0}^{\infty} \left\{ \frac{8}{(2n+1)^2 \pi^2} \exp \left[ \frac{-D_m (2n+1)^2 \pi^2 t}{4 \delta^2} \right] \right\} \quad (2.6)$$

where  $D_m$  = diffusion coefficient of the pollutant in the sink material ( $\text{m}^2/\text{h}$ )

$\delta$  = thickness of the sink material if only one side is exposed to air or one half of the thickness of the sink material if both sides are exposed to air (m)

t = time (h)

According to Equation 2.6, for a given pollutant and a given sink material, the DSS is a function of three variables, i.e., the solid-phase diffusion coefficient ( $D_m$ ), the thickness of the sink material ( $\delta$ ), and the exposure time (t).

More recently, Deng et al. (2010) developed correlations between the DSS and three dimensionless numbers, i.e., dimensionless air change rate ( $N^*$ ), dimensionless mass capacity ( $\Theta$ ), and Fourier number for mass transfer ( $F_{om}$ ). The correlations are shown in the following equations:

$$DSS = 0.234 N^{*0.245} \Theta^{-0.081} F_{om}^{0.61} \quad (\text{for } F_{om} \leq 0.01) \quad (2.7)$$

$$DSS = 0.747 N^{*0.059} \Theta^{-0.003} F_{om}^{0.527} \quad (\text{for } 0.01 < F_{om} \leq 0.2) \quad (2.8)$$

$$DSS = 1 - 1.109 N^{*-0.056} \Theta^{0.63} e^{-2.35 F_{om}} \quad (\text{for } 0.2 < F_{om} \leq 2) \quad (2.9)$$

$$N^* = \frac{N \delta^2}{D_m} \quad (2.10)$$

$$\Theta = \frac{A \delta K_{ma}}{V} \quad (2.11)$$

$$F_{om} = \frac{D_m t}{\delta^2} \quad (2.12)$$

where  $N$  = air change rate ( $\text{h}^{-1}$ )

$\delta$  = thickness of the sink material (m)

$D_m$  = diffusivity in the sink material ( $\text{m}^2/\text{h}$ )

$A$  = exposed area of the sink material ( $\text{m}^2$ )

$V$  = room volume ( $\text{m}^3$ )

$K_{ma}$  = material/air partition coefficient (dimensionless)

t = time (h)

Equations 2.7, 2.8, and 2.9 reduce the computational complexity substantially and, thus, are easier to use for estimating parameters.

As a generalized form,  $M(t)$  in Equation 2.5 can be expressed as shown in Equation 2.13:

$$M(t) = M_{\infty} \times DSS = f(K_{ma}, D_m, C_a, A, \delta, V, N, t) \quad (2.13)$$

Because  $A$ ,  $\delta$ ,  $V$ ,  $N$ , and  $t$  are easily obtained,  $K_{ma}$  and  $D_m$  are the only unknown parameters in the equation if  $M(t)$  and  $C_a$  can be determined experimentally. In this study, we used Equation 2.13 to estimate the partition and diffusion coefficients from the experimental data.

### 2.2.3 Dynamic Sink Models

There are two types of dynamic sink models, i.e., those based on Langmuir isotherms and those based on the material/air partition and solid-phase diffusion. The most commonly used Langmuir sink model is shown in Equations 2.14 and 2.15 (Tichenor et al., 1991):

$$R_a = A k_a C_a \quad (2.14)$$

$$R_d = A k_d M_s \quad (2.15)$$

where  $R_a$  = rate of adsorption ( $\mu\text{g/h}$ )

$A$  = area of sink material ( $\text{m}^2$ )

$k_a$  = adsorption rate constant ( $\text{m/h}$ )

$C_a$  = pollutant concentration in air ( $\mu\text{g/m}^3$ )

$R_d$  = rate of desorption ( $\mu\text{g/h}$ )

$k_d$  = desorption rate constant ( $\text{h}^{-1}$ )

$M_s$  = pollutant concentration adsorbed on the sink surface ( $\mu\text{g/m}^2$ )

The Langmuir sink models are suitable for simulating the short-term sink effect. They work better for non-porous and impenetrable materials, such as metal sheets, than for porous materials. They always underestimate the long-term re-emissions because they ignore the diffusion of the adsorbate in the sink material.

The second class of sink models is based on the material/air partition and solid-phase diffusion (Little and Hodgson, 1996; Yang and Chen, 2001; Kumar and Little, 2003; Lee et al., 2005). In these models, the sink material is characterized by three parameters, i.e., the material/air partition coefficient ( $K_{ma}$ ), the diffusion coefficient in the material ( $D_m$ ), and the thickness of the material ( $\delta$ ). Thus, determination of the partition and diffusion coefficients is the key to using these models. These models require extensive computational effort, but they are more suitable for describing the long-term effect than the Langmuir models, especially for porous materials. Typical output of these models include pollutant concentration in room air as a function of time, pollutant concentration in the sink material as a function of time and depth, and the amount of pollutant accumulated in the sink material as a function of time. As an example, the sink model developed by Little and Hodgson (1996) is shown as Equations 2.16 through 2.19 below:

$$C_m(x, t) = 2 \sum_{n=1}^{\infty} \left\{ \frac{e^{-D_m \lambda_n^2 t} \lambda_n^2 \cos(\lambda_n x)}{[\delta(\alpha - \beta \lambda_n^2)^2 + \lambda_n^2(\delta + \beta) + \alpha] \cos(\lambda_n \delta)} \int_0^t e^{D_m \lambda_n^2 \tau} K_{ma} C_{in}(\tau) d\tau \right\} \quad (2.16)$$

$$\alpha = \frac{Q}{A D_m K_{ma}} \quad (2.17)$$

$$\beta = \frac{V}{A K_{ma}} \quad (2.18)$$

$$\lambda_n \tan(\lambda_n \delta) = \alpha - \beta \lambda_n^2 \quad (2.19)$$

where  $C_m(x,t)$  = pollutant concentration in the sink material at time  $t$  and depth  $x$  ( $\mu\text{g}/\text{m}^3$ )

$x$  = depth in the sink material,  $x = \delta$  at the exposed surface (m)

$t$  = elapsed time (h)

$Q$  = air change flow rate ( $\text{m}^3/\text{h}$ )

$A$  = exposed area of the sink material ( $\text{m}^2$ )

$K_{ma}$  = material/air partition coefficient (dimensionless)

$D_m$  = diffusivity of the pollutant in the sink material ( $\text{m}^2/\text{h}$ )

$\lambda_n$  = the  $n^{\text{th}}$  smallest positive root of nonlinear Equation 2.19 ( $\text{m}^{-1}$ )

$\delta$  = thickness of the sink material (m)

$\tau$  = time for the integral,  $0 \leq \tau \leq t$ , (h)

Some of the applications of the dynamic sink model include estimations of the following:

- Amount of PCBs accumulated in the sink material at a given time
- Concentrations of the PCBs accumulated at different depths of the sink material at a given time
- Re-emission of PCBs from the sink material after the primary source is removed

### 2.3 Material/Material Partitioning

Material/material partitioning occurs when two materials are in direct contact. The amount of pollutant transferred from the source to the sink material depends on several parameters, including the solid/solid partition coefficient, the diffusivities of the pollutant in the source and the sink, and the distribution of the pollutant concentrations in both materials. The upper bound of the total migration can be estimated using Equation 2.20:

$$K_{12} = \frac{C_{m1}}{C_{m2}} \quad (2.20)$$

where  $K_{12}$  = material/material partition coefficient between material 1 and material 2 (dimensionless)



$C_{m1}$  = pollutant concentration in material 1 in equilibrium with material 2 ( $\mu\text{g}/\text{m}^3$ )

$C_{m2}$  = pollutant concentration in material 2 in equilibrium with material 1 ( $\mu\text{g}/\text{m}^3$ )

Although few, if any, material/material partition coefficients are available for common building materials, they can be estimated from their respective material/air partition coefficients (Kumar and Little, 2003):

$$K_{12} = \frac{K_{ma1}}{K_{ma2}} \quad (2.21)$$

where  $K_{ma1}$  = material/air partition coefficient for material 1 (dimensionless)

$K_{ma2}$  = material/air partition coefficient for material 2 (dimensionless)

If the material/air partition coefficients for the source and sink materials are equal, then  $K_{12} = 1$ , which means that the pollutant concentrations in the source and sink will eventually become equal. Note that a major difference between material/air partitioning and material/material partitioning is that the former is controlled by the concentration in the air but the latter is not.

### 3. Experimental Considerations

#### 3.1 Methods for Testing Building Materials

Laboratory testing of the sink effect in buildings started in the late 1980s. Since then several experimental methods have been developed. Thorough reviews of this topic have been published in the literature (An et al., 1997; Zhang et al., 2001, 2002; Yang et al., 2010).

##### 3.1.1 Conventional Chamber Method

The interactions between contaminated air and sink materials have often been studied in environmental chambers (Tichenor et al., 1991). In such studies, the test specimen is placed in the chamber, and a chemical vapor is introduced into the chamber from the air inlet at a constant rate. After a certain interaction time, the source is shut off to allow the chamber to be flushed by clean air. Throughout a test, the concentrations of the chemical in the inlet and outlet air are monitored continuously. A schematic of the experimental setup is shown in Figure 3.1. The time-concentration profiles obtained from the test (Figure 3.2) are used to estimate the sink parameters ( $k_a$  and  $k_d$  in Equations 2.14 and 2.15 or  $K_{ma}$  and  $D_m$  in Equations 2.16 through 2.19).

This test method requires continuous monitoring of the air concentrations at both the inlet and the outlet of the chamber. For chemicals with low volatility, including PCBs, the interior walls of the chamber may serve as a sink and, thus, interfere with the experiment. In addition, this method requires good time resolution for air sampling, which is difficult to achieve for PCBs.

##### 3.1.2 Microbalance Method

Another test method is based on the determination of the mass gain by the sink material during the sorption process, which requires placing a microbalance inside a flow-through chamber (Little and Hodgson, 1996). The test specimen is placed on the balance, and, as was the case in the conventional test method, the source is introduced into the chamber through the air inlet. As the adsorbate accumulates in the test specimen, the microbalance records the mass of the test specimen over time (Figure 3.3). Often, such test results are used to determine the partition and diffusion coefficients for building materials.

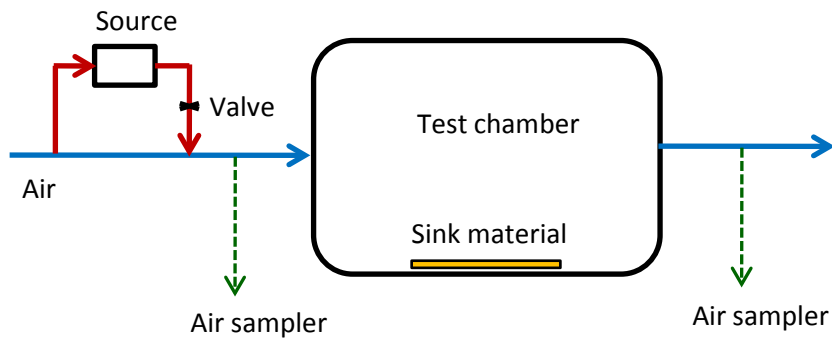


**Figure 3.1.** Schematic of the conventional chamber method for testing sink materials

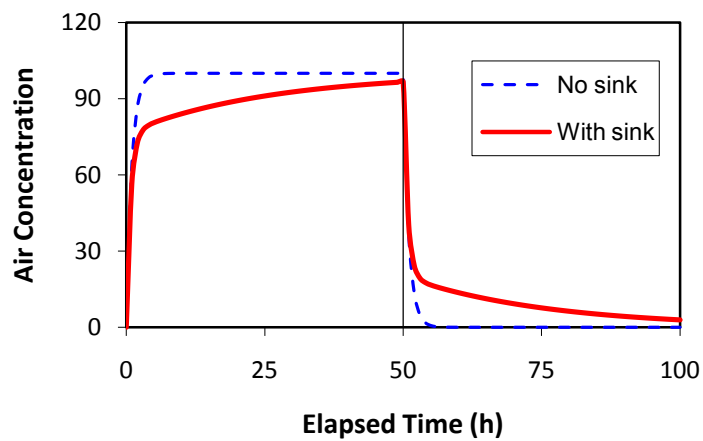


**Figure 3.2.** Typical experimental output of the conventional sink test method (The source is shut off after 50 hours elapse)

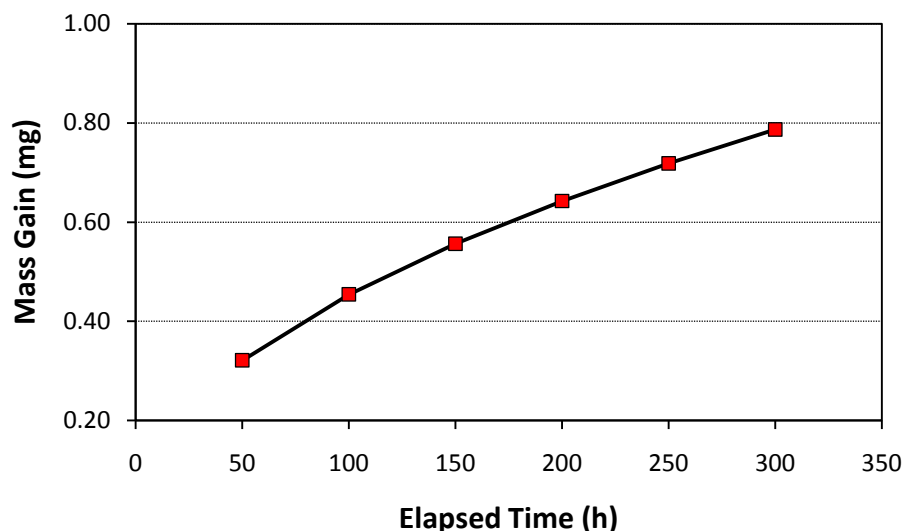


**Figure 3.3. Typical experimental output from a sink test with the microbalance method**

A fundamental difference between the conventional method and the microbalance method is that the former requires two air concentrations be monitored (one at the inlet of the chamber and the other at the outlet), while the latter requires monitoring only the air concentration that interacts with the sink material (i.e., at the outlet). Thus, the microbalance method is more suitable for testing semivolatile chemicals because the test results are not affected by sorption of the chemicals by the walls of the chamber. On the other hand, the microbalance method usually requires that the mass changes of the test material be in the milligram range, which is difficult to achieve for PCBs. The method also requires strict control of the humidity in the chamber, and, often, dry air is used.

### *3.1.3 Other Sink Test Methods*

In addition to the two methods described above, several methods have been developed mainly for the determination of partition and diffusion coefficients for building materials, i.e., the cup method (ASHRAE, 1997), the twin chamber method (Meininghaus et al., 2000; Xu et al., 2008), the diffusion metric method (Bodalal et al., 2000), the twin-compartment method (Hansson and Stymne, 2000), the porosity test method (Tiffonnet et al., 2000). Haghighat et al. (2002) conducted a literature review on this topic. In general, these methods are suitable for testing volatile chemicals.

### *3.1.4 Test Method Used in This Study*

The major challenges for testing the sink effect for PCBs include: (1) low concentrations of the PCBs in air, which leads to long sampling times (at least several hours) or large sampling volume; (2) very small mass gain in the sink material (usually in the microgram range), which makes it difficult to measure the changes using a microbalance; and (3) sorption of PCBs by the walls of the chamber because of the low volatilities of PCBs. The test method used in this study was similar to the microbalance method in principle, but there were significant modifications. The building material was made as small “buttons” and placed in a flow-

through test chamber, which was connected to a PCB source chamber. During a sink test, the buttons were removed from the test chamber at different times and placed directly into the extraction vials for determination of PCB content. The test results consisted of PCB concentrations in the sink material as a function of time, similar to Figure 3.3, and the PCB concentrations in the outlet air. Experimental details are described in Section 4.1. This method has three advantages. First, like the microbalance method, this method requires that the air concentrations be monitored only at the outlet of the chamber and, thus, the test was not affected by the sorption of PCBs by the walls of the chamber. Second, this method allows multiple sink materials to be tested at the same time because the PCB concentrations in the materials were determined individually. Third, this method can detect the PCB concentrations in the sink material in the microgram range and, thus, is more sensitive than the microbalance method. Table 3.1 compares the key features of the three test methods.

**Table 3.1. Comparison of key features for the three sink test methods**

Method	Key Measurements			Allow testing of multiple sink materials?
	Concentration in inlet air	Concentration in outlet air	Concentration in sink material	
Conventional	Yes	Yes	No	No
Microbalance	No	Yes	Yes (gravimetric)	Yes <sup>[a]</sup>
This study	No	Yes	Yes (extraction)	Yes

<sup>[a]</sup> Allowed but not commonly used because each test material requires a microbalance.

### 3.2 Methods for Testing Settled Dust

#### 3.2.1 Existing Methods

Transport of semivolatile pollutants to dust, either through air or through direct contact with a source, is often studied in small or microchambers (Clausen et al., 2004; Schripp et al., 2010; Kofoed-Sørensen et al., 2011). Clausen et al. (2004) used a 51-L glass chamber and 35-mL stainless steel microchambers, known as the Field and Laboratory Emission Cell (FLEC<sup>®</sup>), to study the sorption and subsequent re-emission of di(2-ethylhexyl)phthalate (DEHP). Similar methods were used by Schripp et al. (2010) for testing the transport of phthalates from plasticized polymer to settled dust. The authors used 500-L stainless steel chambers to study the transfer due to dust/air partitioning (Figure 3.4). A plasticized wall paint containing the target compounds [di(2-ethylhexyl) phthalate (DEHP) and di-*n*-butyl phthalate (DnBP)] was used as the source. Three grams of house dust were applied to a stainless steel plate (10 cm by 30 cm), which gave a dust loading of 100 g/m<sup>2</sup>. The chamber was maintained at 23 °C and had a low air change rate (0.12 h<sup>-1</sup>). The tests lasted for 45 days and the results were reported as concentration in dust (mg/kg). These researchers also conducted tests with pure DEHP and DnBP liquids as sources.

The same researchers also used 2.8-L glass flasks to study the transfer of DEHP. Dust was applied to a Petri dish (for testing gas-phase transfer) and to a polymer plate that contained phthalates (for testing transfer due to direct contact with the source). The dust-loaded Petri dish and the dust-loaded polymer plate were placed on different levels of shelves. A constant air flow was maintained during the test. A magnetic stirrer at the

bottom of the flask kept the air well mixed. The tests lasted for 14 days. The dust loading factors were not reported.

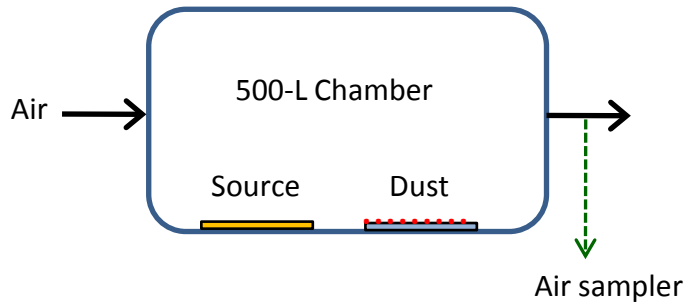


**Figure 3.4. Schematic of the test chamber used by Schripp et al. (2010) for dust/air partitioning experiments**

### *3.2.2 Test Method Used in This Study*

The test method used in this study was similar to the methods used by Clausen et al. (2004) and Schripp et al. (2010), except that a 30-m<sup>3</sup> stainless steel chamber was used to allow multiple test panels to be placed in the chamber and to allow the panels to be removed from the chamber at different times. Details are described in Section 4.2.

## 4. Experimental Methods

### 4.1 Testing of Building Materials

#### 4.1.1 Test Specimens

Twenty materials were tested (Table 4.1). They were selected because they are interior surface materials commonly found in buildings. All the test specimens were new materials. Each specimen was extracted for PCB background before testing.

**Table 4.1. Sink materials tested**<sup>[a]</sup>

No.	Material	Full Name	Manufacturer
1	Concrete	No. 1103 Sand (Topping) Mix	Quikrete
2	Brick	Red patio pavers	Triangle Brick Company
3	Ceiling tile	Ceiling tiles used at the EPA RTP	Unknown
4	Gypsum-A (facing)	Gold Bond 1/2" conventional gypsum board	National Gypsum
5	Gypsum-B (facing)	DensArmor Plus® 1/2" paperless gypsum board	Georgia Pacific
6	Gypsum-A (core)	Gypsum core material for conventional wallboard	National Gypsum
7	Gypsum-B (core)	Gypsum core material for paperless wallboard	Georgia Pacific
8	Oil-based paint	All Surface Enamel Oil-Base Gloss	Sherwin Williams
9	Latex paint, high-gloss	All Surface Enamel Acrylic Latex Gloss	Sherwin Williams
10	Latex paint, eggshell	Eco Spec #223 interior latex eggshell enamel	Benjamin Moore
11	Epoxy coating, solvent free	Sikagard® 62, high-build, protective, 2-component epoxy	Sika Corporation
12	Epoxy coating, polyamide	Macropoxy 646, two-component fast cure epoxy	Sherwin Williams
13	Carpet A	Horizon Collection, 100% Smartstrand Triexta BCF	Mohawk
14	Carpet B	GL070 Wisdom Collection, Duracolor premium fiber w/Antron Legacy	Lees
15	Vinyl flooring B	Roll-type felt backed vinyl flooring; no pad	Unknown
16	Oak flooring, pre-finished	CB726 Westchester Plank with Dura-luster Urethane	Armstrong
17	Laminate flooring	Plastic oak laminate flooring	Pergo
18	Painted metal	Office furniture metal cabinet	Unknown
19	Medium density fiberboard	Backing support substrate for plastic laminate countertop	Unknown
20	Plastic laminate countertop	Countertop material from backsplash kit	Formica

<sup>[a]</sup> Mention of trade names and manufacturers is for product identification only. It is not an endorsement of the products, nor is it meant to discriminate against similar products that were not tested.

#### 4.1.2 Test Facility

All but one of the sink tests were conducted in two 53-L stainless steel chambers, a source chamber and a material test chamber connected in series (Figure 4.1). A scouting test utilized only one of the chambers.



**Figure 4.1. Picture of source chamber (top) and test chamber (bottom)**

These chambers conformed to ASTM Standard Guide D5116-10 — Standard Guide for Small-Scale Environmental Chamber Determinations of Organic Emissions from Indoor Materials/Products (ASTM, 2010). The stainless steel chambers had nominal measurements of 51 cm (width) by 25 cm (height) by 41 cm (depth). Clean air, free of volatile organic compounds (VOCs), was supplied to the chambers through a dedicated clean air system, which consisted of house-supplied high-pressure oil-free air, a pure air generator (Aadco model 737-11A, Cleves, OH), a dryer (Hankinson model SSRD10-300, Canonsburg, PA), a Supelco activated charcoal canister, a Supelco micro sieve canister and gross particle filters (Grainger Speedaire, Chicago, IL). Each chamber was equipped with inlet and outlet manifolds for the air supply, a K-type thermocouple for temperature measurement in the chamber, and two resistance temperature detector (RTD) probes (HyCal model HTT-2WC-RP-TTB, Elmonte, CA) for measuring the relative humidity of the supplied air and the air inside the chamber. The relative humidity of the air supplied to the chamber was controlled by blending dry air with air that was humidified by bubbling through an impinger submerged in a temperature-controlled water bath. All air transfer lines and sampling lines were made of glass, stainless steel, or polytetrafluoroethylene (PTFE). An OPTO 22 data acquisition system (OPTO 22, Temecula, CA) continuously recorded the temperature and relative humidity of the air, the barometric pressure and temperature in the laboratory, and the outputs of the mass flow controllers. A 1½-in (3.8 cm) computer cooling fan (RadioShack, Fort Worth, TX) was placed in the chamber to provide mixing for all of the small chamber tests. The two chambers were housed in a temperature-controlled incubator (model 39900, Forma Scientific, Marietta, OH). All the sink test materials were placed in the lower test chamber while the upper chamber contained the PCB source. Figure 4.2 shows a schematic of the air flow between the source chamber and test chamber as well as the polyurethane foam (PUF) sampling locations for the sink tests.



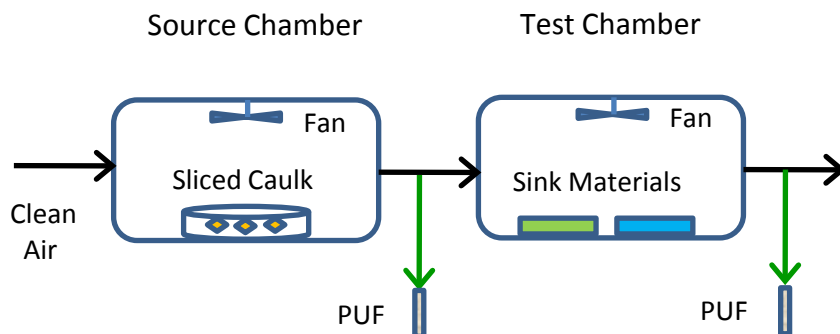


**Figure 4.2. Schematic of the air flow between chambers showing the PUF sampling locations**

#### 4.1.3 Test Procedure

##### 4.1.3.1 Sink Tests and PCB Source

During this study, four PCB sink tests (S-1 through S-4) were conducted using the same PCB source for exposure:

- **S-1:** Multiple materials. Source and test chambers combined (scouting test).
- **S-2:** Multiple materials. Separate source and test chambers.
- **S-3:** Multiple materials. Separate source and test chambers
- **S-4:** Concrete panels and buttons. Separate source and test chambers. Re-emission measured after source shut-off.

Sink materials (listed in Table 4.1) were exposed to a roughly constant concentration of Aroclor 1254 emitted from a caulking material that was obtained from a field study. This caulk sample has been previously characterized and showed stable emissions (Guo et al., 2011). More details about this source are presented in Appendix A. The caulking material was prepared using approximately 10 g of field caulk cut into <1 mm thick strips, which were placed in an open-face Petri dish (Figure 4.3). The Petri dish was placed in the source chamber to provide a stable source of Aroclor 1254 for sink tests (S-2) through (S-4). Aroclor 1254 was used as the source for the sink tests because many studies (e.g., Herrick et al., 2004; Guo, et al., 2011) have shown that Aroclor 1254 was the most frequently used PCB product for mixing caulking materials and sealants before the use of PCBs was banned by the U.S. Congress in 1978. Typical indoor parameters were established in both the source chamber and the test chamber [23 °C, 50% RH, and one air change per hour (ACH)] for all of the sink tests. Test S-1 incorporated both the PCB source and test materials in the same chamber and was controlled to the same environmental parameters as the other tests.



**Figure 4.3. Field caulk source containing Aroclor 1254**

#### 4.1.3.2 Procedure for Sink Tests S-1, S-2, and S-3

The test materials for Tests S-1 through S-3 were prepared as “buttons” with a nominal diameter of 1.2 cm. This diameter assured that the material would accommodate the opening of a 20-mL scintillation vial used for the hexane/sonication extraction method, described in Section 4.4.2, below. The total exposed areas for the test substrates varied from 2.5 cm<sup>2</sup> to 17 cm<sup>2</sup>, depending on the material. Most materials were prepared so that the thickness was negligible and did not contribute to the exposed surface area. Samples with non-negligible thicknesses were concrete, brick, carpet and vinyl flooring with padding. For these samples, the areas of the edges associated with the thickness of the samples were considered to be part of the exposed area. Table 4.2 details the materials tested and the material preparation methods that were used.

**Table 4.2. Test materials and sample preparation methods**

No.	Material	Sink test IDs	Preparation and material information
1	Concrete	S-1, S-2, S-3, S-4	Mix of commercial grade Portland cement and sand; for repairing and topping damaged concrete surfaces. Prepared according to manufacturer’s recommendation and molded in butter board to appropriate size.
2	Brick	S-3	Manufactured and purchased locally; cut to size with a wet saw.
3	Ceiling Tile	S-1, S-2	Ceiling material used at EPA RTP; cut to test size with a ½” round hole arch punch.
4	Gypsum-A (facing)	S-1, S-3	Standard indoor gypsum board, paper side only unpainted; cut to test size with a ½”round hole arch punch.
5	Gypsum-B (facing)	S-3	Mold and mildew resistant paperless gypsum board , GREENGUARD certified). Fiberglass side only, unpainted; cut to test size with a ½”round hole arch punch.
6	Gypsum-A (core)	S-3	Calcium Sulfate Dihydrate (Gypsum); cut to size with a General No. S31 ½” drill fitted plug cutter.
7	Gypsum-B (core)	S-3	Used for moisture -prone interior walls; cut to size with a General No. S31 ½” drill fitted plug cutter.
8	Oil-based paint	S-2	Painted on Gypsum-A; painted paper surface only; cut to test size with a ½”round hole arch punch.
9	Latex paint, high-gloss	S-2	Painted on Gypsum-A; painted paper surface only; cut to test size with a ½”round hole arch punch.

No.	Material	Sink test IDs	Preparation and material information
10	Latex paint, eggshell	1,3	Painted on Gypsum-A (S-1) and painted on Gypsum-B (S-3); painted paper surface only; cut to test size with a ½”round hole arch punch.
11	Epoxy coating, solvent free	2	Used as a protective lining for secondary containment structures. Painted on Gypsum-A; painted paper surface only; cut to test size with a ½”round hole arch punch.
12	Epoxy coating, polyamide	2	Designed to protect metal, concrete, and marine applications; painted on Gypsum-A; painted paper surface only; cut to test size with a ½”round hole arch punch.
13	Carpet A	2	1333/Windwalker/natural grain-textured cut pile; carpet with backing; cut to size with scissors.
14	Carpet B	3	Birdhouse 12' width, used in schools and offices; carpet with backing; cut to size with scissors.
15	Vinyl flooring B	2	Used for kitchen and bath indoor flooring; cut to test size with a ½”round hole arch punch.
16	Oak flooring, pre-finished	2	Solid oak flooring with a factory varnish finish; cut to size with a General No. S31 ½” drill fitted plug cutter.
17	Laminate flooring	2	Floating snap together laminate flooring; cut to size with a General No. S31 ½” drill fitted plug cutter.
18	Painted metal	3	Acquired from disassembled file cabinet at EPA; cut to size with hydraulic metal punch.
19	Medium density fiberboard	3	Substrate backing for Formica countertop material; cut to size with a General No. S31 ½” drill fitted plug cutter.
20	Plastic laminate countertop	3	Purchased as a backsplash kit from Lowes Home Improvement; cut to size with a General No. S31 ½” drill fitted plug cutter.
21	Vinyl flooring A	1	Stone pattern vinyl for residential use only; cut to test size with a ½”round hole arch punch.

Each test material for sink tests S-1, S-2, and S-3 was mounted on aluminum pin mounts (18-mm diameter mounting surface × 8-mm pin height, part # 16119, Ted Pella, Inc., Redding, CA) with double-sided tape. The mounted materials were then placed on a custom-made 10-cm-diameter, aluminum, pin-mounted support block, referred to as “the stage” (Figure 4.4). The stages had positions for 7 to 12 pin mounts, dependent on the data needs of the test. During a test, the sample “buttons” were removed from the chamber at different exposure times. The samples were placed in 20-mL scintillation vials and extracted by the hexane/sonication extraction method and analyzed by gas chromatography/mass spectrometry (GC/MS) as detailed in Guo et al. (2011). A set of unexposed samples was prepared for each material to establish background conditions. Table 4.3 provides the sample numbers of each material collected at each sampling point and the scheduled elapsed time from the start of the test for the sampling point(s) for each test.

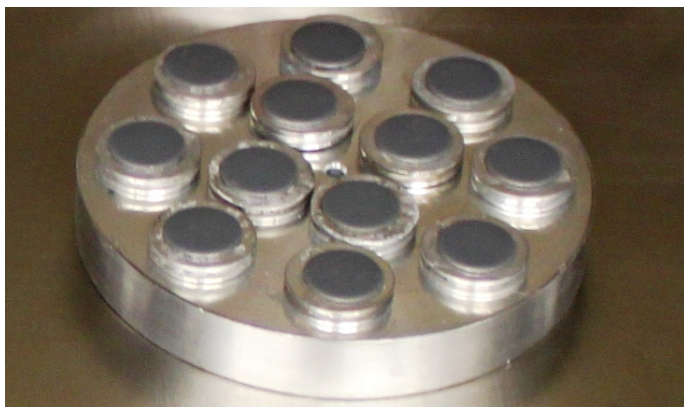


**Figure 4.4. Stage with 12 pin mounts for Test S-3**

**Table 4.3. Sample sets of each material collected at specified sampling points**

Test ID	Number of materials	Number of sampling points	Elapsed times for sampling (h)	Number of “buttons” for each sample
S-1	7	1	169	7
S-2	9	3	98, 173, and 269	3
S-3	12	6	75, 171, 240, 338, 412, and 507	2

Prior to each test, the test chamber was cleaned by wiping all interior surfaces with isopropyl alcohol wipes (Walgreens, Deerfield, IL) followed by washing with water containing detergent. An inlet air flow was set to achieve 1 ACH at 23 °C and 50% RH. An empty-chamber background PUF sample was collected overnight at a sampling flow rate of approximately 600 mL/min for 16 hr. After the empty-chamber background samples were removed, 12 stages containing the sink materials were placed in the test chamber in an arrangement that was three rows deep and four rows wide. Figures 4.5 and 4.6 show the placement of each sink material for tests S-2 and S-3. An overnight PUF was collected to determine the background of the sink materials.

A PUF sample was collected from the effluent of the source chamber to determine the initial dosing concentration. After the background PUF sample for the materials was removed, the effluent from the source chamber was directed to the inlet of the test chamber to start the test (time zero). PUF samples were collected at the outlet of the test chamber at scheduled times for all three sink tests.

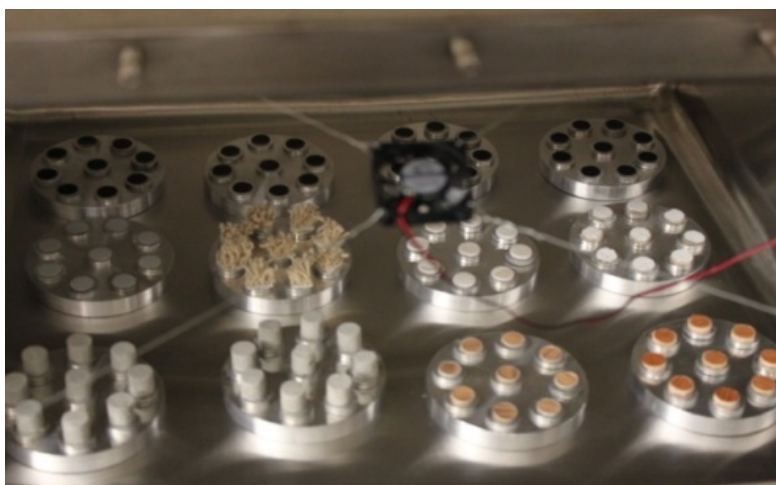


**Figure 4.5. Twelve support blocks with sink materials for Test S-2**



**Figure 4.6. Twelve support blocks with sink materials for Test S-3**

The test chamber was exposed to PCBs for at least 75 hours prior to the removal of the first set of samples (Table 4.3). The sample removal procedure involved redirecting the source chamber effluent back to the source chamber exhaust manifold. The test chamber was then sealed and relocated to a nearby fume hood. The test chamber was opened and the specified number of sample “buttons” removed from each stage. The buttons for each material were placed in a single, labeled, pre-weighed scintillation vial for hexane/sonication extraction and analysis. After a set of each material was collected, the chamber was resealed and returned to the incubator. The source effluent was reconnected and the PCB exposure continued for approximately 96 hours until the next samples were collected. This process was repeated until all of the sample “buttons” were collected. Each chamber-opening event lasted for approximately 5 minutes. Because the sampling interval was rather long (75 to 96 hours), the decrease of PCB concentrations in the chamber air due to the opening had little effect on the time-averaged PCB concentrations in chamber air. Because the re-emission of PCBs from the sink material is very slow (See Section 6.2.3 below), the PCB loss from the sample buttons during the transport from the chamber to the extraction vials should be minimal.

#### 4.1.3.3 Procedure for Sink Test S-4 with Concrete

Sink test S-4 was designed to observe the re-emissions from the sink material after being exposed to PCBs. The test was performed with a single sink material – concrete. This material was selected because it is one of the most common interior surface materials in school buildings. The concrete was molded to a nominal size of 15 cm by 15 cm by 0.8 cm. Stainless steel wire was used to suspend six panels between the air manifolds in the chamber (Figure 4.7). The chamber loading (i.e., the area of the material divided by the volume of the chamber) was  $5.8 \text{ m}^2/\text{m}^3$ .

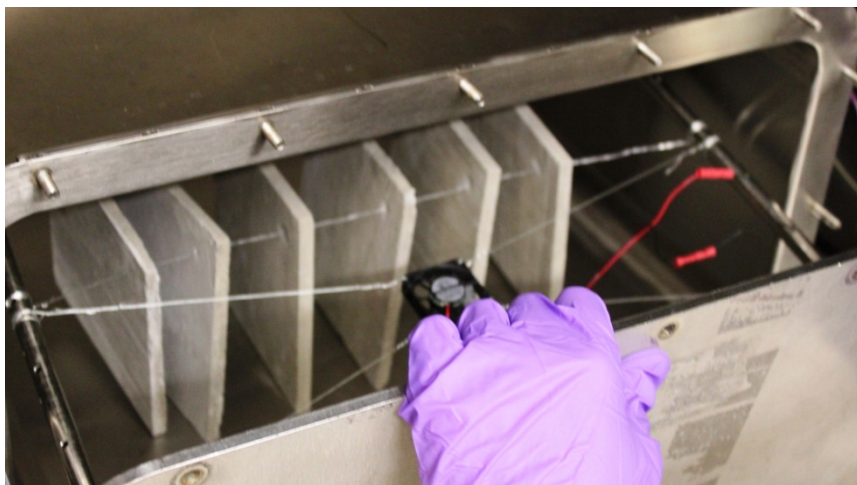


**Figure 4.7. Concrete panel placement in Test S-4**

In addition to the concrete panels, four concrete buttons were prepared using the same concrete. These buttons were placed in a custom-made cage (Figure 4.8.), which was inserted into the chamber through a hole in the wall of the chamber, and the cage was held in place with air-tight fittings. This device allowed concrete buttons to be removed from the chamber for the determination of PCB content at the end of the dosing period with minimal disruption to the air concentration in the chamber.



**Figure 4.8. The cage that held the concrete buttons**

The concrete panels and the concrete buttons were installed into the cleaned chamber. The areas and weights of these materials are present in Appendix B of this document. The loaded chamber was placed in the incubator and a clean air source connected to the inlet. A single PUF sample was collected from the effluent of the source chamber overnight at a sampling flow rate of approximately 600 mL/min for 16 hours to determine the initial PCB exposure concentration and duplicate PUF samples were collected overnight at a



sampling flow rate of approximately 300 mL/min for 16 hours from the effluent of the test chamber to determine baseline background concentrations. A 100 mL/min vacuum flow was attached to the inlet manifold of the materials chamber. During the PCB exposure period, PUF samples were collected at the inlet during the same sampling points as the outlet samples. After the background samples were removed, the clean air source was disconnected from the test chamber and the effluent from the source chamber was connected to the test chamber inlet. Inlet and outlet PUF samples were collected at timed intervals for the 167-hour PCB dosing period. At 167 hours two of the concrete buttons were removed from the holder and placed in a labeled and pre-weighed scintillation vial for future hexane/sonication extraction and analysis. The PCB source was disconnected from the inlet of the test chamber and replaced with the conditioned clean air source.

PUF samples were collected immediately from the outlet of the test chamber to determine the decay in PCB Aroclor 1254 concentration in the chamber. Chamber air samples continued to be collected for the following 140 hour decay period.

#### **4.1.3.4 Chamber Air Sampling**

Air samples were collected onto PUF sampling cartridge (pre-clean certified, Supelco, St. Louis, MO) by using a mass flow controller and a vacuum pump. The sampling flow rate was set by the mass flow controller and measured frequently by using the Gilibrator<sup>TM</sup> air flow calibrator (Scientific Instrument Services, Ringoes, NJ) before and after each sampling period. After collection, the glass holder with the sample inside was wrapped in a sheet of aluminum foil, placed in a sealable plastic bag, and stored in the refrigerator at 4 °C until extracted by the EPA Soxhlet Method 8082A (U.S. EPA, 2007) as discussed in Section 4.4.3.

### **4.2 Testing of Settled Dust**

#### **4.2.1 *Test Specimens***

Two types of dust were tested, i.e. house dust and Arizona Test Dust (ATD). The house dust was obtained from EPA's National Exposure Research Laboratory. The dust sample was collected from the vacuum cleaner bags from a local housekeeping service company in Research Triangle Park, North Carolina. The dust was sieved to <150 µm to remove large objects. The Arizona Test Dust (0 to 10 µm nominal diameters, Powder Technology, Inc., Burnsville, MN) was a test dust made from Arizona sand. It was included in the tests for evaluating the effect of the composition of the dust on PCB transfer. The microscopic images of the two dust samples are shown in Figures 4.9 through 4.12. Their physical and chemical properties are summarized in Table 4.4.

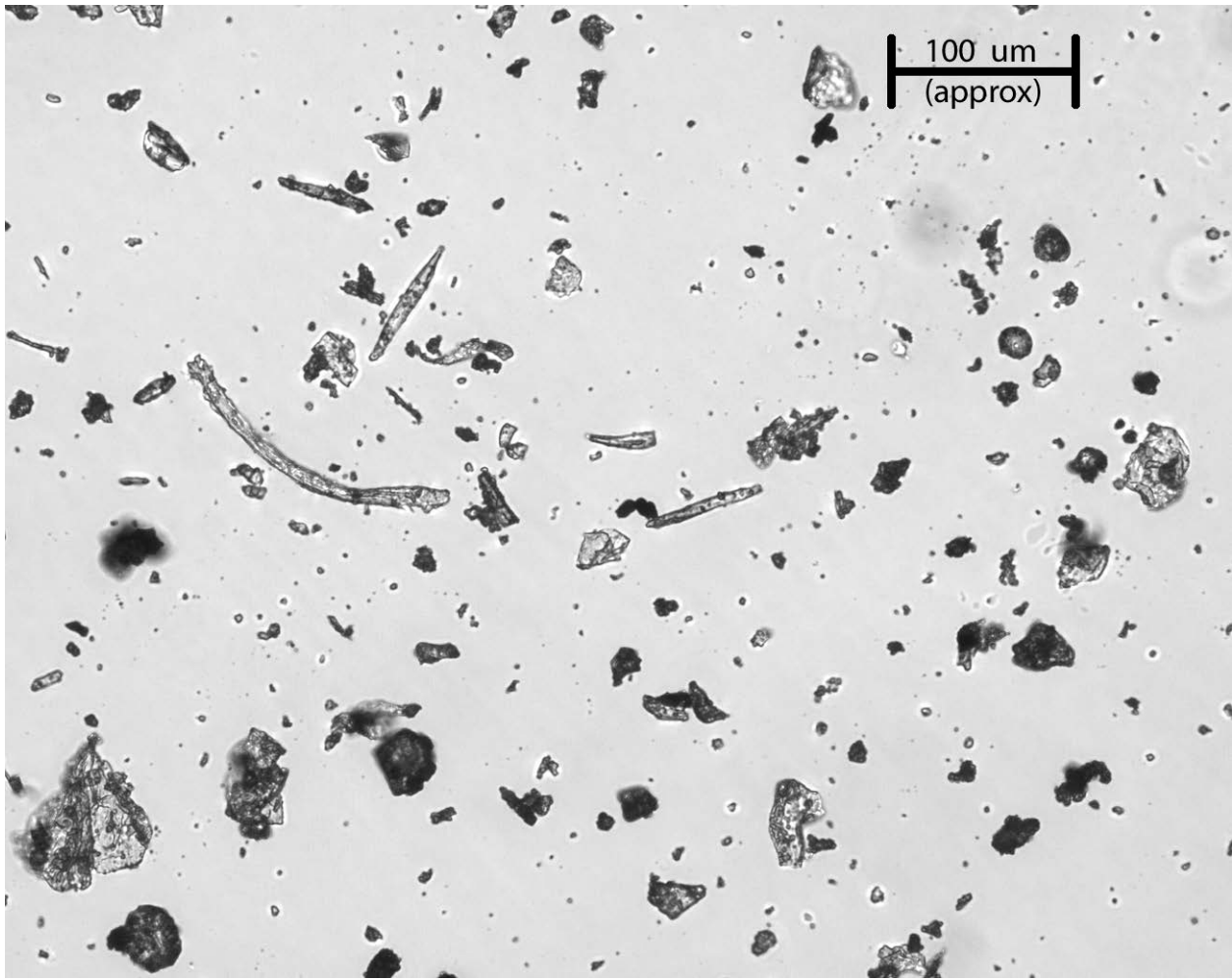


**Figure 4.9.** Optical microscopic image for the house dust that was tested



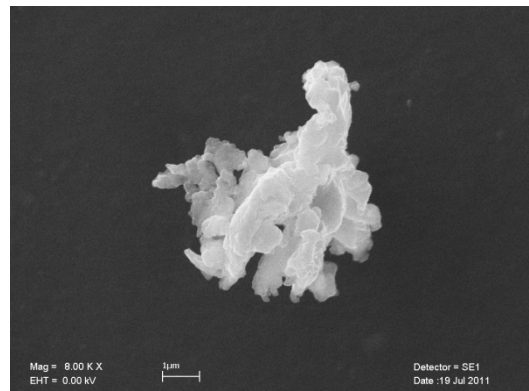
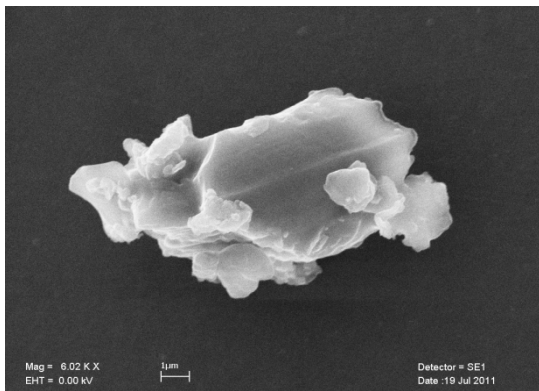
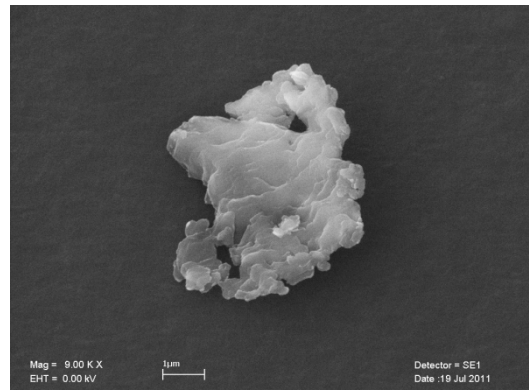
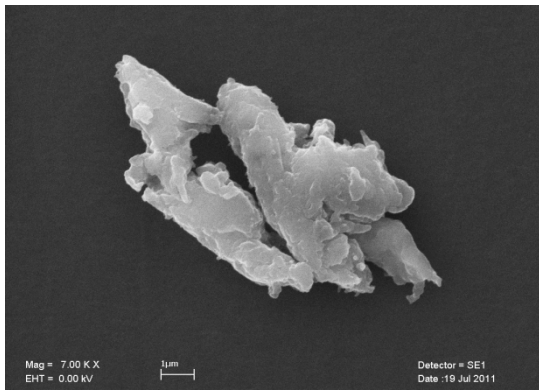


**Figure 4.10. Scanning electron microscope images of individual house dust particles  
(The scale is 1 μm)**

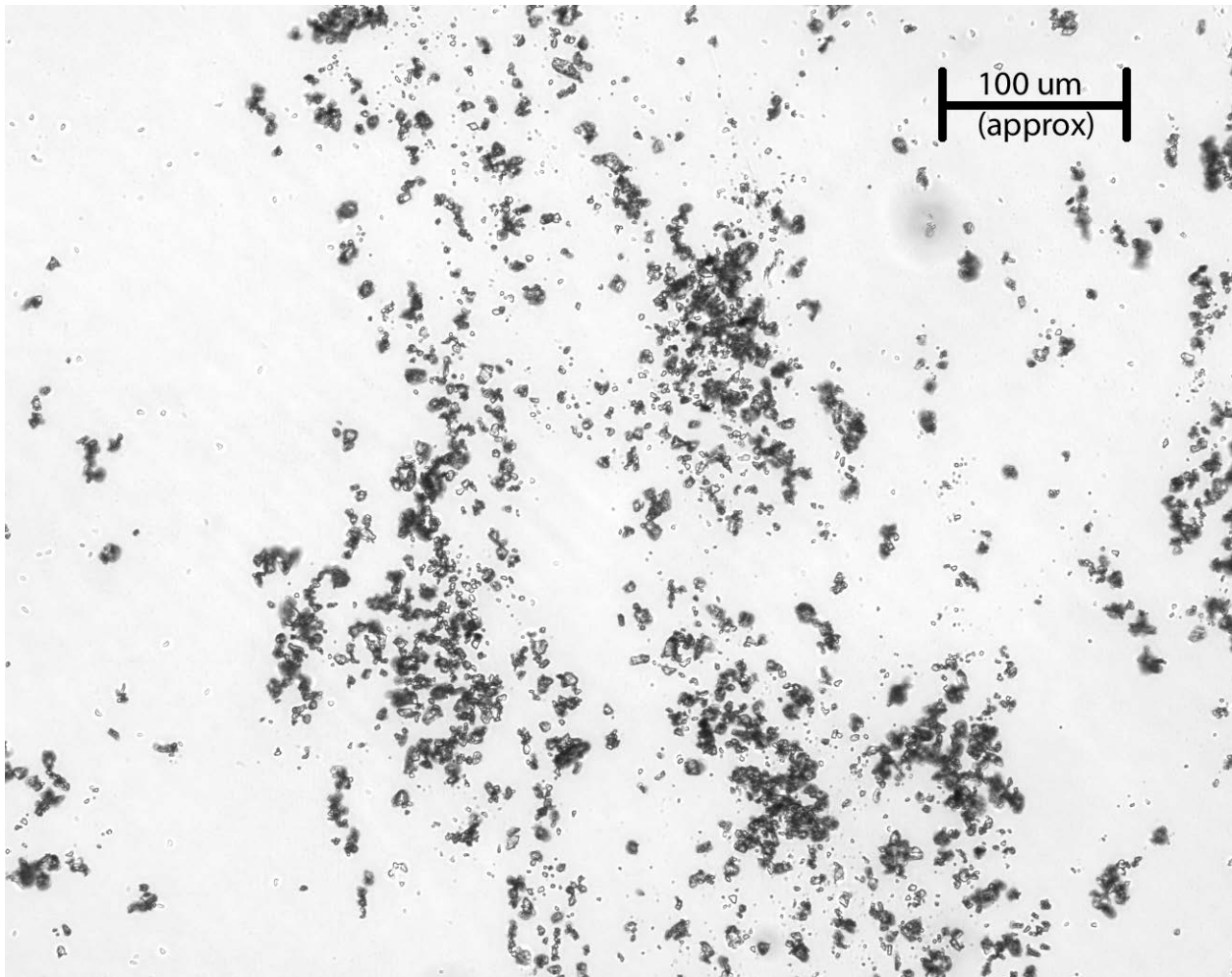


**Figure 4.11. Optical microscopic image of Arizona Test Dust**

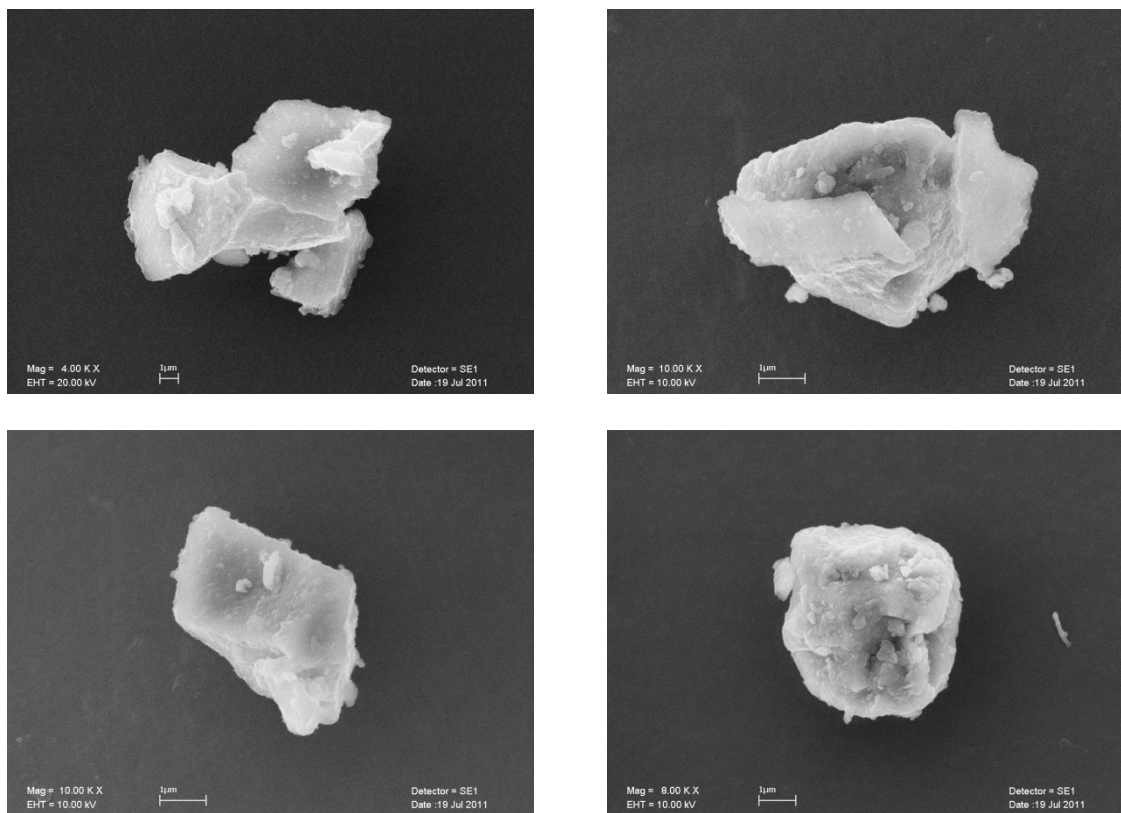


**Figure 4.12.** Scanning electron microscope images of individual ATD particles (The scale is 1 μm)

**Table 4.4. Selected properties of the two dust samples that were tested**

Property		Dust Type	
		House dust	ATD
Weight by volume <sup>[a]</sup>	g/mL	0.589 ± 0.027	0.842 ± 0.033
Surface area <sup>[b, c]</sup>	m <sup>2</sup> /g	0.629 ± 0.03	5.22 ± 0.26
Particle size — mean <sup>[b, d]</sup>	μm	78.3 ± 1.47	4.28 ± 0.012
Particle size — range <sup>[b, e]</sup>	μm	5 to 180	0.5 to 10
Total carbon <sup>[b, f]</sup>	% (w/w)	23.8 ± 1.2	0.49 ± 0.00
Organic carbon <sup>[b, g]</sup>	% (w/w)	19.3 ± 1.1	0.45 ± 0.11

<sup>[a]</sup> Arithmetic mean ± standard deviation (SD) (n=2); measured at room temperature by gravimetric method.

<sup>[b]</sup> Analyzed by a commercial analytical laboratory.

<sup>[c]</sup> Arithmetic mean ± SD (n=2); method: Brunauer-Emmett-Teller (BET) method with N<sub>2</sub>.

<sup>[d]</sup> Weighted mean value ± SD (n=2); method: light scattering (ISO 13320).

<sup>[e]</sup> Method: light scattering (ISO 13320).

<sup>[f]</sup> Arithmetic mean ± SD (n=2); method: pyrolysis.

<sup>[g]</sup> Arithmetic mean ± SD (n=4); method: EPA Method 9060A.

#### 4.2.2 Test Facility

One compartment of a two-compartment chamber (TCC) system was used to study the transport of PCBs to settled dust. The TCC consisted of two adjoining compartments, an air distribution system, a process control and monitoring system, and contaminant generation and sampling systems. Each of the compartments was 3.66 m wide, 3.05 m deep, and 2.74 m high. Each compartment had leak-tight penetrations to accommodate entry, electrical power, environmental sensors, instrument sampling and media injection. A centrally-mounted ceiling fan ensured homogenous mixing of the air. The chamber and associated systems were constructed of nonemitting and nonshedding materials such as stainless steel and PTFE. A partition with openings sized for installation of commercially-available building components such as windows and doors (test specimens) separated the two compartments. Openings not fitted with test specimens were sealed using stainless steel cover plates. The chamber was designed to operate as a single unit or as two stand-alone units (Figure 4.13).

The air distribution system cleaned and distributed air throughout the chamber (Figure 4.14). An ultra-low particulate air (ULPA) filter and carbon bed provided air to the chamber that was free of particulate matter and VOCs. Multiple airflow configurations were achieved by pushing or pulling air through the chamber using variable rate blowers (Hitachi SJ300 Voltage/Frequency Drive, FUJI VFC400A-7W Regenerative Blower). Modes of air flow included single-pass or continuous circulation, either between compartments or within compartments. Air flow was calculated by measuring pressure drop across an orifice plate (Flow-Lin, Arlington, TX) using a Veltron DPT-plus differential pressure transmitter (Air Monitor Corp., Santa Rosa, CA). Flow rates from 0.5 to 40 cfm (0.85 to 68 m<sup>3</sup>/h) were generated to produce chamber air exchange rates between 0.03 and 2.2 air changes per hour (ACH).



**Figure 4.13. Two-Compartment Chamber System (The compartment on the left was used for this study)**

An integrated, programmable control system (OPTO 22, Temecula, CA) was used to control the air flow, and to monitor and record the operating parameters. Compartment pressures were monitored using Veltron Series II differential pressure transmitters; temperature and humidity transmitters (HyCal, Model HCT-839R-806-L) monitored each compartment and the chamber's surrounding environment (i.e., building space); pressure, temperature and humidity were not controlled. Pressure differentials, temperature and humidity vary seasonally, and the ambient conditions had typical ranges of 0-25 Pa,  $20 \pm 5$  °C, 50% RH  $\pm$  20% RH, respectively.

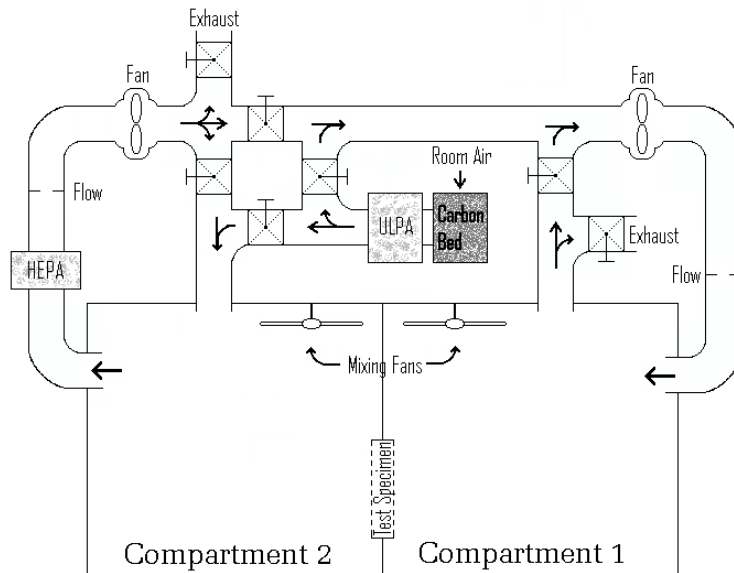


**Figure 4.14. Schematic of the Two-Compartment Chamber System**

For this study, Compartment 2 was isolated and operated in the single-pass mode (i.e., no air re-circulation). Air flow was pulled through the compartment from the filter/carbon bed and exhausted to the building's ventilation system. Mylar<sup>®</sup> film was installed over the existing test specimen of the partition to minimize exposure to the specimen's rough surface and to minimize contamination to or from the test specimen. The flow rate setting varied from test to test, i.e., from 2 to 15 cfm (approximately 0.11 to 0.85 ACH). The ceiling fan was operated at 50 % capacity to mix the air in the compartment uniformly. Flow rate, temperature, humidity, and pressure data were recorded continuously during the tests.

#### *4.2.3 Test Procedure*

##### 4.2.3.1 Preparation of Test Panels

The base of the test panels was an aluminum sheet (25 cm × 25 cm × 0.028 cm). Two types of panels were prepared, i.e., the source panels and the reference panels. The source panels were coated with a PCB-spiked, oil-based primer (Sherwin-Williams) or two-part polysulfide caulk (THIOLKOL 2235M Industrial Polysulfide Joint Sealant, PolySpec, Huston, TX). The reference panels were coated with the same materials but they were not spiked with PCBs.

To add PCBs to the primer, a calculated amount of PCBs (Aroclor 1254 or 1242) was mixed with the primer in a glass vial. Then, the vial was sealed and shaken in a paint shaker (Red Devil 5400, Red Devil Equipment Co., Plymouth, MN) for 15 minutes. To add PCBs to the polysulfide caulk, calculated amount of PCBs was added to the activator (Part B), which was then added to the resin (Part A). The two parts were mixed manually with a 2.54-cm-wide steel utility spatula for approximately five minutes.

Before painting, a 21-cm circle was cut from a sheet of adhesive paper (3M<sup>™</sup> Permanent-Adhesive Shipping Labels). Then, the aluminum panel was covered with the adhesive paper and taped down with painter tape (Figure 4.15). The panels were placed in the ventilated hood for painting with an air-brush (model # 175-7, Badger Air-Brush Co., Franklin Park, IL). The panels were cured in the hood for five days before being placed in the test chamber. A steel utility spatula (25 cm wide) was used to apply the polysulfide sealant to the panels.

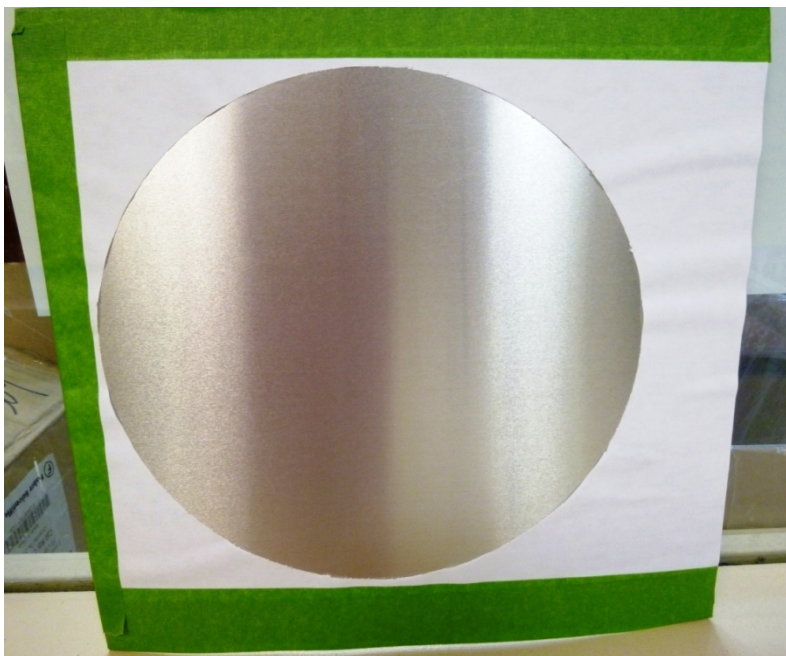


**Figure 4.15. Aluminum sheet covered by white shipping label with a 21-cm circle cutout**

#### 4.2.3.2 Loading Dust to Test Panels

The procedure for loading the dust on the test panels was as follows:

- For the standard dust loading (1 g of dust per panel), weigh  $1.000 \pm 0.005$  g of dust by using a tared aluminum weigh boat; other dust loadings of 0.25, 0.5, and 2 g per panel were also tested.
- Place a No. 100 sieve on the test panel; make certain that the sieve is aligned with the perimeter of the painted circle (Figure 4.16).
- Use a spatula with a spooned end to spread the dust evenly on the mesh of the sieve.
- Use a 2.54-cm wide foam paint brush to push the dust in a circular motion until all of the dust passes through the sieve.
- Lift the sieve slowly.

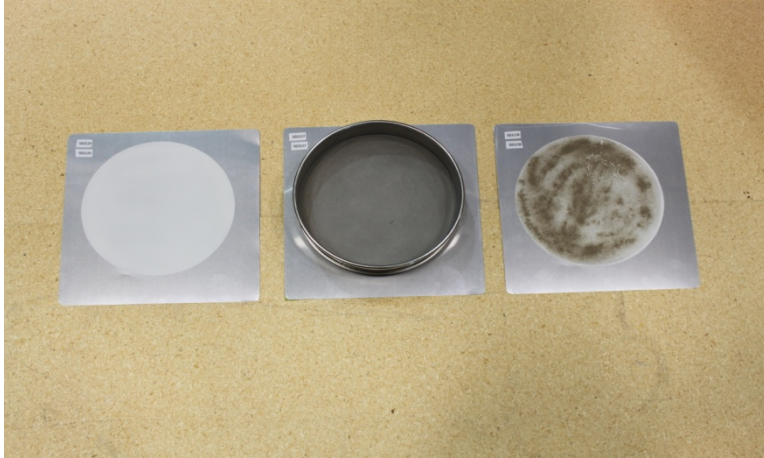


**Figure 4.16. Loading dust to test panels (from left to right: before loading the dust, with the painted area covered by the sieve, and after loading the dust)**

#### 4.2.3.3 Chamber Testing

Four tests were conducted for settled dust, i.e., D-1 through D-4. To start a test:

- Take an overnight air sample with the PUF sampler prior to the test.
- Set the chamber air flow rate (approximately 3.4 m<sup>3</sup>/h for tests D-1 and D-2, 25 m<sup>3</sup>/h for test D-3, and 8.5 m<sup>3</sup>/h for test D-4).
- Set the ceiling fan speed at 50% of the full power.
- Open the chamber door.
- Place the test panels on the floor of the chamber (Figure 4.17).
- Close the chamber door.
- Record the time when the test starts.



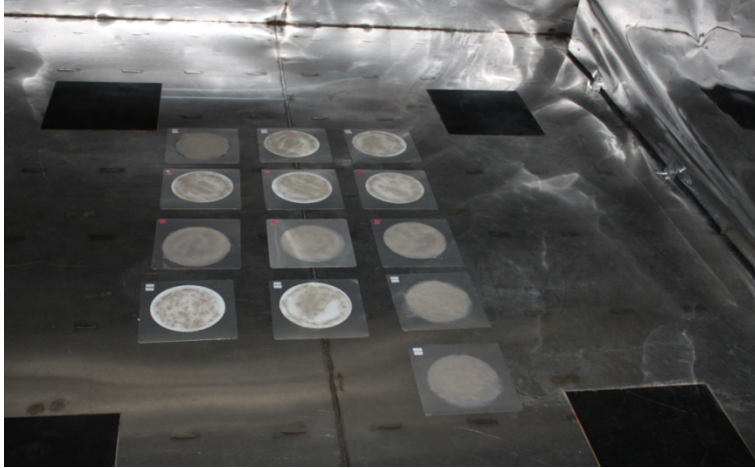


**Figure 4.17. Test panels placed on the chamber floor**

To remove test panels from the chamber:

- Take an overnight air sample with the PUF sampler prior to opening the chamber door.
- Open the chamber door.
- Record the time.
- Move the panels from the center nearer the door for easy access (This takes about one minute).
- Take one panel out of the chamber for dust collection.
- Close the chamber door.
- Repeat the last two steps until all dust samples have been collected for the given sampling point.

#### 4.2.3.4 Collecting Dust from Test Panels

For safety, dust collection was performed in a portable fume hood near the test chamber. The procedure was as follows:

- Place a piece of aluminum foil (roughly 30 cm × 30 cm) on the table.
- Place a centrifuge tube holder on the aluminum foil (Figure 4.18).
- Place a 20-mL scintillation vial in the tube holder (Figure 4.18).

- Fold the test panel to form a U shape (Figure 4.19).
- Hold the folded test panel with one hand and use a spatula to tap the outside of the folder panel to allow the dust to settle on the bottom of the U-shaped panel (Figure 4.20).
- To collect the dust into the scintillation vial, tilt the folded panel to about 45° to allow the dust to “flow” into the scintillation vial (Figure 4.21); tap the panel lightly with a spatula if necessary.



**Figure 4.18. Securing the scintillation vial with a centrifuge tube holder**

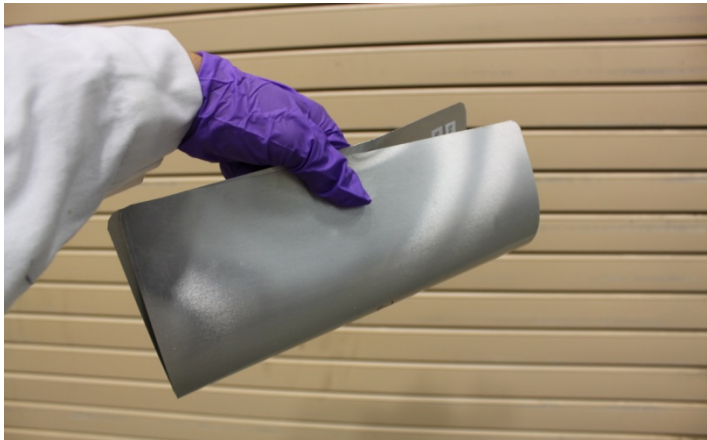


**Figure 4.19. Test panel folded into a U shape**

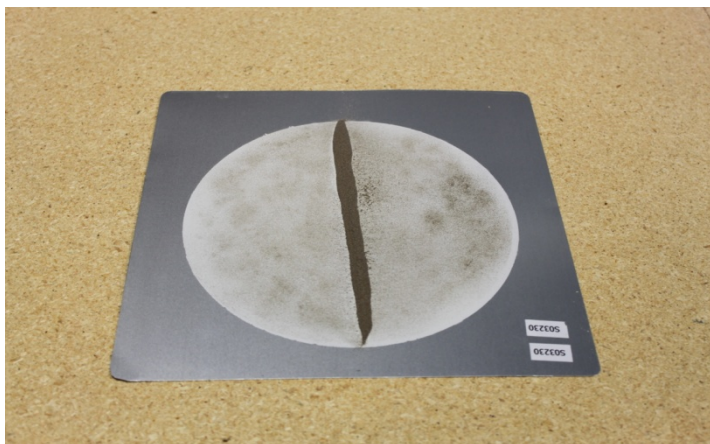


**Figure 4.20.** Test panel after folding and tapping. The dust formed a line along the bottom of the folded panel

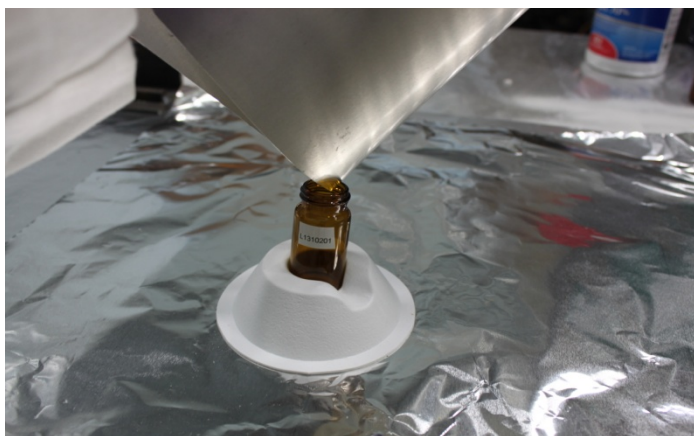


**Figure 4.21.** Dust being transferred to the scintillation vial

For the dust applied on the primer surfaces, the average collection efficiency was 73%. For panels covered with caulk, the collection efficiency was lower because of the sticky surfaces, averaging 52%. It was not required to collect 100% of the dust from panels, because the PCB content in the dust was expressed on a weight of PCB/weight of dust basis (i.e.,  $\mu\text{g PCB/g dust}$ ).

### **4.3 Testing of PCB Sorption by the Walls of the Test Chambers**

#### *4.3.1 Background and Significance*

When a PCB source is tested for emissions in an environmental chamber, the interior walls of the chamber may act as a PCB sink, resulting in lower concentrations in the air inside the chamber. Thus, sorption by the walls of the chamber can be an error source for emissions testing. To evaluate the magnitude of this potential error source, the two types of chambers that were used to test the primary PCB sources (Guo et al., 2011), i.e., the 44-mL microchambers for testing caulk samples (Figure 4.22) and the 53-L chamber for

testing light ballasts (Figure 4.1), were evaluated for the sink effect. While both chambers were made of stainless steel, the surfaces of the microchambers were treated with SilcoSteel<sup>®</sup>, a process for “passivating” active metal surfaces.

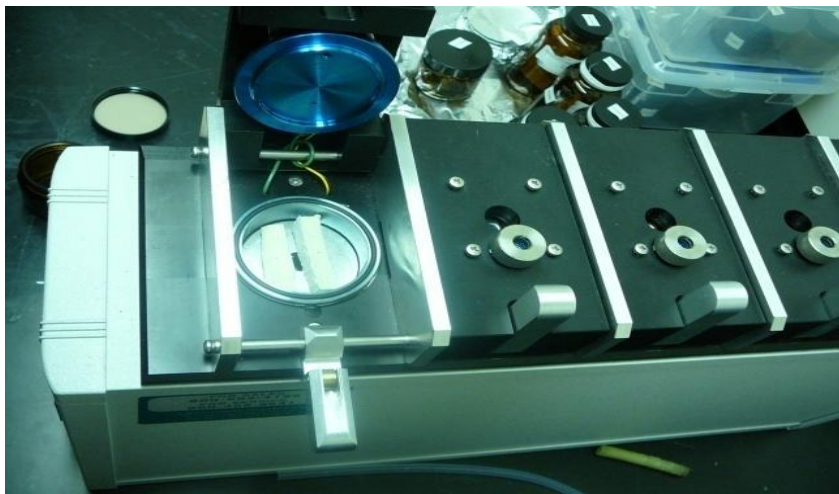


**Figure 4.22. Markes Microchamber/Thermal Extractor (μ-CTE)**

#### *4.3.2 Procedure for Testing the 44-mL Microchambers*

The amounts of PCBs adsorbed by the walls of the chamber were determined by taking wipe samples immediately after the emissions tests. After the caulk sample was removed from the chamber, a wipe sample was collected from the walls of the chamber by using PCB Wipe Sampling Kits (WT-KIT, Dextsil, Hamden, CT) according to the procedure described in ASTM D6661-01 (ASTM, 2006) but without using the wipe template. The area of the interior surfaces of the microchamber was approximately 67 cm<sup>2</sup>. The wipe pad was placed in a 20-mL scintillation vial for extraction by the sonication method followed by GC/MS analysis (See Section 4.3.2).

#### *4.3.3 Procedure for Testing of the 53-Liter Environmental Chamber*

PCB sorption by the interior walls of the 53-L environmental chamber was evaluated by using the two-chamber system described in Section 4.1.2. The test chamber was cleaned by wiping all the interior surfaces with isopropyl alcohol wipes (Walgreens, Deerfield, IL) followed by washing with water containing detergent. The inlet air flow was set to achieve 1 ACH at 23 °C and 50% relative humidity. Prior to the test, a chamber background PUF sample was collected overnight at a sampling flow rate of approximately 600 mL/min for 16 hours. To start the test, the effluent of the source chamber was directed to the inlet of the empty test chamber. PUF air samples were collected from both the inlet and outlet of the test chamber. The amounts of PCBs adsorbed by walls of the chamber were calculated based on the difference of the two air concentrations.

## 4.4 Sample Extraction and Analysis

### 4.4.1 Target Congeners

In this study, 10 target congeners were selected for Aroclor 1254 and 9 for Aroclor 1242 (Table 4.5). These congeners were selected based on the following considerations: (1) inclusion of some predominant components in the Aroclor, (2) inclusion of some predominant components in the emissions (i.e., in the air), (3) inclusion of some dioxin-like congeners, (4) good separation by GC/MS, and (5) coverage of congeners with different chlorine numbers and vapor pressures. The target congeners for Aroclor 1254 were analyzed in all the tests conducted; those for Aroclor 1242 were analyzed only in dust experiment D-4, in which a source of Aroclor 1242 was present.

It is neither necessary nor practical to test each of the 209 PCB congeners because, once the behavior of a handful congeners is understood, the behavior of other congeners can be predicted from quantitative structure-activity relationship (QSAR) models. Appendices D and F include examples of using the QSAR models to predict the sink behavior for non-target congeners.

**Table 4.5. List of target congeners and their selected properties**

Congener #	Short Name	IUPAC Name	CASRN	Cl No.	P <sup>[a]</sup> (torr)	Notes
13	PCB-13	3,4'-Dichlorobiphenyl	2974-90-5	2	$6.24 \times 10^{-4}$	[b]
15	PCB-15	4,4'-Dichlorobiphenyl	2050-68-2	2	$5.82 \times 10^{-4}$	[b]
17	PCB-17	2,2',4'-Trichlorobiphenyl	37680-66-3	3	$5.82 \times 10^{-4}$	[b],[c]
18	PCB-18	2,2',5'-Trichlorobiphenyl	37680-65-2	3	$6.38 \times 10^{-4}$	[b]
22	PCB-22	2,3,4'-Trichlorobiphenyl	38444-85-8	3	$1.97 \times 10^{-4}$	[b]
44	PCB-44	2,2',3,5'-Tetrachlorobiphenyl	41464-39-5	4	$1.14 \times 10^{-4}$	[b]
49	PCB-49	2,2',4,5'-Tetrachlorobiphenyl	41464-40-8	4	$1.36 \times 10^{-4}$	[b]
52	PCB-52	2,2',5,5'-Tetrachlorobiphenyl	35693-99-3	4	$1.50 \times 10^{-4}$	[b],[c]
64	PCB-64	2,3,4',6-Tetrachlorobiphenyl	52663-58-8	4	$1.06 \times 10^{-4}$	[b]
66	PCB-66	2,3',4,4'-Tetrachlorobiphenyl	32598-10-0	4	$4.42 \times 10^{-5}$	[c]
77	PCB-77	3,3',4,4'-Tetrachlorobiphenyl	32598-13-3	4	$1.43 \times 10^{-5}$	[c]
101	PCB-101	2,2',4,5,5'-Pentachlorobiphenyl	37680-73-2	5	$2.99 \times 10^{-5}$	[c]
105	PCB-105	2,3,3',4,4'-Pentachlorobiphenyl	32598-14-4	5	$5.82 \times 10^{-5}$	[c]
110	PCB-110	2,3,3',4',6-Pentachlorobiphenyl	38380-03-9	5	$1.68 \times 10^{-5}$	[c]
118	PCB-118	2,3',4,4',5-Pentachlorobiphenyl	31508-00-6	5	$8.42 \times 10^{-6}$	[c]
154	PCB-154	2,2',4,4',5,6'-Hexachlorobiphenyl	60145-22-4	6	$1.36 \times 10^{-5}$	[c]
187	PCB-187	2,2',3,4',5,5',6-Heptachlorobiphenyl	52663-68-0	7	$2.79 \times 10^{-6}$	[c]

<sup>[a]</sup> Vapor pressure from method B in Fischer et al. (1992).

<sup>[b]</sup> Target congener for Aroclor 1242.

<sup>[c]</sup> Target congener for Aroclor 1254.

#### 4.4.2 Extraction of Solid Samples

Solid samples (i.e., building materials and dust) were extracted by using the sonication method that was used for extracting caulk samples (Guo et al., 2011). The samples were extracted using a sonicator (Ultrasonic Cleaner FS30, Fisher Scientific, Pittsburgh, PA) with 10 mL of hexane (ultra grade or equivalent, Fisher Scientific, Pittsburgh, PA) and approximately 100 mg of sodium sulfate (anhydrous grade or equivalent, Fisher Scientific, Pittsburgh, PA) for 30 min in a scintillation vial. Before extraction, 100  $\mu$ L of the 5 ng/mL recovery check standards, including 2,4,5,6-tetrachloro-*m*-xylene (TMX),  $^{13}\text{C}$ -PCB-77, and  $^{13}\text{C}$ -PCB-206, were added to the extraction solution. After extraction, 990  $\mu$ L of the extract was placed in a 1-mL volumetric flask containing 10  $\mu$ L of 10- $\mu$ g/mL internal standards, including  $^{13}\text{C}$ -PCB-4,  $^{13}\text{C}$ -PCB-52 and  $^{13}\text{C}$ -PCB-194, and then transferred to GC vials for analysis. The final concentrations of each recovery check standard and each internal standard were 50 ng/mL and 100 ng/mL, respectively.

The sonication method was chosen for solid samples because (1) Its extraction efficiency is as good as the Soxhlet method (Guo et al., 2011); (2) It involves fewer steps than the Soxhlet method and, thus, reduces the chance of sample loss; (3) It consumes much less solvent. As a disadvantage, this method cannot extract large samples such as PUF samples.

#### 4.4.3 Extraction of Air Samples

PUF samples were extracted using Soxhlet systems by following EPA Method 8082A (U.S. EPA, 2007). The PUF samples were placed in individual Soxhlet extractors with about 250 mL of hexane. Fifty microliters of recovery check standards (concentration of 5  $\mu$ g/mL) were spiked onto the PUF samples inside the Soxhlet extractor. The samples were extracted for 16 to 24 h. The extract was concentrated to about 50 to 75 mL using a Snyder column. Then the concentrated solution was filtered through anhydrous sodium sulfate into a 100-mL borosilicate glass tube and further concentrated to about 1 mL using a RapidVap N2 Evaporation System (Model 791000, LabConco, MO). The 1-mL solution was cleaned up with sulfuric acid (certified plus grade or equivalent, Fisher, Pittsburgh, PA) and brought up to 5 mL with the rinse solution (i.e., hexane for rinsing the concentration tube) in a 5 mL volumetric flask. One milliliter of the 5-mL solution was separated and 10  $\mu$ L of 10-ng/ $\mu$ L internal standards were added, after which the extract was transferred to GC vials for analysis by GC/MS. The final concentrations of each recovery check standard and each internal standard were 50 ng/mL and 100 ng/mL, respectively.

#### 4.4.4 Sample Analysis

The analytical method used for this project was a modification of EPA Method 8082A (U.S. EPA, 2007) and EPA Method 1668B (U.S. EPA, 2008a). The procedures are detailed in Part 1 of this report series (Guo et al., 2011).



## 5. Quality Assurance and Quality Control

Quality assurance (QA) and quality control (QC) procedures were implemented in this project by following guidelines and procedures detailed in the approved Category II Quality Assurance Project Plan (QAPP), *Polychlorinated Biphenyls (PCBs) in Caulk: Source Characterization to Support Exposure/Risk Assessment for PCBs in Schools*. Quality control samples consisted of background samples collected prior to the test, field blanks, spiked field controls, and duplicates. Daily calibration check samples were analyzed on each instrument on each day the analyses were conducted. More information is presented in Part 1 of this report series (Guo et al., 2011). Results of QA/QC activities that are specific to this study are described in the following subsections.

### 5.1 GC/MS Instrument Calibration

The GC/MS calibration and quantitation of PCBs were performed by using the relative response factor (RRF) method based on peak areas of extracted ion current profiles for target analytes relative to those of the internal standard. The calibration standards were prepared at six levels ranging from approximately 5 to 200 ng/mL in hexane. Three internal standards were added in each standard solution for different PCB congeners. The calibration curve was obtained by injecting 1  $\mu$ L of the prepared standards in triplicate at each concentration level. Tables 5.1 and 5.2 summarize all GC/MS calibrations conducted for the project, including the practical quantification limit (PQL, i.e., the lowest calibration concentration) and the highest calibration concentration. The percentage relative standard deviation (RSD) of the average RRF meets the DQI goal of 25%.

The Internal Audit Program (IAP) was implemented to minimize the systematic errors. Prepared by personnel other than the analyst, the IAP standards contained three calibrated PCB congeners, and were analyzed after the calibration was completed. The IAP standards were purchased from a supplier (ChemService, West Chester, PA) that was different from the supplier for the calibration standards, and their concentrations of PCB congeners were certified.

Table 5.3 presents the results of the IAP standards analyzed for each calibration. The recoveries of IAP ranged from 76% to 116% and percentage of RSDs ranged from 0.13% to 3.79%. They all met the criteria for IAP analysis, which are  $100 \pm 25\%$  recovery with percentages of RSD from triplicate analyses within 25%.

### 5.2 Detection Limits

After each calibration, the lowest calibration standard was analyzed seven times and the instrument detection limit (IDL) was determined from three times the standard deviations of the measured concentrations of the standard. The IDLs for all calibrated PCB congeners are listed in Table 5.4. The detection limits for the sonication method are presented in Table 5.5. The detection limits for the Soxhlet method were reported in the report entitled *Laboratory Study of Polychlorinated Biphenyl (PCB) Contamination and Mitigation in Buildings, Part 1. Characterization of Selected Primary Sources* (Guo et al., 2011).

**Table 5.1. GC/MS calibration for PCB congeners from Aroclor 1254 <sup>[a]</sup>**

Date	08/06/2010		10/12/2010		2/14/2011		6/20/2011		7/18/2011		PQL (ng/mL)	Hi Cal (ng/mL)
Analytes	RRF	%RSD	RRF	%RSD	RRF	%RSD	RRF	%RSD	RRF	%RSD		
PCB-17	1.07	7.61	0.90	9.37	0.69	6.14	0.67	5.96	0.84	6.64	5.00	200
PCB-52	1.56	6.30	1.23	8.22	1.05	3.53	0.94	5.07	1.11	5.19	5.01	200
PCB-101	1.28	9.09	1.18	7.48	0.90	7.86	0.77	8.15	0.98	7.88	5.01	200
PCB-154	1.41	14.84	1.20	8.19	0.90	7.80	0.72	8.66	0.94	7.37	4.98	199
PCB-110	1.58	11.07	1.52	7.83	1.18	12.1	0.99	13.28	1.25	9.85	5.01	200
PCB-77	1.34	23.97	1.54	11.93	1.21	19.0	1.14	18.59	1.39	14.31	5.01	200
PCB-66	1.39	11.75	1.40	8.24	1.07	7.22	1.10	8.26	1.39	8.64	5.03	201
PCB-118	1.27	14.78	1.42	7.96	1.03	10.9	0.89	11.19	1.31	11.17	5.05	202
PCB-105	1.12	15.84	1.32	8.44	0.95	11.0	0.81	11.46	1.07	10.14	5.00	200
PCB-187	0.83	13.12	0.93	8.54	0.68	9.78	0.51	11.40	0.70	9.00	4.98	199
TMX (RCS)	0.62	4.21	0.40	5.89	0.40	4.11	0.36	5.32	0.46	7.51	5.01	200
<sup>13</sup> C-PCB-77 (RCS)	1.30	24.89	1.15	15.54	1.12	16.7	0.95	16.77	1.20	15.50	5.00	200
<sup>13</sup> C-PCB-206 (RCS)	1.61	12.81	1.01	7.42	1.08	11.5	0.84	13.43	1.03	14.15	5.00	200

<sup>[a]</sup> The Data Quality Indicator (DQI) goal for %RSD was 25%.



**Table 5.2. GC/MS calibration for PCB congeners from Aroclors 1242 and 1248**

Date	5/10/2011		6/3/2011		PQL (ng/mL)	Hi Cal (ng/mL)
Analytes	RRF	%RSD	RRF	%RSD		
PCB-13	0.80	15.00	1.36	7.92	5.03	201
PCB-18	0.61	5.27	0.64	3.87	5.03	201
PCB-17	0.65	10.05	0.73	10.42	5.00	200
PCB-15	0.76	14.28	1.35	9.93	5.03	201
PCB-22	0.66	8.19	0.84	5.21	4.95	198
PCB-52	0.97	6.05	0.99	6.04	5.01	200
PCB-49	1.03	6.83	1.06	8.33	5.02	201
PCB-44	0.81	7.83	0.80	6.95	4.98	199
PCB-64	1.28	6.66	1.28	7.98	4.98	199
TMX (RCS)	0.42	4.94	0.40	5.34	5.01	201
<sup>13</sup> C-PCB-77 (RCS)	0.71	9.01	0.91	7.37	5.00	200
<sup>13</sup> C-PCB-206 (RCS)	0.97	5.91	0.92	14.81	5.00	200

<sup>[a]</sup> The DQI goal for %RSD was 25%.

**Table 5.3. IAP results for each calibration**

<b>Calibration</b>	<b>Analyte</b>	<b>IAP Concentration (ng/mL)</b>	<b>Avg. Recovery %</b>	<b>%RSD (n=3)</b>
8/6/2010	PCB-52	70.80	114	0.46
	PCB-101	69.60	90	1.48
	PCB-77	70.80	93	1.10
10/12/2010	PCB-52	150	92	1.22
	PCB-101	150	86	1.64
	PCB-77	150	80	1.37
2/14/2011	PCB-52	100	104	0.13
	PCB-101	100	94	0.33
	PCB-77	100	80	0.64
5/10/2011	PCB-13	50.0	107	3.24
	PCB-15	50.0	114	2.61
	PCB-44	50.0	108	1.70
6/3/2011	PCB-13	40.0	94	3.79
	PCB-15	40.0	114	3.49
	PCB-44	40.0	108	0.79
6/20/2011	PCB-52	40.0	106	0.42
	PCB-101	40.0	93	0.33
	PCB-77	40.0	76	0.77
7/18/2011	PCB-52	80.0	116	0.38
	PCB-101	80.0	104	1.20
	PCB-77	80.0	94	1.40

<sup>[a]</sup> The DQI goal for %RSD was 25%.

**Table 5.4. Instrument detection limits (IDLs) for PCB congeners on GC/MS (ng/mL)**

For Aroclor 1254						For Aroclors 1242/1248		
Analytes	8/6/2010	10/12/2010	2/14/2011	6/20/2011	7/18/2011	Analytes	5/10/2011	6/3/2011
PCB-17	0.77	0.48	0.69	0.41	0.40	PCB-13	1.39	0.40
PCB-52	0.44	0.44	0.32	0.50	0.26	PCB-18	0.64	0.28
PCB-101	1.01	0.43	0.35	0.39	0.52	PCB-17	1.03	0.74
PCB-154	0.54	0.17	0.47	0.28	0.58	PCB-15	1.20	0.41
PCB-110	0.98	0.25	0.38	0.27	0.45	PCB-22	1.04	0.60
PCB-77	1.17	0.21	0.41	0.25	0.42	PCB-52	0.59	0.27
PCB-66	0.94	0.42	0.13	0.52	0.34	PCB-49	0.79	0.45
PCB-118	1.31	0.35	0.23	0.28	0.47	PCB-44	1.05	0.56
PCB-105	1.72	0.44	0.24	0.34	0.31	PCB-64	0.90	0.42
PCB-187	0.91	0.33	0.26	0.34	0.37	TMX (RCS)	0.96	0.57
TMX (RCS)	0.77	1.05	0.43	0.81	0.34	<sup>13</sup> C-PCB-77 (RCS)	1.77	1.11
<sup>13</sup> C-PCB-77 (RCS)	1.13	0.34	0.21	0.21	0.30	<sup>13</sup> C-PCB-206	1.84	0.98
<sup>13</sup> C-PCB-206 (RCS)	2.50	1.36	0.44	0.80	1.33	--	--	--

**Table 5.5. Method detection limits (MDLs) of the sonication extraction method for PCB congeners on GC/MS<sup>[a]</sup>**

Analytes for Aroclor 1254	MDL (ng/mL)	MDL (ng/sample)
PCB-17	0.50	5.00
PCB-52	0.23	2.34
PCB-101	0.61	6.11
PCB-154	0.33	3.29
PCB-110	0.55	5.48
PCB-77	0.74	7.44
PCB-66	0.36	3.64
PCB-118	0.50	4.95
PCB-105	0.95	9.51
PCB-187	0.35	3.51
TMX (RCS)	1.09	10.9
<sup>13</sup> C-PCB-77 (RCS)	0.99	9.86
<sup>13</sup> C-PCB-206 (RCS)	0.56	5.61

<sup>[a]</sup> Determined by using wipe samples.

### 5.3 Environmental Parameters

The temperature and RH sensors used to measure environmental conditions for the small chamber tests were calibrated in EPA's Metrology Laboratory in July 2010; the sensors used for the dual chamber system were calibrated in November 2009 and March 2011. Environmental data in the small chambers, such as temperature and RH, were recorded by the OPTO 22 data acquisition system (DAS). The air exchange rate of the small chamber was calculated based on the average flow rate of outlet air measured with a Gilibrator at the start and end of each small chamber test. The measurement device was a primary reference method calibrated by EPA's Metrology Laboratory. Measured environmental parameters are presented in Tables 6.3 and 6.6 in Section 6.

### 5.4 Quality Control Samples

Data quality control samples discussed here include background, field blank and duplicate samples. For all the tests, background air samples were collected. A typical background sample showed the contribution of the contamination in the empty chamber, the sampling device, and the clean air supply. The results are summarized in Table 5.6. Concentrations of all PCB congeners detected in the background of the 53-L chamber were below the PQL. Some of the PCB concentrations in dual chamber tests were above the PQL, possibly due to carryover from previous tests. The dual chamber was only flushed with a high flow rate of laboratory air for 48 hours before tests started. For dust tests, it was not required that the PCB concentrations

in the chamber background be below the PQL because the actual air concentrations were used to calculate the normalized sorption concentrations and rates.

Duplicate samples were used to estimate the precision of the sampling and analysis methods. The DQI was  $RSD < 25\%$ . Table 5.7 summarizes the number of duplicates/triplicates analyzed for each test and the number of duplicates/triplicates that failed. The data were not reported when the DQI was not met. Overall, the precision of the sampling and analysis methods was good.

Field blank samples were acquired to determine background contamination on the sampling media due to media preparation, handling, and storage. Field blank samples were handled and stored in the same manner as the samples. The results are presented in Table 5.7. No field blank samples were analyzed for sink test S-4. Field blank data for dust test D-4 and sink test S-3 were not reported due to RCS failure. For the data reported in Table 5.8, the target PCB congener concentrations in the field blank were below PQL for all samples.

On each day of analysis, at least one daily calibration check (DCC) sample was analyzed to document the performance of the instrument. DCC samples were analyzed at the beginning and during the analysis sequence on each day. Table 5.9 and Table 5.10 summarize the average recovery of the DCCs for the tests in the 53-L and 30-m<sup>3</sup> chambers, respectively. The recoveries met the laboratory criterion of 75 to 125% recovery for acceptable performance of the GC/MS instrument.

**Table 5.6. Concentration of PCBs ( $\mu\text{g}/\text{m}^3$ ) in the chamber background<sup>[a]</sup>**

Analyte	Test ID									Analyte	Test ID
	D-1	D-2	D-3	S-1 <sup>b</sup>	S-1 <sup>c</sup>	S-2 <sup>b</sup>	S-2 <sup>c</sup>	S-3	S-4 <sup>b,d</sup>		
PCB-17	<del>0.00</del>	<del>0.00</del>	<del>0.00</del>	<del>0.01</del>	<del>0.01</del>	<del>0.00</del>	<del>0.00</del>	<del>0.01</del>	<del>0.00</del>	PCB-13	<del>0.00</del>
PCB-52	0.01	0.06	0.01	<del>0.00</del>	<del>0.00</del>	<del>0.01</del>	<del>0.01</del>	0.19	0.19	PCB-18	<del>0.00</del>
PCB-101	<del>0.00</del>	0.04	<del>0.00</del>	<del>0.00</del>	<del>0.00</del>	<del>0.01</del>	<del>0.01</del>	<del>0.04</del>	<del>0.05</del>	PCB-17	<del>0.00</del>
PCB-154	<del>0.00</del>	<del>0.00</del>	<del>0.00</del>	<del>0.00</del>	<del>0.00</del>	<del>0.00</del>	<del>0.00</del>	<del>0.00</del>	<del>0.00</del>	PCB-15	<del>0.00</del>
PCB-110	<del>0.00</del>	0.02	<del>0.00</del>	<del>0.00</del>	<del>0.00</del>	<del>0.01</del>	<del>0.01</del>	<del>0.02</del>	<del>0.03</del>	PCB-22	<del>0.00</del>
PCB-77	<del>0.00</del>	<del>0.00</del>	<del>0.00</del>	<del>0.00</del>	<del>0.00</del>	<del>0.00</del>	<del>0.00</del>	<del>0.00</del>	<del>0.00</del>	PCB-52	0.01
PCB-66	<del>0.00</del>	0.01	<del>0.00</del>	<del>0.00</del>	<del>0.00</del>	<del>0.00</del>	<del>0.00</del>	<del>0.01</del>	<del>0.01</del>	PCB-49	<del>0.00</del>
PCB-118	<del>0.00</del>	0.01	<del>0.00</del>	<del>0.00</del>	<del>0.00</del>	<del>0.00</del>	<del>0.00</del>	<del>0.01</del>	<del>0.02</del>	PCB-44	<del>0.00</del>
PCB-105	<del>0.00</del>	<del>0.00</del>	<del>0.00</del>	<del>0.00</del>	<del>0.00</del>	<del>0.00</del>	<del>0.00</del>	<del>0.00</del>	<del>0.01</del>	PCB-64	<del>0.00</del>
PCB-187	<del>0.00</del>	<del>0.00</del>	<del>0.00</del>	<del>0.00</del>	<del>0.00</del>	<del>0.00</del>	<del>0.00</del>	<del>0.00</del>	<del>0.00</del>	—	—

<sup>[a]</sup> Values in strikethrough are below PQL.

<sup>[b]</sup> Empty chamber.

<sup>[c]</sup> Chamber with substrates.

<sup>[d]</sup> Average of duplicates

**Table 5.7. Summary of duplicate samples for tests**

Test ID	Number of duplicates/triplicates	Number of duplicates/triplicates failed
D-1	8	1
D-2	13	1
D-3	5	2
D-4	12	1
S-1	3	0
S-2	4	1
S-3	5	2
S-4	4	0

**Table 5.8. Concentration of PCBs in the field blank samples (ng/PUF sample) <sup>[a][b]</sup>**

Analyte	Test ID				
	D-1	D-2	D-3	S-1	S-2
PCB-17	0.00	0.00	0.00	0.00	0.00
PCB-52	0.00	0.00	0.97	0.00	0.00
PCB-101	0.00	5.59	0.00	0.00	0.00
PCB-154	0.00	0.00	0.00	0.00	0.00
PCB-110	0.00	5.65	0.00	0.00	0.00
PCB-77	0.00	0.00	0.00	0.00	0.00
PCB-66	0.00	0.00	0.00	0.00	0.00
PCB-118	0.00	5.37	0.00	0.00	0.00
PCB-105	0.00	2.72	0.00	0.00	0.00
PCB-187	0.02	0.00	0.00	0.00	0.00

<sup>[a]</sup> Values in strikethrough are below PQL.

<sup>[b]</sup> To convert (ng/PUF sample) to air concentration units (ng/m<sup>3</sup>), divide the former by sampling volume (m<sup>3</sup>).

**Table 5.9. Average recoveries of DCCs for dust tests in the 30-m<sup>3</sup> chamber**

Test ID	Analyte	Average Recovery	SD	%RSD	N <sup>[a]</sup>
D-1, D-2, D-3	PCB-17	104%	0.06	5.84	56
	PCB-52	107%	0.07	6.39	56
	PCB-101	101%	0.04	4.16	56
	PCB-154	98.1%	0.05	5.46	56
	PCB-110	104%	0.05	4.97	56
	PCB-77	111%	0.08	7.25	56
	PCB-66	104%	0.06	5.91	56
	PCB-118	103%	0.05	5.14	56
	PCB-105	104%	0.07	6.62	56
	PCB-187	98.3%	0.08	8.16	56
	TMX (RCS)	102%	0.04	4.24	56
	<sup>13</sup> C-PCB-77 (RCS)	108%	0.06	5.43	56
	<sup>13</sup> C-PCB-206 (RCS)	96.2%	0.03	3.60	56
D-4	PCB-13	106%	0.06	5.77	23
	PCB-18	107%	0.06	5.85	23
	PCB-17	106%	0.04	4.05	23
	PCB-15	102%	0.06	5.73	23
	PCB-22	108%	0.05	8.39	23
	PCB-52	102%	0.09	1.90	23
	PCB-49	101%	0.02	1.52	23
	PCB-44	104%	0.03	2.71	23
	PCB-64	104%	0.03	3.17	23
	TMX (RCS)	105%	0.05	4.44	23
	<sup>13</sup> C-PCB-77 (RCS)	108%	0.12	11.0	23
	<sup>13</sup> C-PCB-206 (RCS)	101%	0.04	3.90	23

<sup>[a]</sup> N is the number of DCCs analyzed.



**Table 5.10. Average recoveries of DCCs for the sink tests in the 53-L chamber**

Analyte	Average Recovery	SD	%RSD	N <sup>[a]</sup>
PCB-17	104%	0.05	4.54	78
PCB-52	102%	0.04	4.12	78
PCB-101	105%	0.06	5.76	78
PCB-154	103%	0.08	7.49	78
PCB-110	106%	0.06	6.00	78
PCB-77	109%	0.08	7.53	78
PCB-66	107%	0.08	7.47	78
PCB-118	104%	0.10	9.21	78
PCB-105	108%	0.10	9.06	78
PCB-187	105%	0.12	11.39	78
TMX (RCS)	106%	0.05	4.66	78
<sup>13</sup> C-PCB-77 (RCS)	109%	0.07	6.39	78
<sup>13</sup> C-PCB-206 (RCS)	99.0%	0.05	5.19	78

<sup>[a]</sup> N is the number of DCCs analyzed.

## 5.5 Recovery Check Standards

Three recovery check standards (RCSs), TMX, <sup>13</sup>C-PCB-77, and <sup>13</sup>C-PCB-206, were spiked in each of the samples before extraction to serve as the laboratory controls (LCs). When the measured concentrations of PCBs in the sample were above the highest calibration level, which happened mostly during bulk analysis, the extract was diluted, and the analysis of the sample was repeated. In such cases, recoveries of RCS were not reported. The analytical results were considered acceptable if the percent recovery of laboratory controls was in the range of 60-140% for at least two of the three recovery check standards.

## 5.6 Precision for Chamber Tests

### 5.6.1 Congener Concentrations in Building Materials

To estimate the precision of the measurements of sorption concentrations, three sink materials were tested in duplicate. The results are presented in Tables 5.11 through 5.13. Note that the RSDs were calculated only for the data pairs that were above the PQL.

**Table 5.11. Precision of duplicate measurements for sorption concentrations for oil-based paint in Test S-2 <sup>[a]</sup> <sup>[b]</sup>**

Elapsed time (h)	Sample	Congener Sorption Concentration (µg/cm <sup>2</sup> )									
		#17	#52	#101	#154	#110	#77	#66	#118	#105	#187
98.0	A	0.014	0.381	0.129	<del>0.012</del>	0.061	<del>0.000</del>	0.025	0.020	<del>0.004</del>	<del>0.000</del>
	B	<del>0.014</del>	0.305	0.096	<del>0.008</del>	0.044	<del>0.000</del>	0.017	0.014	<del>0.004</del>	<del>0.000</del>
173.0	A	0.024	0.732	0.246	0.020	0.117	<del>0.000</del>	0.045	0.041	<del>0.010</del>	<del>0.000</del>
	B	<del>0.022</del>	0.732	0.253	<del>0.018</del>	0.116	<del>0.000</del>	0.046	0.039	<del>0.009</del>	<del>0.000</del>
269.0	A	0.030	1.083	0.395	0.029	0.207	<del>0.000</del>	0.085	0.081	0.020	<del>0.001</del>
	B	0.022	0.821	0.284	0.022	0.151	<del>0.000</del>	0.065	0.058	0.015	<del>0.000</del>

<sup>[a]</sup> Values in strikethrough are below PQL.

<sup>[b]</sup> Statistics: Total number of duplicates: 30; number of data pairs above PQL: 18; RSD range: 0% to 25.8%; average RSD = 15.5%.

**Table 5.12. Precision of duplicate measurements for sorption concentrations for concrete sample in Test S-2 <sup>[a]</sup> <sup>[b]</sup>**

Elapsed time (h)	Sample	Congener Sorption Concentration (µg/cm <sup>2</sup> )									
		#17	#52	#101	#154	#110	#77	#66	#118	#105	#187
98.0	A	0.008	0.236	0.078	0.007	0.034	<del>0.000</del>	0.012	<del>0.010</del>	<del>0.002</del>	<del>0.000</del>
	B	0.007	0.216	0.062	0.006	0.028	<del>0.000</del>	0.010	<del>0.008</del>	<del>0.002</del>	<del>0.000</del>
173.0	A	0.011	0.393	0.160	0.015	0.076	<del>0.000</del>	0.029	<del>0.025</del>	0.006	<del>0.000</del>
	B	0.011	0.374	0.128	0.013	0.066	<del>0.000</del>	0.022	0.022	0.005	<del>0.000</del>
269.0	A	0.014	0.550	0.217	0.020	0.104	<del>0.000</del>	0.046	0.046	0.011	<del>0.000</del>
	B	0.013	0.517	0.199	0.019	0.097	<del>0.000</del>	0.040	0.044	0.011	<del>0.000</del>

<sup>[a]</sup> Values in strikethrough are below PQL.

<sup>[b]</sup> Statistics: Total number of duplicates: 30; number of data pairs above PQL: 21; RSD range: 1.8% to 18.1%; average RSD = 8.5%.

**Table 5.13. Precision of duplicate measurements for sorption concentrations for brick sample in Test S-3 <sup>[a]</sup> <sup>[b]</sup>**

Elapsed Time (h)	Sample	Congener Sorption Concentration ( $\mu\text{g}/\text{cm}^2$ )									
		#17	#52	#101	#154	#110	#77	#66	#118	#105	#187
74.2	A	<del>0.0003</del>	0.0134	0.0083	<del>0.0010</del>	0.0055	<del>0.0000</del>	<del>0.0012</del>	<del>0.0023</del>	<del>0.0008</del>	<del>0.0000</del>
	B	<del>0.0004</del>	0.0241	0.0136	<del>0.0013</del>	0.0077	<del>0.0000</del>	<del>0.0020</del>	0.0032	<del>0.0009</del>	<del>0.0000</del>
170.9	A	<del>0.0005</del>	0.0202	0.0159	<del>0.0018</del>	0.0122	<del>0.0000</del>	<del>0.0026</del>	0.0053	<del>0.0019</del>	<del>0.0000</del>
	B	<del>0.0005</del>	0.0202	0.0165	<del>0.0020</del>	0.0137	<del>0.0000</del>	0.0034	0.0063	<del>0.0022</del>	<del>0.0000</del>
240.1	A	<del>0.0006</del>	0.0247	0.0197	<del>0.0023</del>	0.0168	<del>0.0000</del>	0.0032	0.0059	<del>0.0028</del>	<del>0.0001</del>
	B	<del>0.0004</del>	0.0159	0.0133	<del>0.0016</del>	0.0135	<del>0.0000</del>	0.0031	0.0047	<del>0.0024</del>	<del>0.0000</del>
338.3	A	<del>0.0006</del>	0.0260	0.0258	<del>0.0030</del>	0.0244	<del>0.0001</del>	0.0042	0.0116	0.0048	<del>0.0002</del>
	B	<del>0.0005</del>	0.0145	0.0126	<del>0.0015</del>	0.0151	<del>0.0000</del>	0.0034	0.0069	0.0030	<del>0.0015</del>
412.3	A	<del>0.0005</del>	0.0237	0.0227	<del>0.0028</del>	0.0222	<del>0.0000</del>	0.0041	0.0105	0.0045	<del>0.0003</del>
	B	<del>0.0005</del>	0.0158	0.0155	<del>0.0018</del>	0.0190	<del>0.0001</del>	0.0039	0.0091	0.0042	<del>0.0002</del>
507.0	A	<del>0.0006</del>	0.0257	0.0253	<del>0.0030</del>	0.0260	<del>0.0000</del>	0.0046	0.0123	0.0055	<del>0.0003</del>
	B	<del>0.0007</del>	0.0194	0.0197	<del>0.0024</del>	0.0238	<del>0.0000</del>	0.0046	0.0119	0.0051	<del>0.0000</del>

<sup>[a]</sup> Values in strikethrough are below PQL.

<sup>[b]</sup> Statistics: Total number of duplicate: 60; Number of data pairs above PQL = 30; RSD range: 0.0% to 48.4%; average RSD = 18.6%.

### 5.6.2 Congener Concentrations in Settled Dust

The precision data for PCB sorption concentrations in dust samples are presented in Table 5.14. The 131 replicate measurements were for individual congeners, and only the measurements that were above the PQLs were counted.

**Table 5.14. Precision of PCB sorption concentrations as determined by replicate measurements**

	Dust category	
	From PCB panels	From PCB-free panels
Number of replicates	94	37
RSD (range)	0.68% ~ 45.2%	0.97% ~ 36.7%
RSD (mean)	9.2%	12.1%

## 6. Results

### 6.1 Terminology and Definitions

In this study, several sets of terminology were used to describe the accumulation of PCB congeners in sink materials and the rates of the accumulation. The definitions of the terms we used are presented below.

#### 6.1.1 Terminology for Material/Air Partitioning

The terminologies used for the material/air partition are summarized in Table 6.1.

**Table 6.1. Terminology used for PCB transport to building materials**

Term	Symbol	Units
Sorption concentration	$C_m$	$\mu\text{g}/\text{cm}^2$
Normalized sorption concentration	$C_m^*$	$(\mu\text{g}/\text{cm}^2)_{\text{sink}}/(\mu\text{g}/\text{m}^3)_{\text{air}}$
Sorption rate	$R_m$	$\mu\text{g}/\text{cm}^2/\text{h}$
Normalized sorption rate	$R_m^*$	$(\mu\text{g}/\text{cm}^2/\text{h})_{\text{sink}}/(\mu\text{g}/\text{m}^3)_{\text{air}}$

*Sorption concentration* ( $C_m$ ) is the congener concentration in the building material as a result of the material/air partition. Sorption concentration has the units ( $\mu\text{g}/\text{cm}^2$ ), which can be converted to other units such as ( $\mu\text{g}/\text{cm}^3$ ) or ( $\mu\text{g}/\text{g}$ ) when the density and dimensions of the sink material are given. Sorption concentrations were experimentally determined.

*Normalized sorption concentration* ( $C_m^*$ ) is the sorption concentration that corresponds to an air concentration of  $1 \mu\text{g}/\text{m}^3$  and is defined by Equation 6.1:

$$C_m^* = \frac{C_m}{C_a} \quad (6.1)$$

where  $C_m^*$  = normalized sorption concentration  $[(\mu\text{g}/\text{cm}^2)_{\text{sink}}/(\mu\text{g}/\text{m}^3)_{\text{air}}]$

$C_m$  = sorption concentration ( $\mu\text{g}/\text{cm}^2$ )

$C_a$  = time-averaged concentration in chamber air ( $\mu\text{g}/\text{m}^3$ )

*Sorption rate* ( $R_m$ ) is defined by Equation 6.2.

$$R_m = \frac{C_m}{t} \quad (6.2)$$

where  $R_m$  = sorption rate ( $\mu\text{g}/\text{cm}^2/\text{h}$ )

$C_m$  = sorption concentration ( $\mu\text{g}/\text{m}^2$ )

t = exposure time (h)

Note that  $R_m$  is the time-averaged sorption rate between time 0 and t. It is not the sorption rate at time t.

*Normalized sorption rate* ( $R_m^*$ ) is the sorption rate that corresponds to an air concentration of  $1 \mu\text{g}/\text{m}^3$  and is defined by Equation 6.3:

$$R_m^* = \frac{R_m}{C_a} \quad (6.3)$$

where  $R_m^*$  = normalized sorption rate [ $(\mu\text{g}/\text{cm}^2/\text{h})_{\text{sink}}/(\mu\text{g}/\text{m}^3)_{\text{air}}$ ]

$R_m$  = sorption rate ( $\mu\text{g}/\text{cm}^2/\text{h}$ )

$C_a$  = concentration in chamber air ( $\mu\text{g}/\text{m}^3$ )

### 6.1.2 Terminology for Dust/Air and Dust/Source Partitioning

Two sets of terminology were used for PCB transport from the source to settled dust, i.e., one for the dust/air partition and the other for the dust/source partition. They are distinguished by the words “sorption” and “migration” (Table 6.2).

**Table 6.2. Terminology used for PCB transport to settled dust**

Partition Type	Term	Symbol	Unit
Dust/air	Sorption concentration	$C_D$	$\mu\text{g}/\text{g}$
	Normalized sorption concentration	$C_D^*$	$(\mu\text{g}/\text{g})_{\text{dust}}/(\mu\text{g}/\text{m}^3)_{\text{air}}$
	Sorption rate	$R_D$	$\mu\text{g}/\text{g}/\text{h}$
	Normalized sorption rate	$R_D^*$	$(\mu\text{g}/\text{g}/\text{h})_{\text{dust}}/(\mu\text{g}/\text{m}^3)_{\text{air}}$
Dust/source	Migration concentration	$C_s$	$\mu\text{g}/\text{g}$
	Normalized migration concentration	$C_s^*$	$(\mu\text{g}/\text{g})_{\text{dust}}/(\text{mg}/\text{g})_{\text{source}}$
	Migration rate	$R_s$	$\mu\text{g}/\text{g}/\text{h}$
	Normalized migration rate	$R_s^*$	$(\mu\text{g}/\text{g}/\text{h})_{\text{dust}}/(\text{mg}/\text{g})_{\text{source}}$

The terminologies for the dust/air partition are the same as those used for the material/air partition (Equations 6.1 through 6.3), except that the sorption concentration for dust is in ( $\mu\text{g}/\text{g}$ ).

*Migration concentration* ( $C_s$ ) is the congener concentration in settled dust as a result of direct contact with a source. It has the units ( $\mu\text{g}/\text{g}$ ). Migration concentrations were experimentally determined.

*Normalized migration concentration* ( $C_s^*$ ) is the migration concentration that corresponds to the congener concentration of  $1 \text{ mg}/\text{g}$  [i.e., 1000 parts per million (ppm)] in the source and is defined by Equation 6.4:

$$C_s^* = \frac{C_s}{y} \quad (6.4)$$

where  $C_s^*$  = normalized migration concentration,  $[(\mu\text{g/g})_{\text{dust}}/(\text{mg/g})_{\text{source}}]$

$C_s$  = migration concentration in settled dust ( $\mu\text{g/g}$ )

$y$  = congener concentration in the source ( $\text{mg/g}$ )

The time-averaged *migration rate* ( $R_s$ ) is defined by Equation 6.5:

$$R_s = \frac{C_s}{t} \quad (6.5)$$

where  $R_s$  = migration rate ( $\mu\text{g/g/h}$ )

$C_s$  = migration concentration ( $\mu\text{g/g}$ )

$t$  = exposure time (h)

*Normalized migration rate* ( $R_s^*$ ) is the migration rate which corresponds to a congener concentration of 1  $\mu\text{g/g}$  in the source, and is defined by Equation 6.6:

$$R_s^* = \frac{R_s}{y} \quad (6.6)$$

where  $R_s^*$  = normalized migration  $[(\mu\text{g/g/h})_{\text{dust}}/(\text{mg/g})_{\text{source}}]$

$R_s$  = migration rate ( $\mu\text{g/g/h}$ )

$y$  = congener concentration in the source ( $\text{mg/g}$ )

Normalized concentrations and rates described above allow for comparison of sink behaviors between different congeners.

## 6.2 PCB Transfer from Air to Interior Surface Materials

### 6.2.1 Test Summary

Four tests (S-1 through S-4) were conducted. The first test (S-1) was a scouting test with the source and sink materials in the same chamber. Tests S-2 and S-3 measured the sorption concentrations as a function of time for 20 materials. The results were used to estimate the material/air partition coefficients and solid-phase diffusion coefficients. Test S-4 was designed to observe the re-emissions from the concrete panels after the source was shut off. The test conditions are summarized in Table 6.3.

**Table 6.3. Environmental conditions (mean  $\pm$  SD) for small chamber sink tests**

Test ID	Temperature ( °C)	RH (%)	Air Flow Rate (mL/min)
S-1	23.1 $\pm$ 0.0	49.5 $\pm$ 0.8	944 $\pm$ 11
S-2	23.0 $\pm$ 0.1	47.0 $\pm$ 1.6	938 $\pm$ 8
S-3	23.2 $\pm$ 0.12	47.2 $\pm$ 1.37	845 $\pm$ 19
S-4	23.1 $\pm$ 0.03	53.7 $\pm$ 4.15	923 $\pm$ 43

### 6.2.2 General Sorption Patterns

#### 6.2.2.1 Sorption Concentrations

The sorption concentrations increased over time in a pattern similar to that predicted by the DSS models described in Section 2. Figures 6.1 and 6.2 show the sorption concentration profiles for the oil-based paint and concrete.

The sorption concentrations varied greatly from material to material (Figures 6.3 and 6.4), indicating significant difference in sorption capacity.

#### 6.2.2.2 Normalized Sorption Concentrations

Congener #52 (2,2',5,5'-tetrachlorobiphenyl) was the most abundant congener in all the sink materials tested (See Figures 6.1 and 6.2 as examples.) However, this does not mean that the sorption favors congener #52. Rather, the observed abundance of congener #52 was simply because congener #52 had highest concentrations in the air inside the chamber (Figures 6.5 and 6.6).

Calculating the normalized sorption concentration allowed the comparison of sorption behavior between congeners in the same material. Although congener #52 had the highest concentration in every sink material (Figures 6.1 and 6.2), its normalized sorption concentration is the second lowest (Figures 6.7 and 6.8), next only to congener #17, which is more volatile than congener #52.



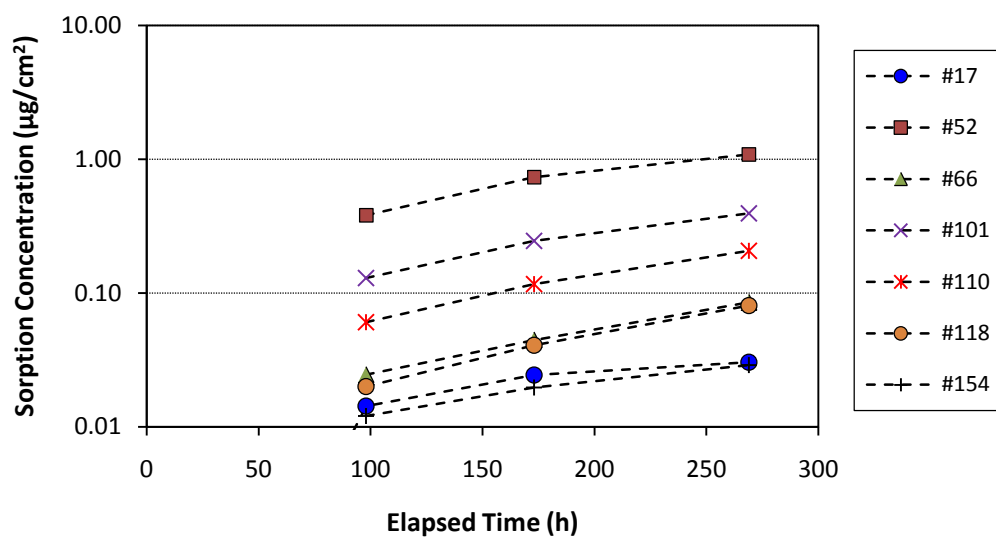
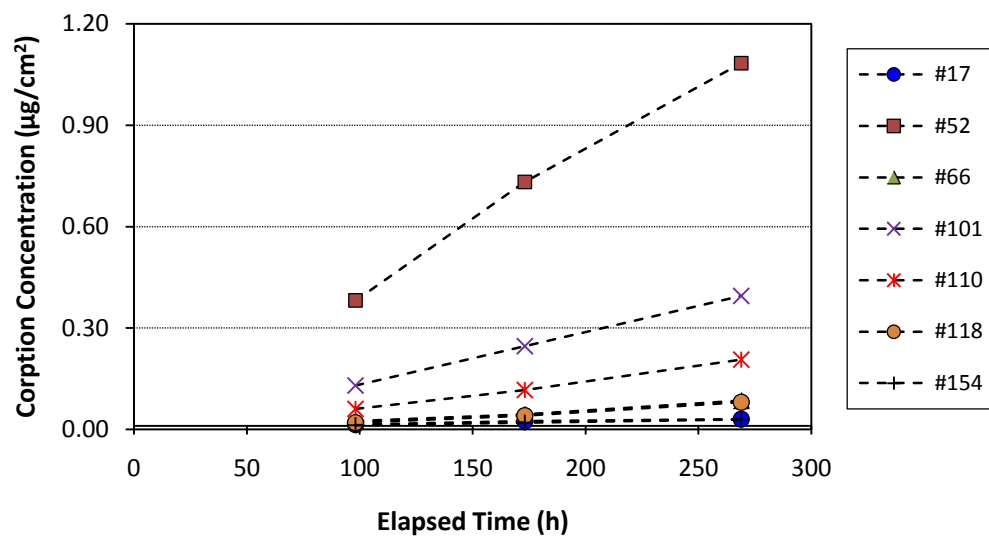


**Figure 6.1. Sorption concentrations for the oil-based paint applied on gypsum board in Test S-2 (top: normal scale; bottom: semi-log scale)**

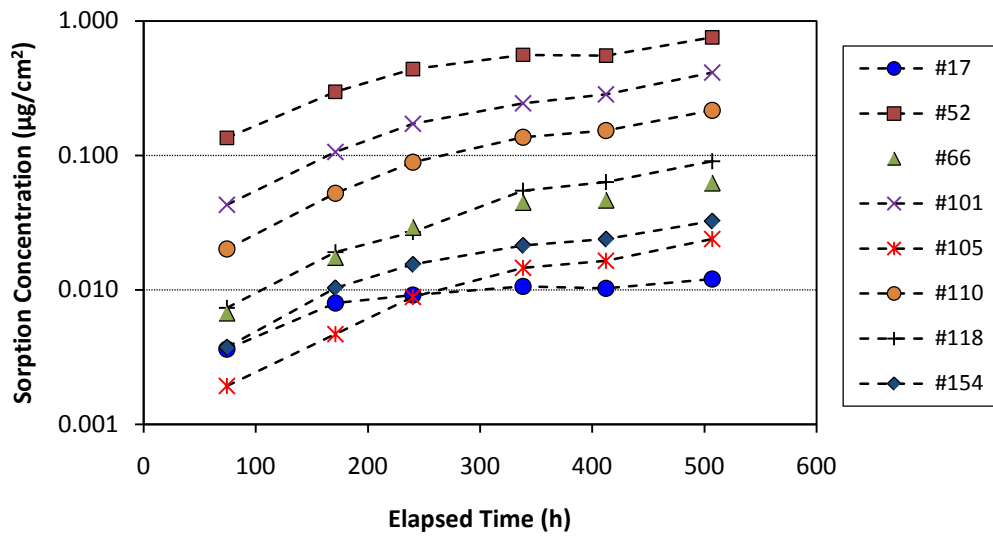
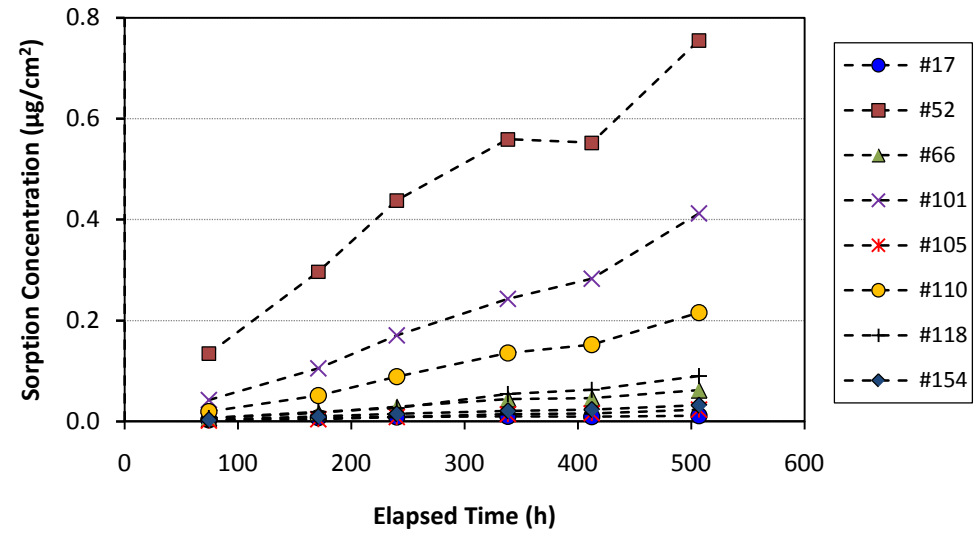


**Figure 6.2.** Sorption concentrations for concrete in Test S-3 (top: normal scale; bottom: semi-log scale)

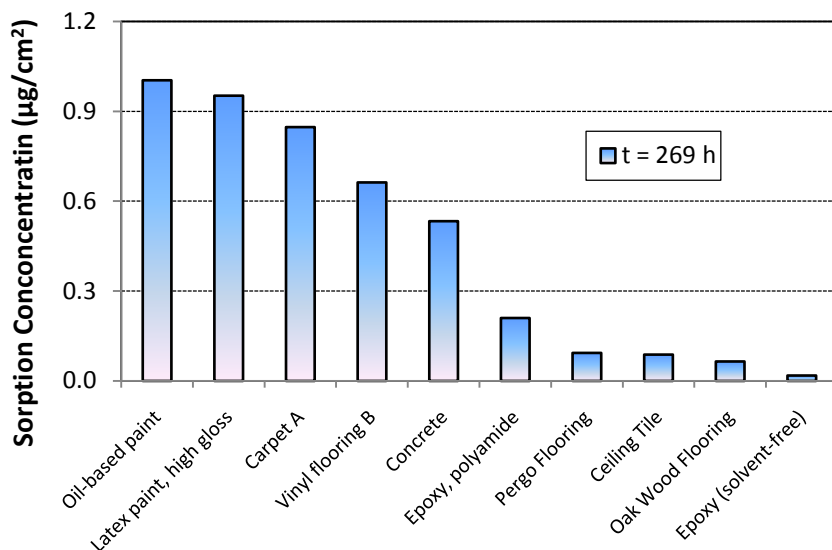


Figure 6.3. Sorption concentrations for congener #52 for 10 materials in Test S-2

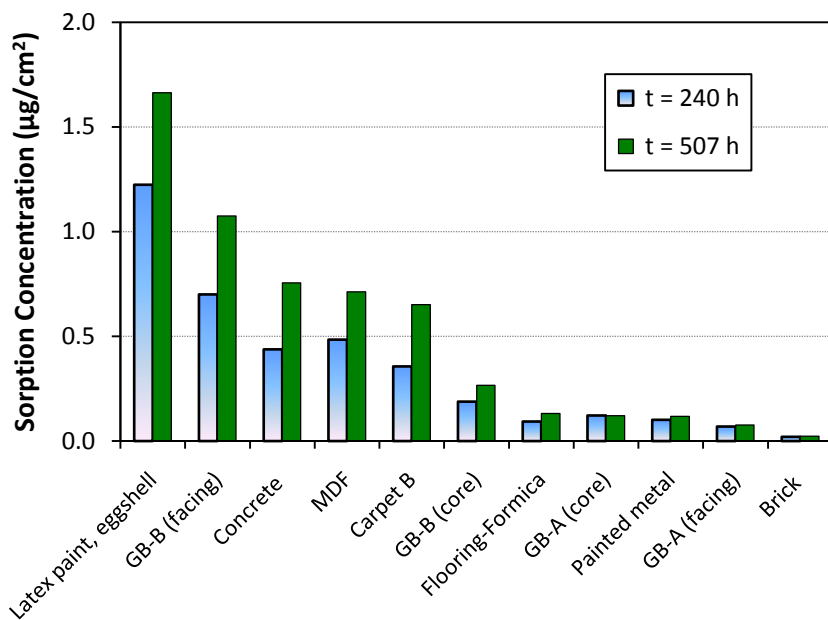
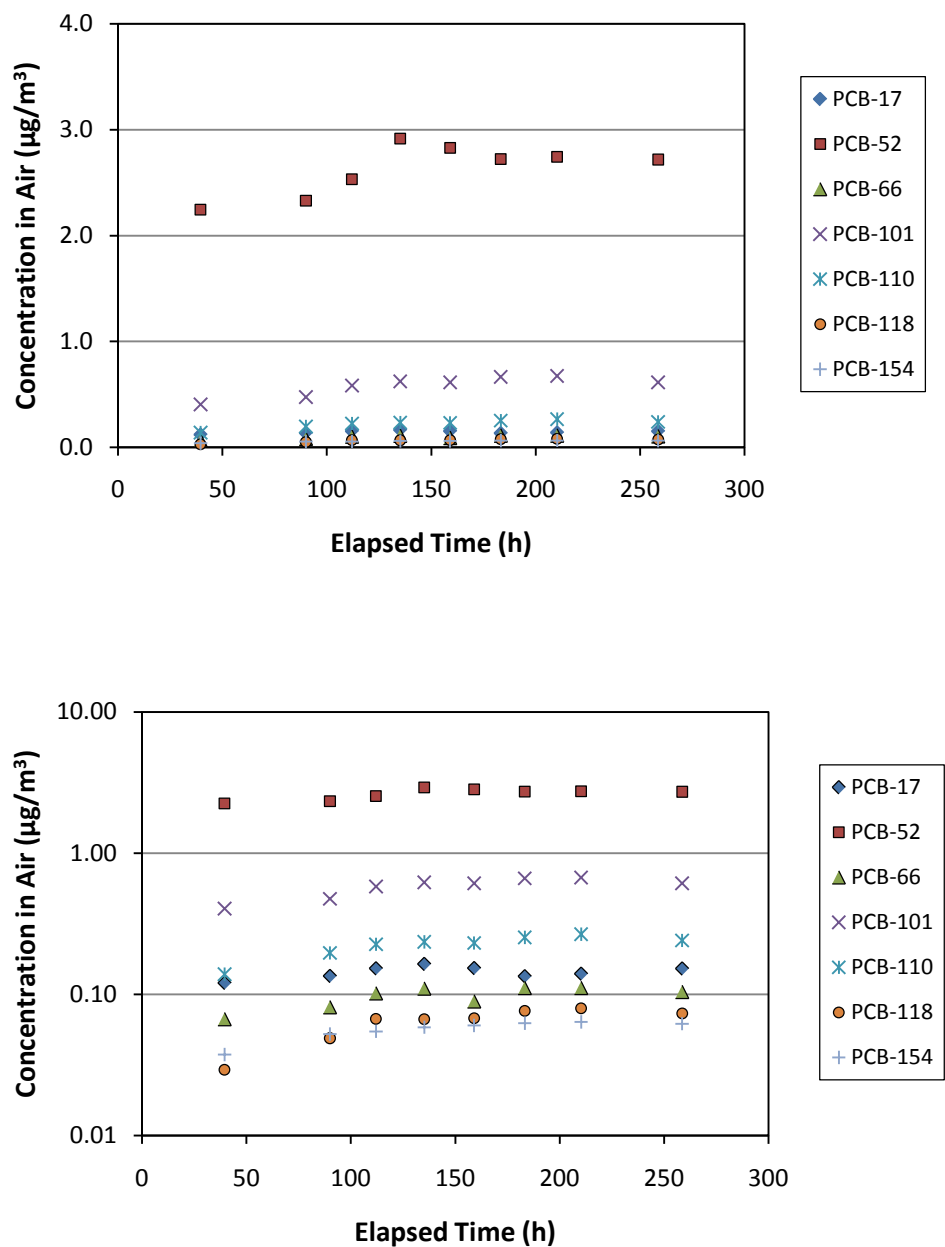
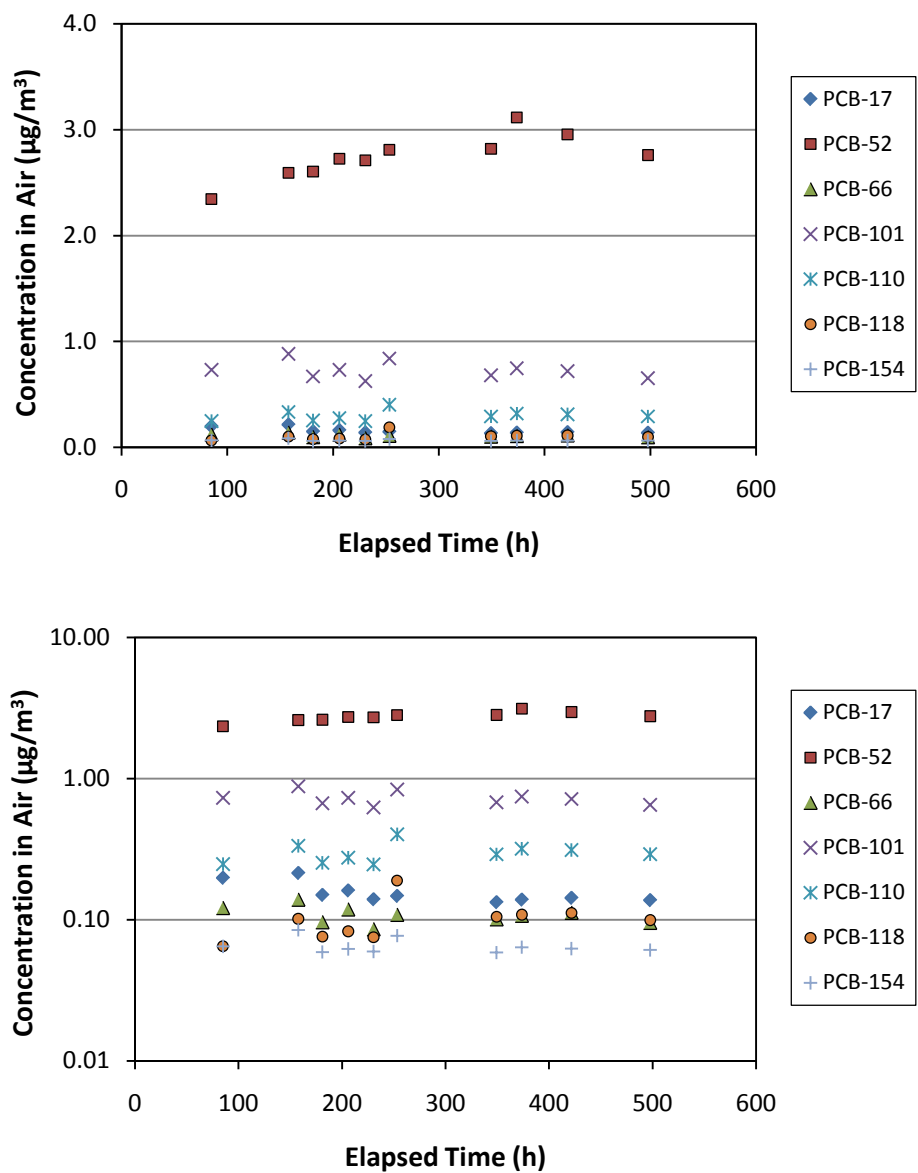


Figure 6.4. Sorption concentrations for congener #52 for 11 materials in Test S-3



**Figure 6.5. Concentrations of PCB congeners in the air inside the test chamber for Test S-2 (top: normal scale; bottom: semi-log scale)**



**Figure 6.6.** Concentrations of PCB congeners in the air inside the test chamber for Test S-3 (top: normal scale; bottom: semi-log scale)

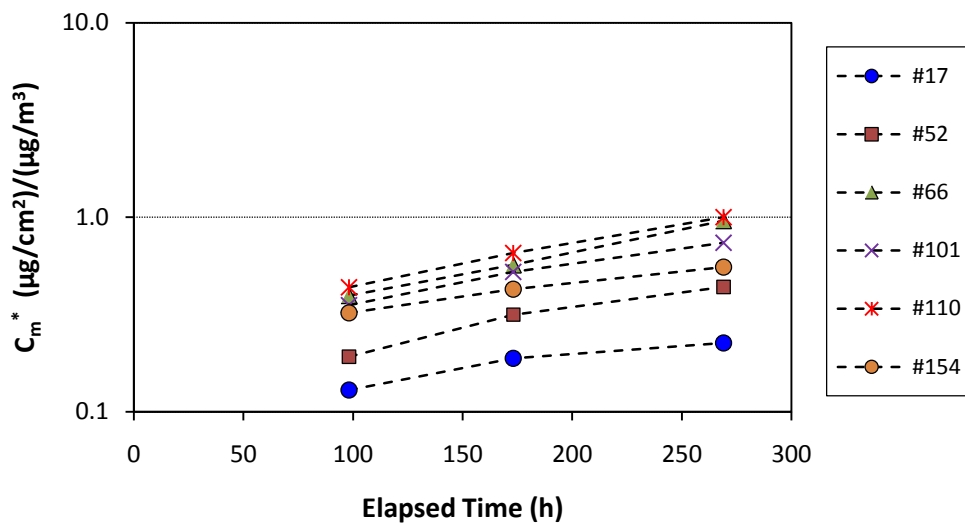


**Figure 6.7.** Normalized sorption concentrations ( $C_m^*$ ) for the oil-based paint applied on gypsum board in Test S-2

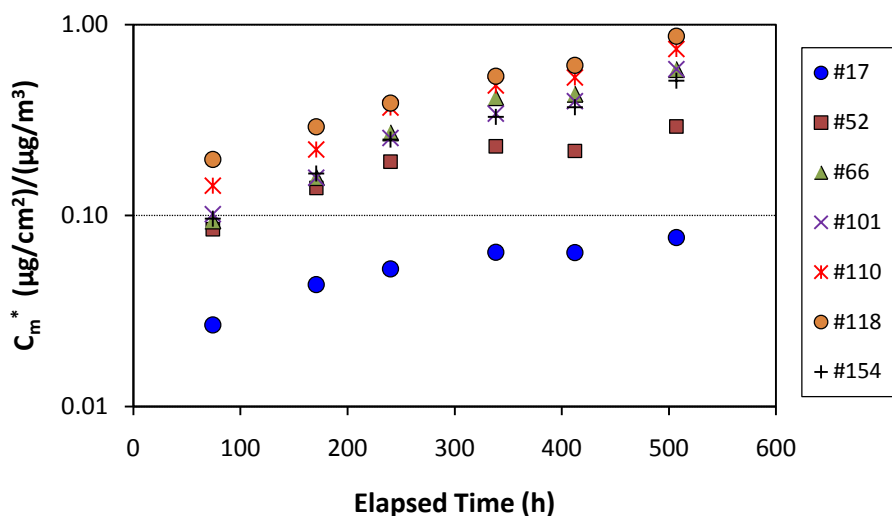


**Figure 6.8.** Normalized sorption concentrations ( $C_m^*$ ) for concrete in Test S-3

Introduction of normalized sorption concentration also makes it possible to compare the data from different tests. Figure 6.9 through 6.11 compare the normalized sorption concentrations for congener #52, congener #110 and Aroclor 1254 for all 20 materials tested in Tests S-2 and S-3. Note that Aroclor concentrations are calculated values (U.S. EPA, 2008b; Guo, et al., 2011).

As shown in Figures 6.9 through 6.11, petroleum-based paint, latex paint, and certain carpets showed strongest adsorption among the materials tested. Note that the area for carpet was based on the physical dimensions, not the actual surface areas.

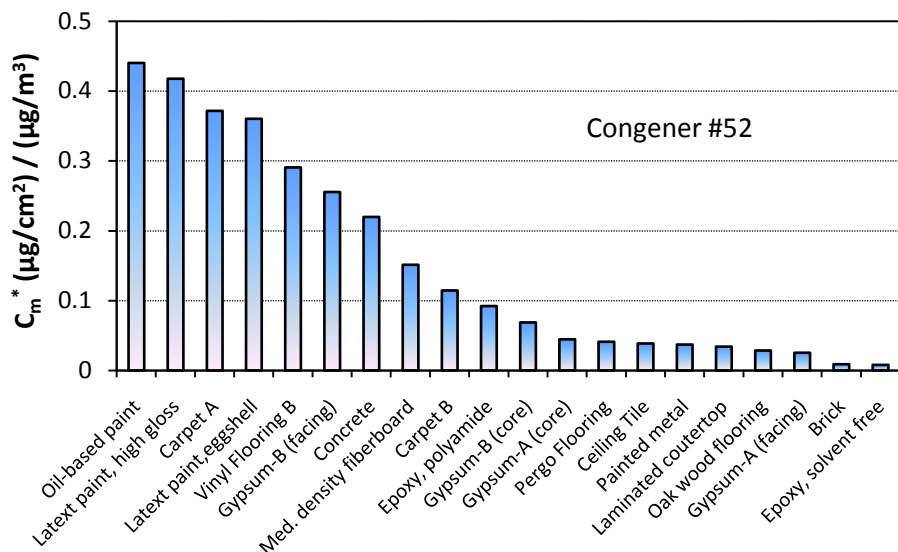


**Figure 6.9.** Normalized sorption concentrations ( $C_m^*$ ) for congener #52 for the materials in Test S-2 ( $t = 269$  h) and Test S-3 ( $t = 240$  h)

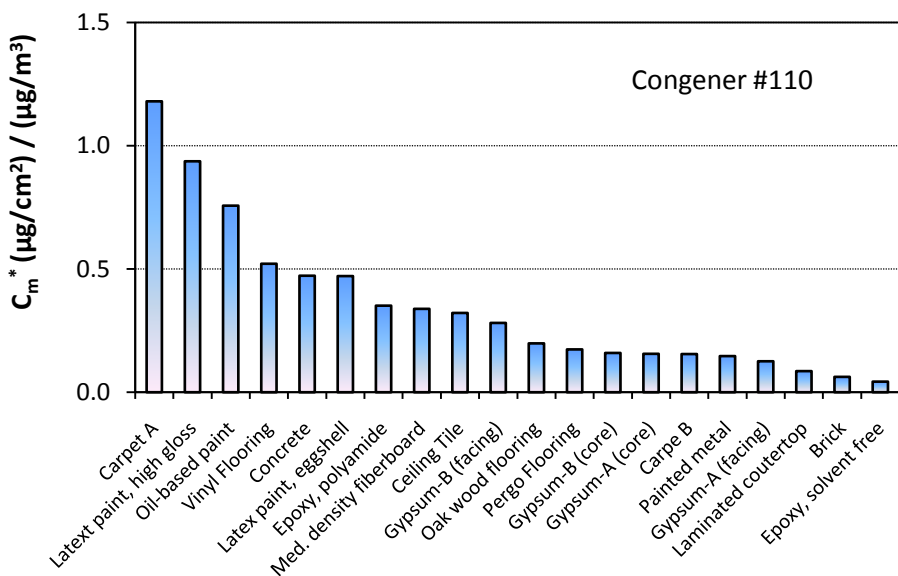


**Figure 6.10.** Normalized sorption concentrations ( $C_m^*$ ) for congener #110 for the materials in Test S-2 ( $t = 269$  h) and Test S-3 ( $t = 240$  h)

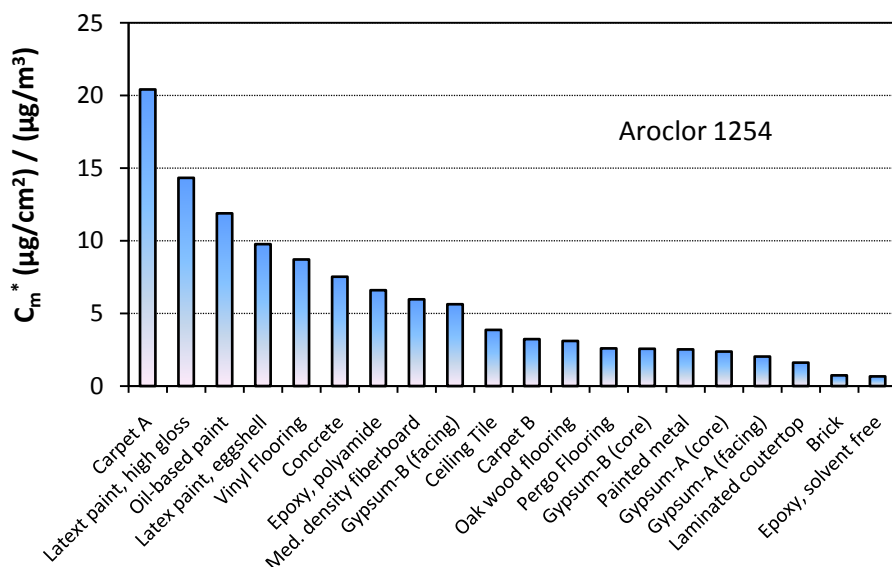


**Figure 6.11. Normalized sorption concentrations ( $C_m^*$ ) for Aroclor 1254 for the materials in Test S-2 ( $t = 269$  h) and Test S-3 ( $t = 240$  h)**

#### 6.2.2.3 Sorption Rate

Although the sorption concentrations kept increasing over time (Figures 6.1 and 6.2), the rate of the increase decreased as the PCB congeners accumulated in the sink material. If the exposure time is sufficiently long, the sink material will become saturated, and the sorption rate will approach zero. Figures 6.12 through 6.14 show the time-averaged sorption rates as a function of time for gypsum board paper, brick, and concrete.

The rate appears to decrease faster for congeners with higher volatility. For concrete, the rates for congeners #101, #110, and #118 were rather stable over the entire test period (Figure 6.14).

#### 6.2.2.4 Normalized Sorption Rate

Similar to normalized sorption concentration, the normalized sorption rate, defined by Equation 6.3, allowed the comparison of the sorption rates for different congeners. Although congener #52 had the highest sorption rate among the four congeners (Figure 6.4), its normalized sorption rate was the lowest among the four congeners (Figure 6.15). Thus, as shown in Figure 6.15, the normalized sorption rate favored the less volatile congeners.



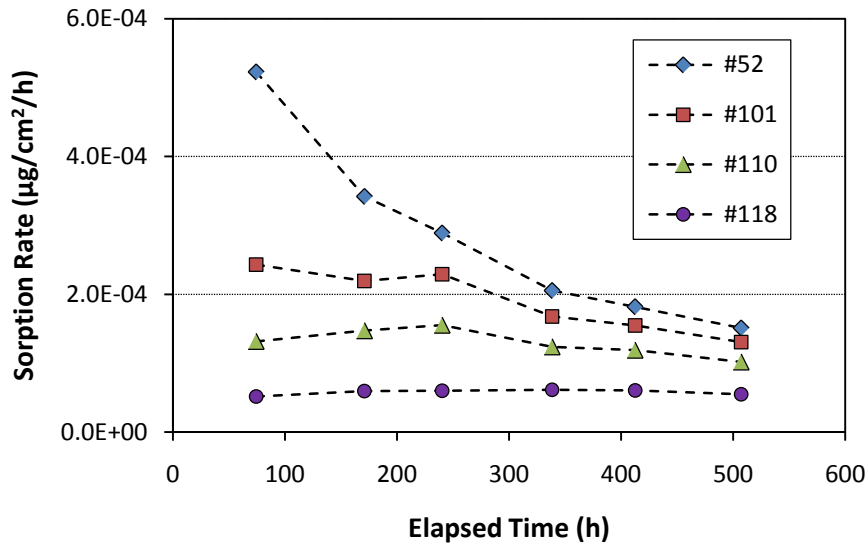


**Figure 6.12.** Sorption rate as a function of time for gypsum board paper in Test S-3

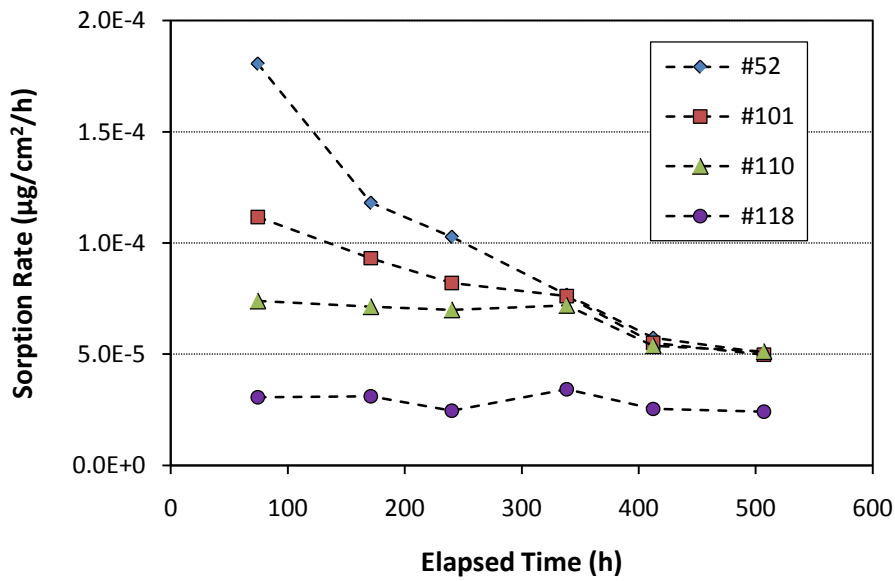


**Figure 6.13.** Sorption rate as a function of time for brick in Test S-3

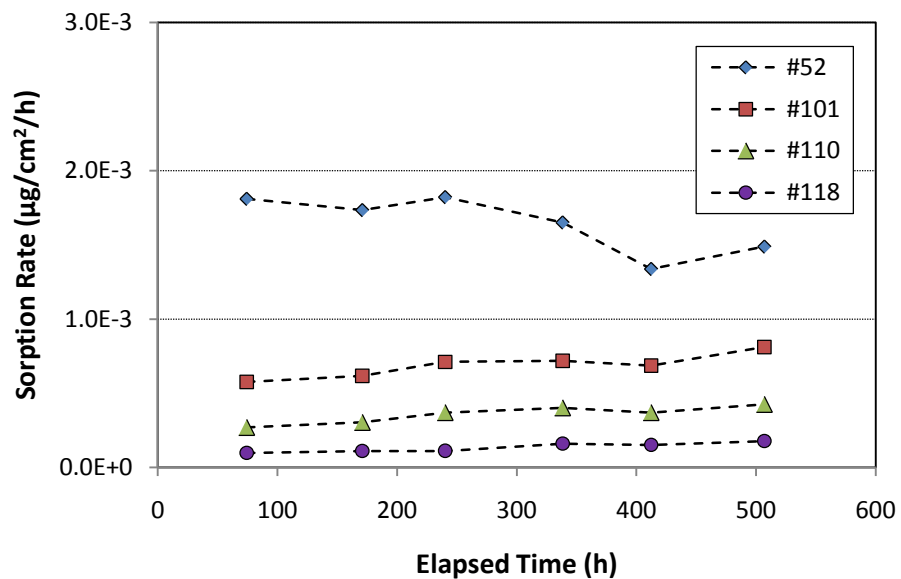


Figure 6.14. Sorption rate as a function of time for concrete in Test S-3

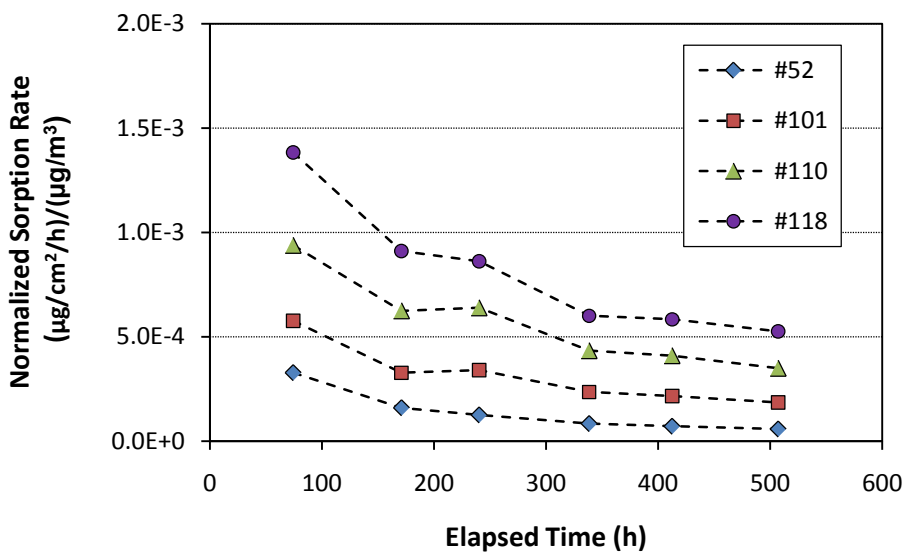


Figure 6.15. Normalized sorption rates for four congeners in concrete (Test S-3)

### 6.2.3 General Re-emission Patterns

Test S-4 was designed to observe the re-emission of PCBs from concrete panels after the source was shut off at 167.2 elapsed hours. The concentration profiles for the outlet air for the three congeners with the most data above the PQLs are shown in Figure 6.16.

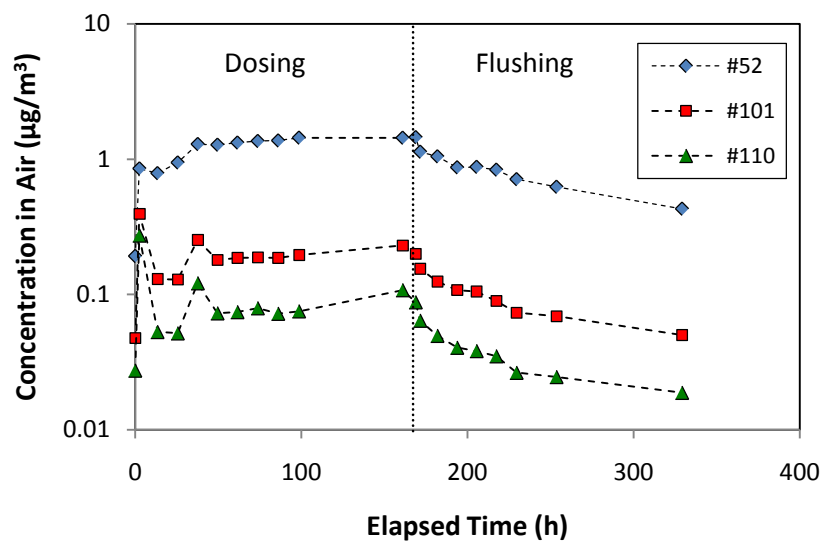


Figure 6.16. Air concentration profiles in Test S-4 for concrete panels

Prior to stopping the PCB source to the test chamber, a set of concrete “buttons” was removed from the chamber to determine the sorption concentrations at the end of the dosing period.

The amounts of congeners re-emitted from the concrete panels during the 160-hour purging period were calculated by the following mass balance equation:

$$W_{RE} = W_{out} - V C_0 + V C_t \quad (6.7)$$

where  $W_{RE}$  = congener mass re-emitted from the concrete panels during the purging period ( $\mu\text{g}$ )

$W_{out}$  = congener mass leaving the chamber during the purging period, from Equation 6.8 ( $\mu\text{g}$ )

$V$  = chamber volume ( $\text{m}^3$ )

$C_0$  = congener concentration in the air inside the chamber prior to purging the chamber ( $\mu\text{g}/\text{m}^3$ )

$C_t$  = congener concentration in the air inside the chamber at the end of the purging period ( $\mu\text{g}/\text{m}^3$ )

$$W_{out} = Q \sum_{i=1}^{n-1} \frac{(C_i + C_{i+1})(t_{i+1} - t_i)}{2} \quad (6.8)$$

where  $Q$  = air change flow rate ( $\text{m}^3/\text{h}$ )

$n$  = number of concentration data points during the purging period

$C_i$  and  $C_{i+1}$  = air concentrations at sampling times  $t_i$  and  $t_{i+1}$ , respectively ( $\mu\text{g}/\text{m}^3$ )

As shown in Table 6.4, only a small fraction of the adsorbed congeners was re-emitted into the air during the purging period, suggesting that the re-emission was a slow process. The results also show that the re-emission favored volatile congeners (Figure 6.17).

**Table 6.4. Congeners re-emitted from concrete panels during the 160-hour purging period <sup>[a]</sup>**

	Congener ID					
	#52	#66	#101	#110	#118	#154
Sorption concentration before purging ( $\mu\text{g}/\text{cm}^2$ )	0.104	0.006	0.033	0.017	0.007	<del>0.003</del>
Mass in concrete before purging ( $\mu\text{g}$ )	322	19.9	103	53.0	21.5	<del>9.5</del>
Mass re-emitted during purging ( $\mu\text{g}$ )	6.44	<del>0.105</del>	0.747	<del>0.281</del>	<del>0.109</del>	<del>0.054</del>
% Re-emitted	2.0%	0.53%	0.73%	0.53%	0.51%	0.57%

<sup>[a]</sup> Values in strikethrough font are below the PQL.

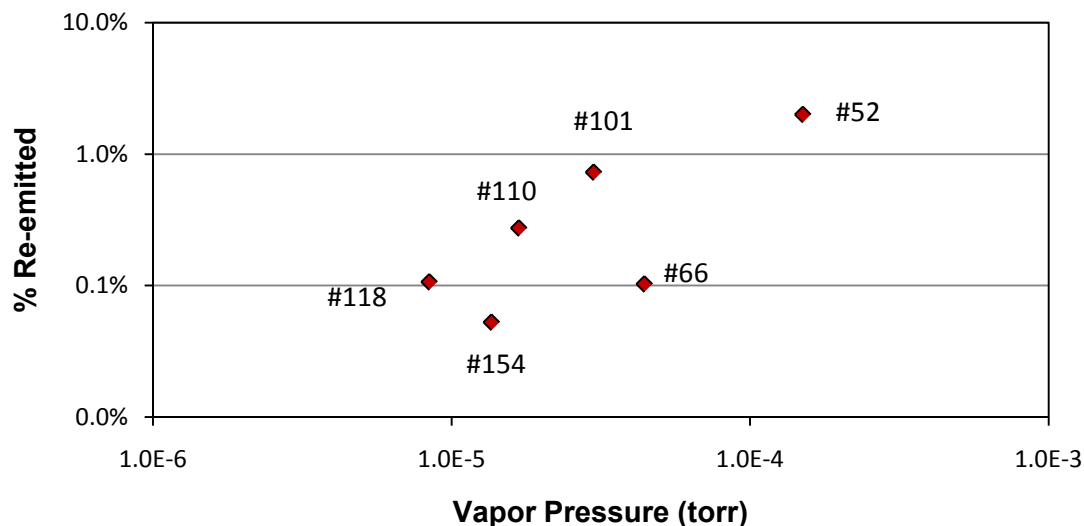


**Figure 6.17. Percent re-emissions from concrete as a function of vapor pressure of the congeners**

The walls of the chamber also adsorbed PCBs from the air. Thus, the re-emission results presented above reflect the combined effects of the concrete panels and the walls of the chamber. The fraction of congeners re-emitted from the concrete panels during the purging period should have been even smaller than the values presented in Table 6.4.

#### 6.2.4 Estimation of Partition and Diffusion Coefficients

Most sink models describe the properties of the sink material with three parameters: the material/air partition coefficient ( $K_{ma}$ ), the diffusion coefficient of the adsorbate in the material ( $D_m$ ), and the thickness of the material ( $\delta$ ). To apply the existing models to PCB contamination in buildings, these three parameters are needed for the congeners of interest. Because a large number of congeners may exist in a given environmental compartment (e.g., over 100 congeners have been identified in Aroclor 1254 alone), determination of partition and diffusion coefficients for all these congeners is time-consuming and costly.

Several studies have shown that, within each class of chemicals, the following correlations exist (Zhao et al., 1999; Bodalal et al., 2001; Cox et al., 2001; Guo, 2002):

$$\frac{K_{ma0}}{K_{mai}} = \left( \frac{P_i}{P_0} \right)^\alpha \quad (6.9)$$

where  $K_{ma0}$  = material/air partition coefficient for the reference constituent in the class (dimensionless)

$K_{mai}$  = material/air partition coefficient for constituent  $i$  in the class (dimensionless)

$P_i$  = vapor pressure for constituent  $i$  (torr)

$P_0$  = vapor pressure for the reference constituent (torr)

$\alpha$  = an empirical value that depends on the properties of the chemical class and the sink material

$$\frac{D_{m0}}{D_{mi}} = \left( \frac{m_i}{m_0} \right)^\beta \quad (6.10)$$

where  $D_{m0}$  = diffusion coefficient for the reference constituent in the class ( $\text{m}^2/\text{h}$ )

$D_{mi}$  = diffusion coefficient for constituent i the class ( $\text{m}^2/\text{h}$ )

$m_i$  = molecular weight for constituent i (g/mol)

$m_0$  = molecular weight for the reference constituent (g/mol)

$\beta$  = an empirical value that depends on the properties of the chemical class and the sink material.

With these correlations, only four parameters, i.e.,  $K_{ma0}$ ,  $D_{m0}$ ,  $\alpha$  and  $\beta$ , are needed to calculate the partition and diffusion coefficients for any constituent in the class. Selection of the reference congener is arbitrary. In this study, congener #52 was selected because of its abundance in the air and in the sink material.

Sorption data from Tests S-2 and S-3 were used to obtain rough estimates of  $K_{ma0}$ ,  $D_{m0}$ , and  $\alpha$  for each test specimen by nonlinear regression. Index  $\beta$  was fixed at 6.5 based on an average value for other classes of chemicals and nonwood materials (Guo, 2002). The dimensions of the test materials are presented in Appendix B. Equation 2.13 was used for parameter estimation. Data-fitting software SCIENTIST 2.0 (MicroMath, Saint Louis, MO) was used for the nonlinear regression. The input data were  $M(t)$  versus time for four congeners: #52, #101, #110 and #154. When data for #154 were unavailable, data for #118 or #66 were used. A more detailed description of the parameter estimation method is provided in Appendix C.

The estimated partition and diffusion coefficients and index  $\alpha$  for the reference congener (#52) for 20 materials are presented in Table 6.5. The meaning of the data in the last two columns ( $K_{ma} \times D_m$  and SSI) is discussed in Section 7.2.

Figures 6.18 through 6.21 show the goodness of fit for four sink materials. Figure 6.19 represents the best fit ( $r^2 = 0.991$ ) and Figure 6.20 represents the worst fit ( $r^2 = 0.957$ ). Oak flooring (Figure 6.21) was one of several cases for which the DSS model was switched from Equation 2.7 to 2.8 during the calculation. Note the discontinuity of the fitting curve for congeners #110 and #118.

Data presented in Table 6.5 can be used to predict the behavior of sink materials in several ways, including:

- Determination of the sorption capacity by using Equation 2.1
- Ranking the sink material based on sink sorption index (SSI) as described in Section 7.2
- Predicting the re-emissions from sink materials as secondary sources after the primary sources are removed by using dynamic sink models such as Equation 2.14 through 2.19.

As discussed in Appendix C, the partition and diffusion coefficients presented in Table 6.5 are rough estimates. More accurate estimation of these parameters requires that they be determined separately. The existing methods for determining these two parameters are mainly for volatile chemicals. Therefore, it is necessary to either develop new experimental methods or modify the existing methods for PCBs.

**Table 6.5. Rough estimates of partition and diffusion coefficients for 20 materials based on data from Tests S-2 and S-3 <sup>[a]</sup>**

Material	<b>K<sub>ma0</sub> (dimensionless)</b>		<b>D<sub>m0</sub> (m<sup>2</sup>/h)</b>		<b><math>\alpha</math></b>		<b>K × D</b>	<b>SSI</b>
	<b>Value</b>	<b>RSD</b>	<b>Value</b>	<b>RSD</b>	<b>Value</b>	<b>RSD</b>		
Concrete <sup>[b]</sup>	2.38×10 <sup>7</sup>	33.6%	2.99×10 <sup>-11</sup>	93.1%	0.554	0.3%	7.12×10 <sup>-4</sup>	3.15
	2.36×10 <sup>7</sup>	36.5%	2.74×10 <sup>-11</sup>	98.6%	0.513	0.0%	6.46×10 <sup>-4</sup>	3.19
	1.59×10 <sup>7</sup>	33.4%	3.21×10 <sup>-11</sup>	79.6%	0.565	0.0%	5.10×10 <sup>-4</sup>	3.29
Brick <sup>[c]</sup>	2.65×10 <sup>6</sup>	59.7%	1.09×10 <sup>-12</sup>	94.6%	1.07	0.0%	2.88×10 <sup>-6</sup>	5.54
	--	--	--	--	--	--	--	--
Ceiling Tile	8.15×10 <sup>6</sup>	33.6%	3.88×10 <sup>-12</sup>	72.5%	1.06	0.0%	3.16×10 <sup>-5</sup>	4.50
GB conventional	3.84×10 <sup>6</sup>	66.4%	1.94×10 <sup>-11</sup>	81.2%	0.909	1.9%	7.46×10 <sup>-5</sup>	4.13
GB paperless	1.31×10 <sup>7</sup>	32.0%	2.08×10 <sup>-10</sup>	66.0%	0.379	0.8%	2.72×10 <sup>-3</sup>	2.57
GB conventional (core)	3.49×10 <sup>6</sup>	35.2%	2.55×10 <sup>-11</sup>	73.4%	0.889	0.0%	8.89×10 <sup>-5</sup>	4.05
GB paperless (core)	5.80×10 <sup>6</sup>	43.7%	5.79×10 <sup>-11</sup>	91.2%	0.582	6.2%	3.36×10 <sup>-4</sup>	3.47
Oil-based paint	2.54×10 <sup>7</sup>	26.0%	1.00×10 <sup>-10</sup>	47.5%	0.408	2.3%	2.55×10 <sup>-3</sup>	2.59
Latex paint, high-gloss <sup>[d]</sup>	1.92×10 <sup>7</sup>	43.6%	2.63×10 <sup>-10</sup>	63.5%	0.520	0.0%	5.054×10 <sup>-3</sup>	2.30
	1.54×10 <sup>7</sup>	53.6%	3.49×10 <sup>-10</sup>	83.6%	0.501	0.1%	5.37×10 <sup>-3</sup>	2.27
Latex paint, eggshell	1.86×10 <sup>7</sup>	17.7%	2.21×10 <sup>-10</sup>	40.5%	0.351	0.0%	4.11×10 <sup>-3</sup>	2.39
Epoxy coating, solvent free <sup>[e]</sup>	5.30×10 <sup>6</sup>	4.0%	1.50×10 <sup>-13</sup>	10.4%	0.908	0.0%	7.95×10 <sup>-7</sup>	6.10
Epoxy coating, polyamide	7.66×10 <sup>6</sup>	29.8%	4.11×10 <sup>-11</sup>	46.5%	0.764	3.8%	3.11×10 <sup>-4</sup>	3.50
Residential carpet	3.33×10 <sup>7</sup>	17.3%	1.23×10 <sup>-11</sup>	40.9%	0.682	0.0%	4.10 ×10 <sup>-4</sup>	3.39
Commercial carpet	7.40×10 <sup>6</sup>	54.5%	2.54×10 <sup>-10</sup>	108%	0.278	12.7%	1.88×10 <sup>-3</sup>	2.73
Vinyl flooring B, no pad	8.14×10 <sup>6</sup>	0.1%	3.63×10 <sup>-10</sup>	0.2%	0.469	0.0%	2.96×10 <sup>-3</sup>	2.53
Oak flooring, pre-finished	5.67×10 <sup>6</sup>	17.9%	3.37×10 <sup>-12</sup>	39.6%	1.03	0.0%	1.91×10 <sup>-5</sup>	4.72



Material	$K_{ma0}$ (dimensionless)		$D_{m0}$ (m <sup>2</sup> /h)		$\alpha$		$K \times D$	SSI
	Value	RSD	Value	RSD	Value	RSD		
Laminate flooring	$6.18 \times 10^6$	14.7%	$4.24 \times 10^{-12}$	35.8%	0.848	0.0%	$2.62 \times 10^{-5}$	4.58
Painted metal	$8.57 \times 10^6$	50.0%	$5.59 \times 10^{-12}$	102%	0.861	5.2%	$4.79 \times 10^{-5}$	4.32
Medium density fiberboard	$9.72 \times 10^6$	37.1%	$1.76 \times 10^{-10}$	91.6%	0.586	4.5%	$1.71 \times 10^{-3}$	2.77
Plastic laminate countertop	$4.41 \times 10^6$	48.5%	$8.08 \times 10^{-12}$	99.1%	0.557	0.0%	$3.56 \times 10^{-5}$	4.45

<sup>[a]</sup> The RSDs for  $K_{ma}$ ,  $D_m$ , and  $\alpha$  were based on three estimates; the coefficients of determination ( $r^2$ ) were greater than 0.95 for all but one case.

<sup>[b]</sup> Tested in triplicate.

<sup>[c]</sup> Tested in duplicate; the results from the second set of data were not reported because of poor fit ( $r^2 = 0.65$ ).

<sup>[d]</sup> Tested in duplicate.

<sup>[e]</sup> Most experimental data were below the PQLs for this material.

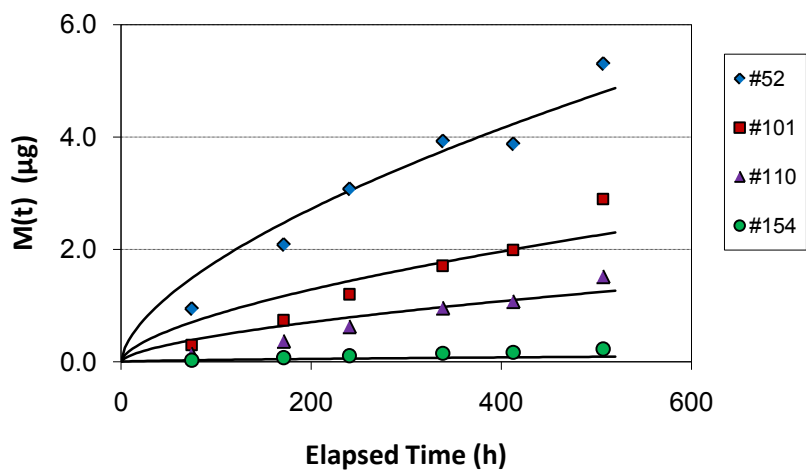


**Figure 6.18.** Amounts of PCB congeners adsorbed by concrete,  $M(t)$ , and the goodness of fit for estimating the partition and diffusion coefficients (data from Test S-3)

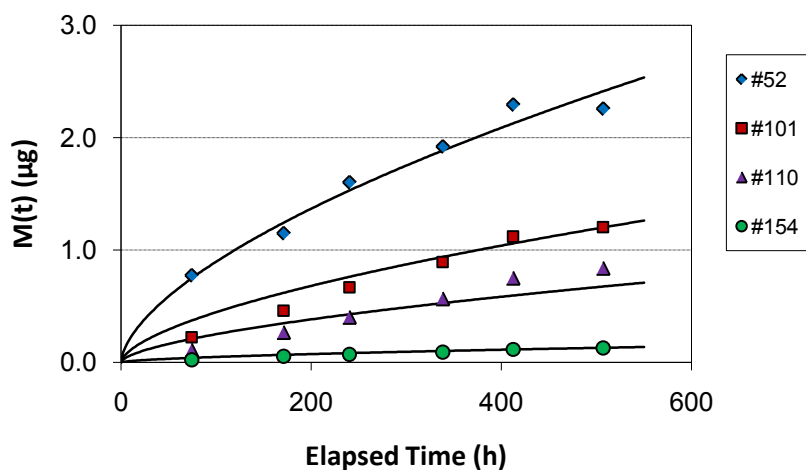


**Figure 6.19.** Amounts of PCB congeners adsorbed by the core of a GREENGUAR-certified gypsum board,  $M(t)$ , and the goodness of fit for estimating the partition and diffusion coefficients (data from Test S-3)

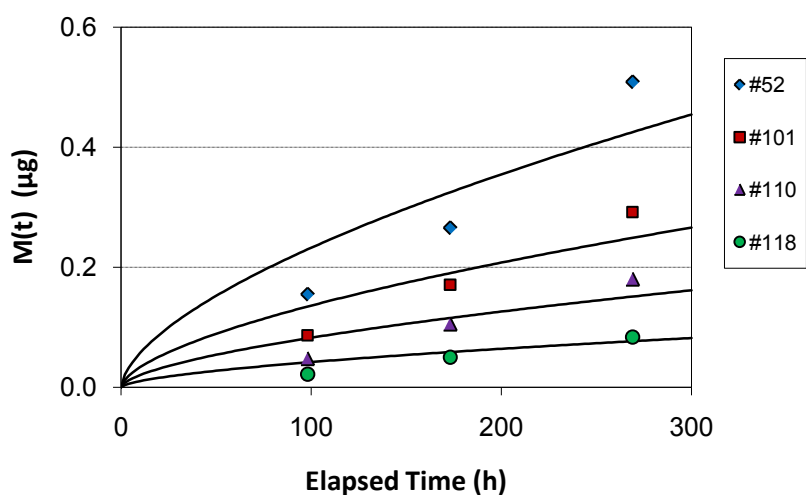


**Figure 6.20.** Amounts of PCB congeners adsorbed by laminated flooring,  $M(t)$ , and the goodness of fit for estimating the partition and diffusion coefficients (data from Test S-2)

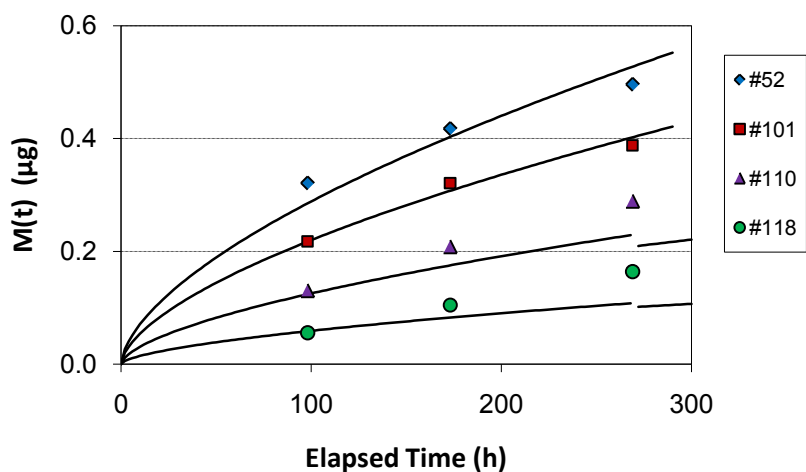


**Figure 6.21.** Amounts of PCB congeners adsorbed by oak flooring,  $M(t)$ , and the goodness of fit for estimating the partition and diffusion coefficients (data from Test S-2)

### 6.3 PCB Transfer to Settled Dust

#### 6.3.1 Test Summary

Four chamber tests were conducted with different combinations of Aroclor type, substrate type, dust type, and dust loading. Test conditions are summarized in Table 6.6. Dust samples collected from the PCB-free

test panels in Test D-2 were used to investigate the sorption of PCBs from air to settled dust. Most dust samples from the PCB-free panels in Tests D-1, D-3, and D-4 were below the practical quantification limits.

**Table 6.6. Summary of chamber tests for settled dust**

Parameter	Test ID			
	D-1	D-2	D-3	D-4
Aroclor	1254	1254	1254	1242
Substrate	primer	primer, caulk	primer	primer
Dust type <sup>[a]</sup>	HD	HD	HD	HD, ATD
Dust loading <sup>[b]</sup>	standard	4 levels	standard	standard
Number of panels	9	19	13	24
Test duration (h)	330	646	381	335
Temperature (°C)	22.9 ± 0.8	22.1 ± 0.2	20.9 ± 0.3 <sup>[c]</sup>	20.7 ± 0.4
RH (%)	49.5 ± 2.2	40.8 ± 4.7	16.7 ± 2.6 <sup>[c]</sup>	49.3 ± 9.1
Air flow setting (m <sup>3</sup> /h)	3.7	8.5	25.4	8.5

<sup>[a]</sup> HD = house dust; ATD = Arizona Test Dust.

<sup>[b]</sup> Standard loading = 30.8 g/m<sup>2</sup>; other three levels were: 7.71, 15.4, and 61.7 g/m<sup>2</sup>.

<sup>[c]</sup> A power outage occurred during test D-3; the chamber flow stopped and data collection ended at elapsed time 182 hours.

### 6.3.2 PCB Transport to Dust Due to Dust/Air Partition

#### 6.3.2.1 Sorption Concentrations

Results of Test D-2 with Aroclor 1254 showed that the sorption concentrations in the dust collected from the PCB-free test panels increased steadily over time (Figure 6.22) despite the decrease in concentrations in the air late in the test (Figure 6.23). Figure 6.22 also shows that the sorption concentrations for the more volatile congeners (#52 and #101) were higher because their concentrations in the air were higher (Figure 6.23). However, the concentrations of all the congeners were rather low, suggesting low sorption rates.

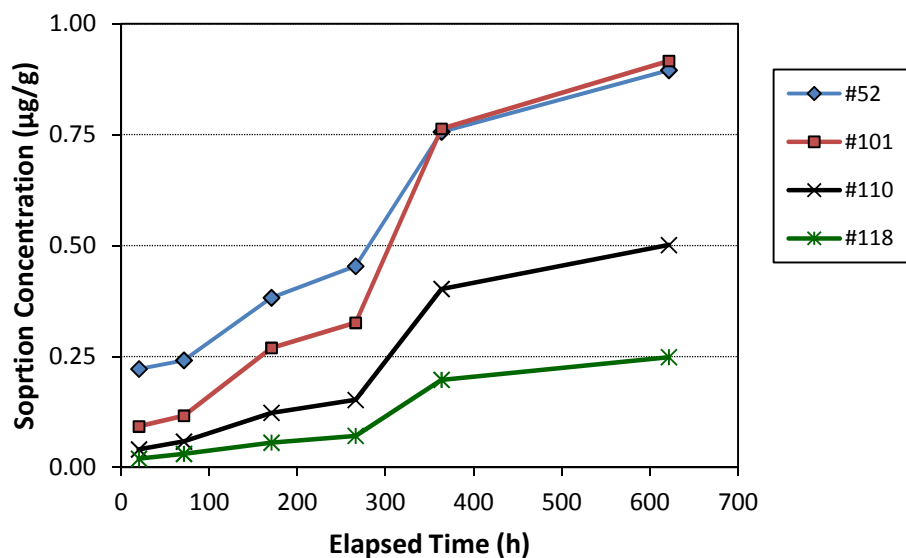


**Figure 6.22.** Experimentally determined sorption concentrations in settled house dust due to dust/air partitioning in Test D-2

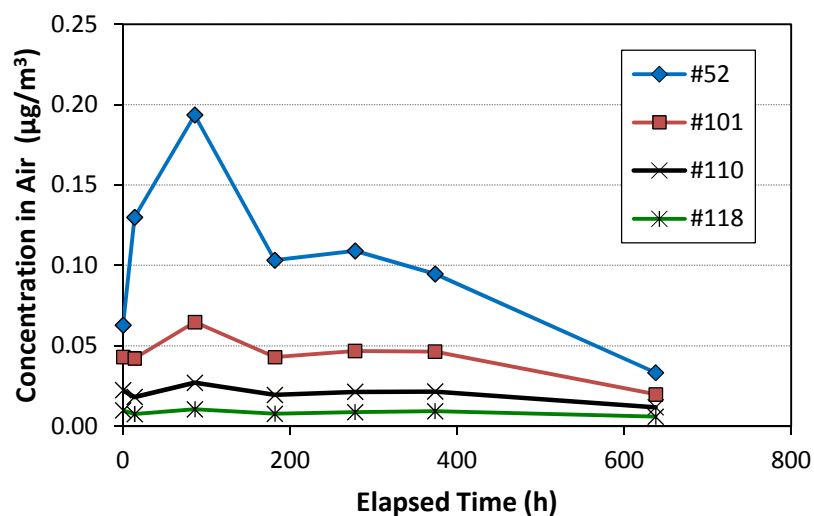


**Figure 6.23.** Concentrations of four congeners in the air inside the chamber in Test D-2. The decrease in these concentrations was caused mainly by the removal of PCB source panels.

Results in Test D-4 with Aroclor 1242 showed that the sorption concentrations at 335 elapsed hours were lower than those at 167 hours (Figure 6.24), suggesting that the sorption of volatile congeners was strongly affected by their concentrations in the air (Figure 6.25).

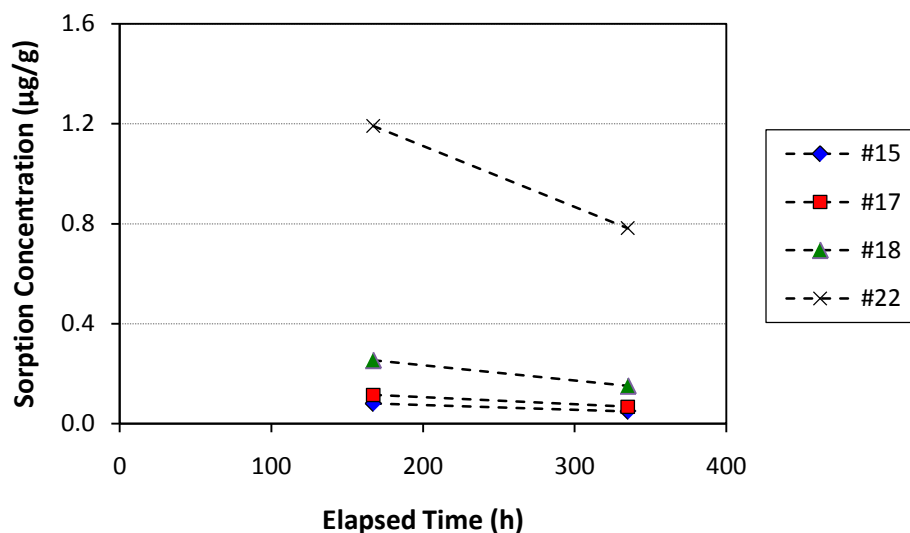


Figure 6.24. Sorption concentrations for congeners #15, #17, #18, and #22 in Test D-4.

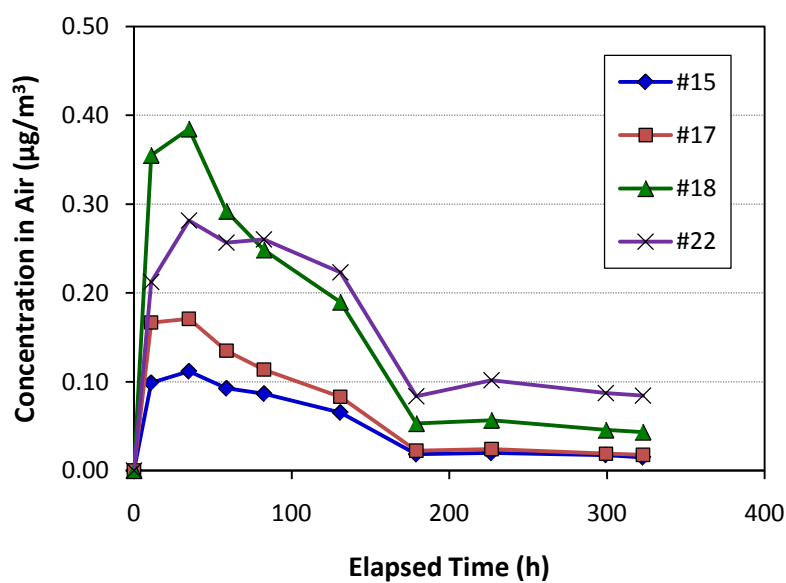


Figure 6.25. Concentrations of congeners #15, #17, #18, and #22 in chamber air (Test D-4)

### 6.3.2.2 Normalized Sorption Concentrations

The normalized sorption concentration is the experimentally determined sorption concentration divided by the time-averaged concentration in the air. Because the congener concentrations in the chamber air were not constant, a continuous curve was generated by applying the third-degree Lagrange interpolation (Pizer and

Wallace, 1983) to the data for the concentrations in the air (Figure 6.26), and the average concentrations in the air were calculated using Equation 6.11:

$$\overline{C_a} = \frac{1}{t} \int_0^t C_a(\tau) d\tau \quad (6.11)$$

where  $\overline{C_a}$  = time-averaged concentration in air ( $\mu\text{g}/\text{m}^3$ )

$C_a(\tau)$  = concentration in air at time  $\tau$  ( $\mu\text{g}/\text{m}^3$ )

$t$  = exposure time (h)

$\tau$  = dummy variable for time (h)

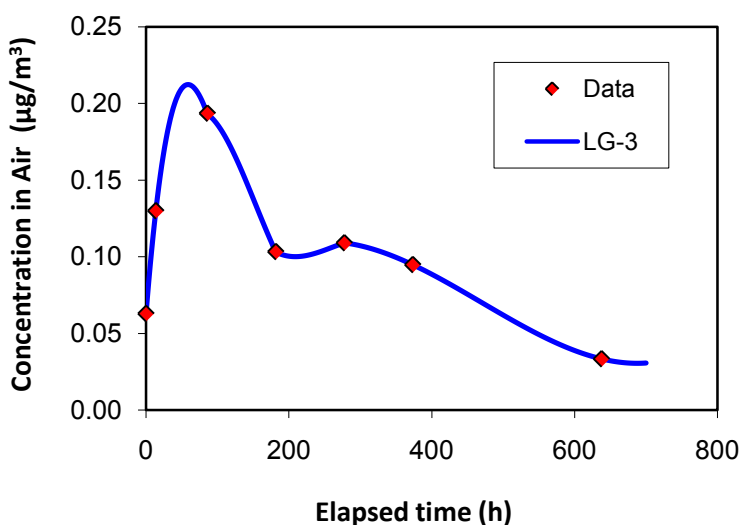


**Figure 6.26. Concentration profile for congener #52 in Test D-2 created by the third-degree Lagrange interpolation (LG-3)**

As shown in Figure 6.27, although the pattern of the normalized sorption concentrations is similar to that of sorption concentrations, the order is reversed, i.e., the more volatile the congener, the smaller the normalized sorption concentration. Clearly, the transport of PCBs from air to settled dust favored the less volatile congeners, as predicted by the sorption capacity (See Figure 2.1, above.)

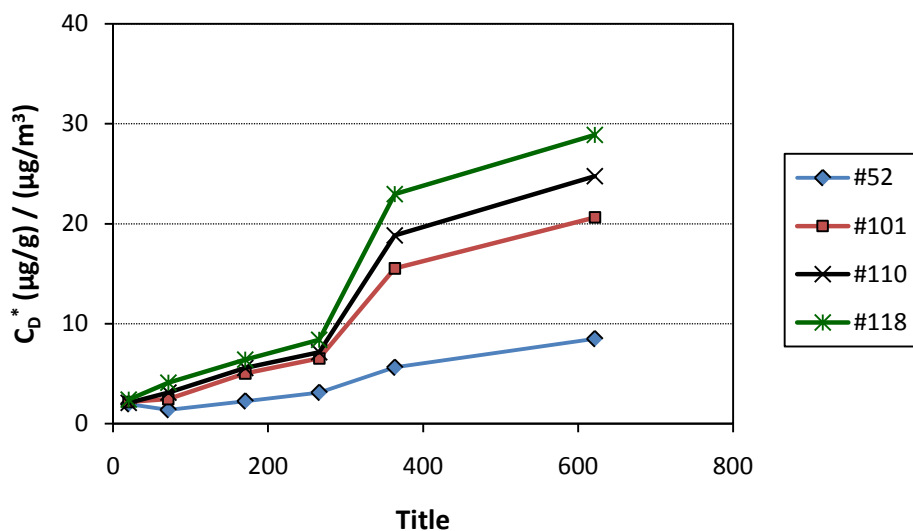


**Figure 6.27. Normalized sorption concentrations ( $C_D^*$ ) for four congeners in Test D-2**

A similar trend was observed in Test D-4 for the more volatile congeners. As shown in Figure 6.28, congener #22, the least volatile congener among the four congeners, had the highest normalized sorption concentration.

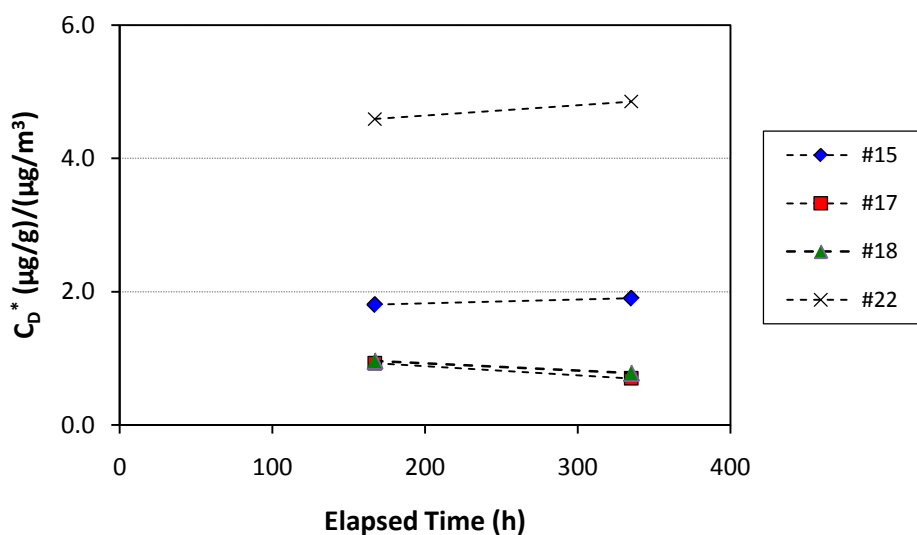


**Figure 6.28. Normalized sorption concentrations ( $C_D^*$ ) for four congeners in Test D-4**

### 6.3.2.3 Sorption Rates

In general, the sorption rate, i.e., sorption concentration divided by the exposure duration, decreased over time (Figure 6.29). The decrease likely was caused by two factors: (1) reduced air concentrations (i.e.,



reduced driving force) and (2) increased resistance to further sorption due to the accumulation of PCBs in the dust.

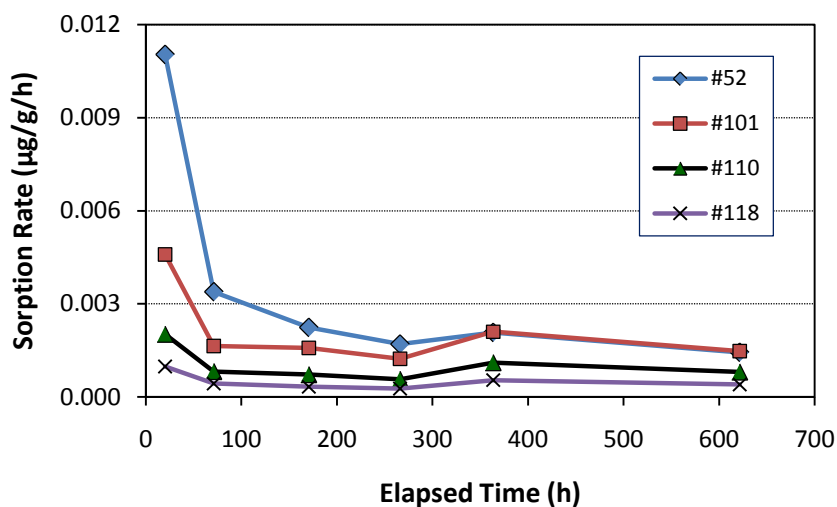


**Figure 6.29.** Sorption rates for congeners #52, #101, #110, and #118 due to dust/air partitioning in Test D-2

Similar trends were observed for congeners in Aroclor 1242 (Figure 6.30).

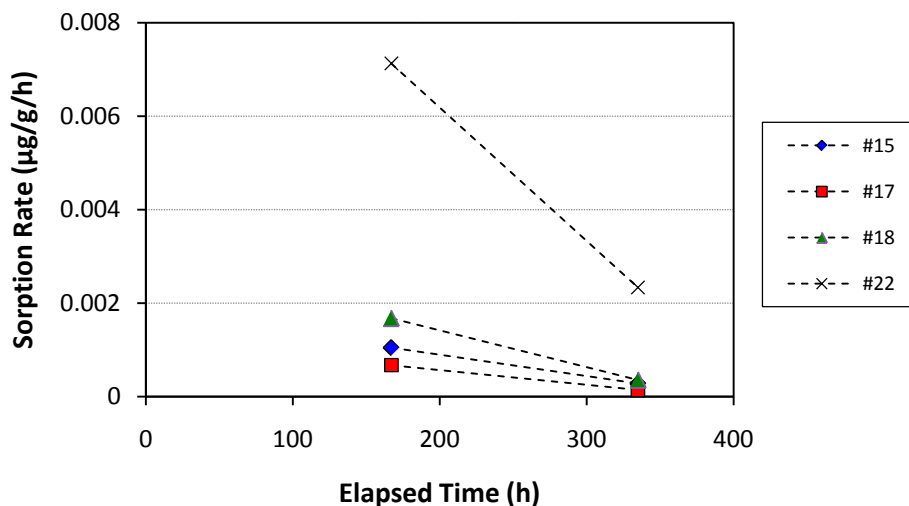


**Figure 6.30.** Sorption rates for congeners #15, #17, #18, and #22 due to dust/air partitioning in Test D-4

#### 6.3.2.4 Normalized Sorption Rates

As shown in Figure 6.29, congener #52, the most volatile congener among the four congeners, had the highest sorption rate because its concentration in the air was higher than the other three congeners (Figure

6.23). However, when the sorption rates were normalized by the concentrations in the air (Equation 6.2), congener #52 had the lowest normalized sorption rate (Figure 6.31). Like the material/air partition (Section 6.2.2.4), the dust/air partition favored the less volatile congeners.

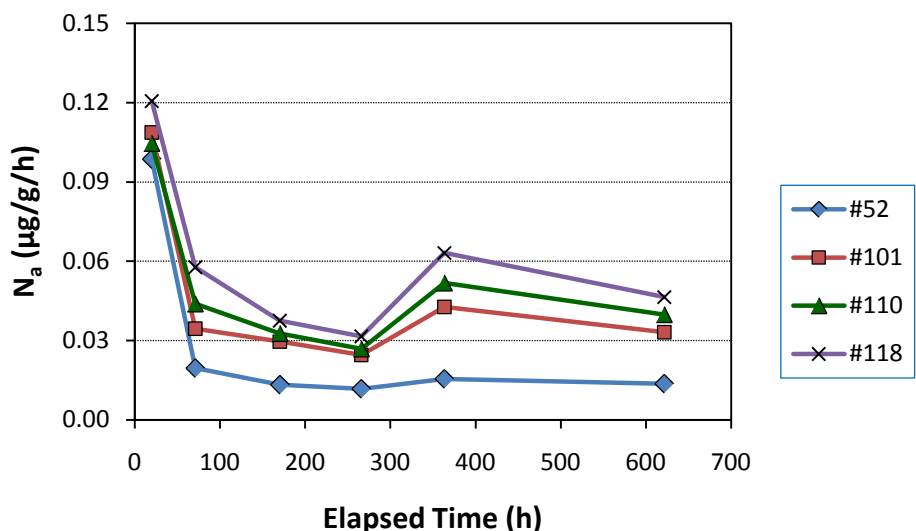


**Figure 6.31. Normalized sorption rates for four congeners due to dust/air partitioning (Test D-2)**

Furthermore, the normalized sorption rates can be linked to the vapor pressures of the congeners (Equation 6.12)

$$\ln R_D^* = a + b \ln P \quad (6.12)$$

where  $R_D^*$  = normalized sorption rate for a congener due to dust/air partitioning  $[(\mu\text{g/g/h})/(\mu\text{g/m}^3)]$

$P$  = vapor pressure of the congener (torr)

$a, b$  = constants (values are shown in Figure 6.32)

Figure 6.32 shows the correlation for four congeners in test D-2. Similar trends can be seen for congeners in Aroclor 1242. In Figure 6.33, congener 22 has the lowest vapor pressure among the four congeners.

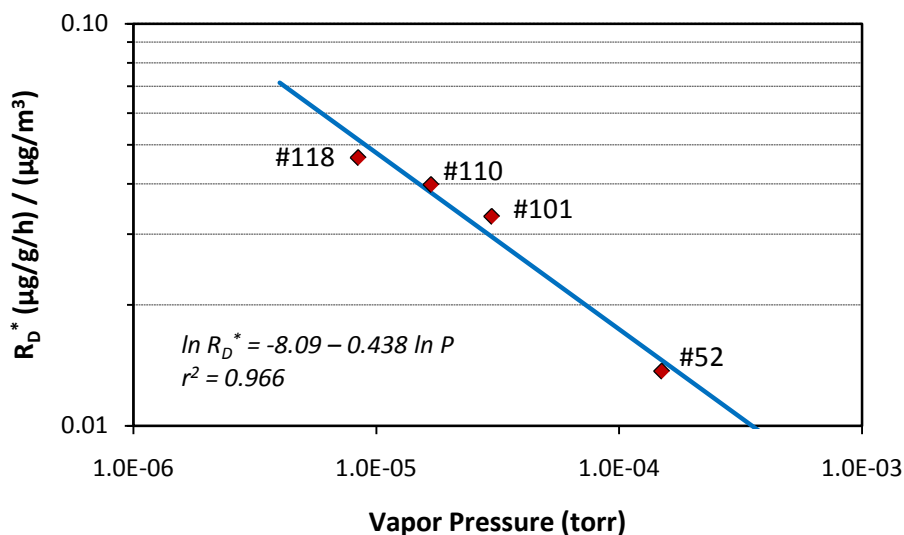


Figure 6.32. Normalized sorption rate ( $R_D^*$ ) as a function of vapor pressure (Test D-2; exposure time = 622 h)

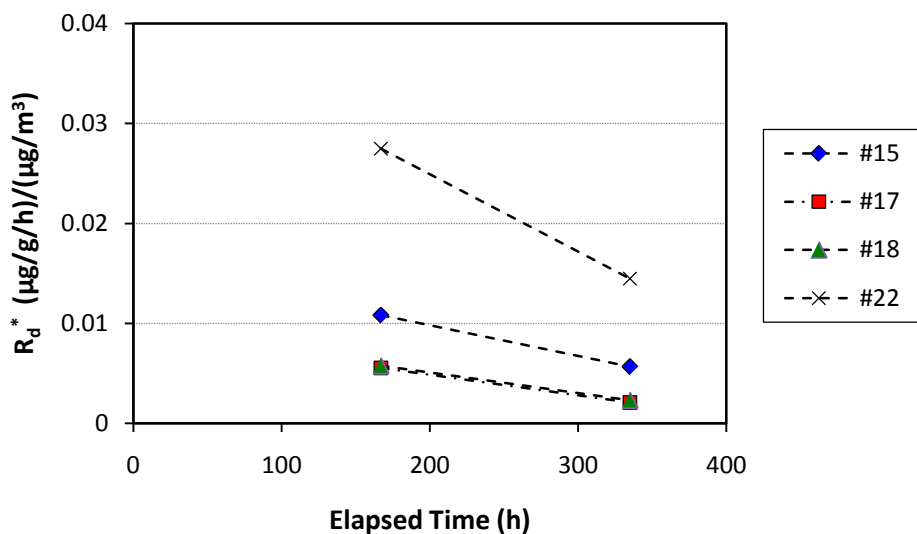
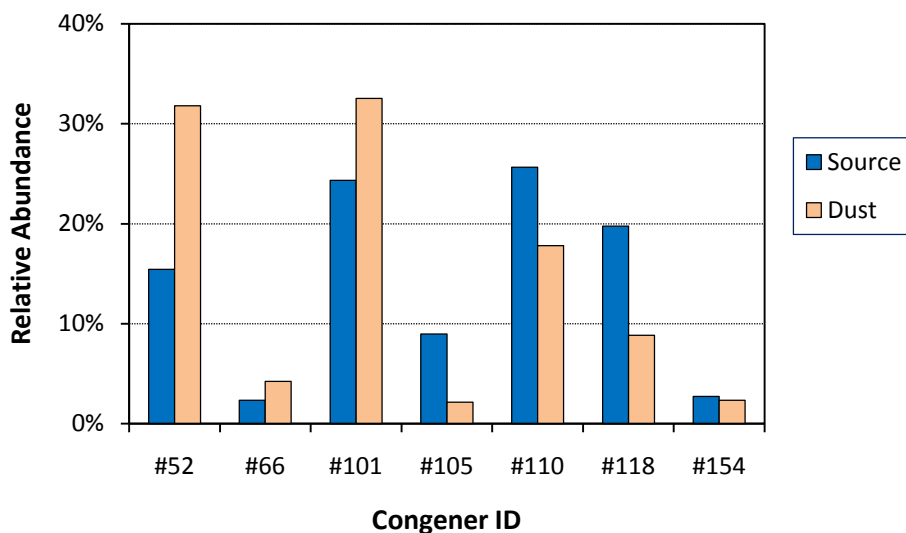


Figure 6.33. Normalized sorption rate ( $R_D^*$ ) for four congeners in Aroclor 1242 (Test D-4)

#### 6.3.2.5 Congener Patterns

Some similarity in congener patterns between the source and the dust was observed. Figure 6.34 compares the relative abundances (i.e., the fractions of individual congeners in the sum of all target congeners) of seven congeners for the source and dust. More discussion on this issue is given in Section 7.3.



**Figure 6.34. Comparison of the congener patterns between the dust collected from PCB-free panels and the source (Test D-2; exposure time = 622 hours)**

### 6.3.3 PCB Transfer Due to Dust/Source Partitioning

#### 6.3.3.1 General Patterns

Dust samples collected from PCB-containing test panels were used to investigate the migration of PCBs from the source to the settled dust due to direct contact. As shown in Figures 6.35 through 6.37, dust/source partitioning is much more effective in PCB transport than dust/air partitioning.

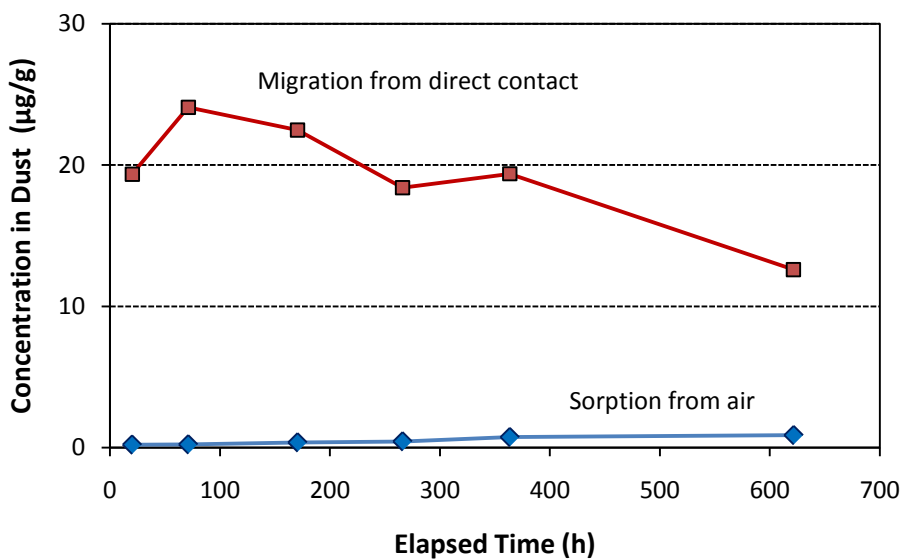


**Figure 6.35. Comparison of PCB accumulations in settled dust for congener #52 in Test D-2**

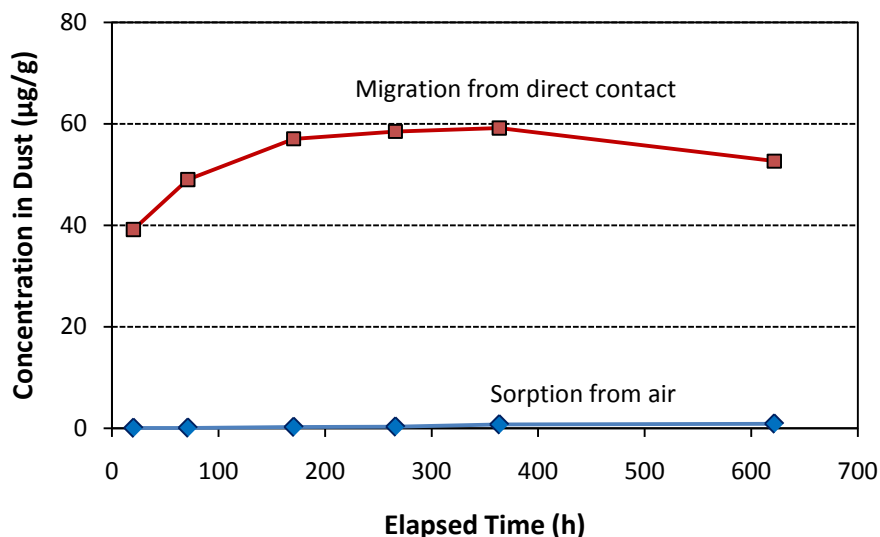


**Figure 6.36. Comparison of PCB accumulations in settled dust for congener #101 in Test D-2**

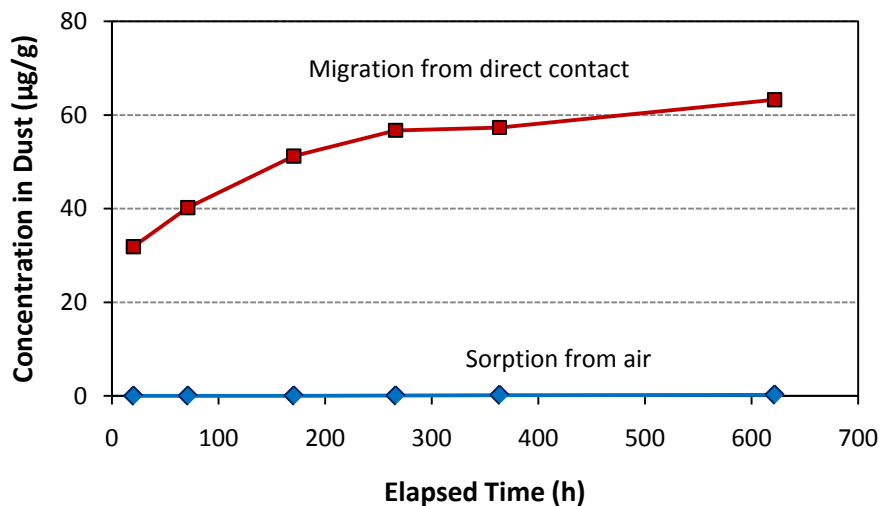


**Figure 6.37. Comparison of PCB accumulations in settled dust for congener #118 in Test D-2**

The migration concentrations for more volatile congeners (such as #52 and #101) decreased with time late in the test (Figures 6.35 and 6.36), suggesting that part of the congener that had accumulated in the dust was re-emitted because of the decrease in the concentration in the air due to the removal of the PCB panels (Figure 6.23). This “escape” phenomenon has been observed by other researchers (Clausen et al., 2004). Although source/dust partitioning was the major transport mechanism, PCB accumulation in dust also was affected by the change in concentrations in the air, especially for more volatile congeners.

### 6.3.3.2 Migration Concentrations

The experimentally determined migration concentrations for the nine congeners in Test D-2 are presented in Figures 6.38.

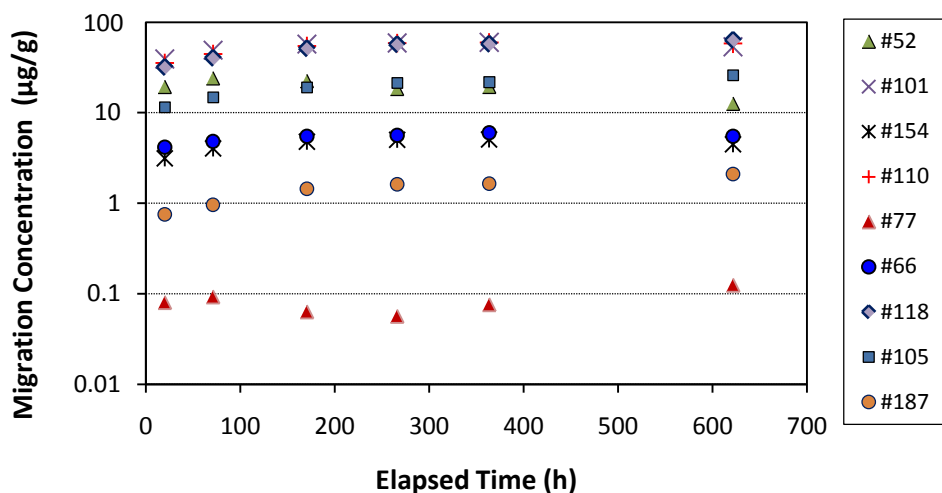


Figure 6.38. Migration concentrations in dust due to direct contact with the source (Test D-2)

### 6.3.3.3 Normalized Migration Concentrations

The normalized migration concentration was calculated by dividing the experimentally determined migration concentration by the congener concentration in the source (Equation 6.4). As shown in Figure 6.39, the migration due to dust/source partitioning was not significantly affected by the volatilities of the congeners.

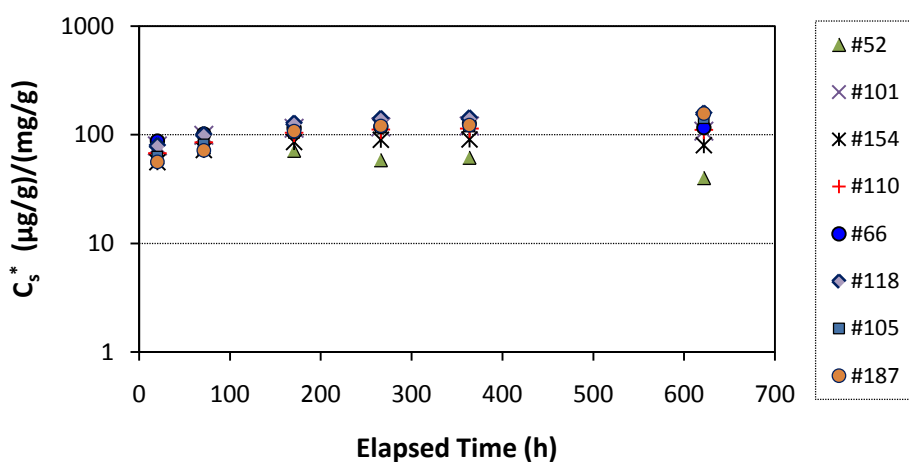
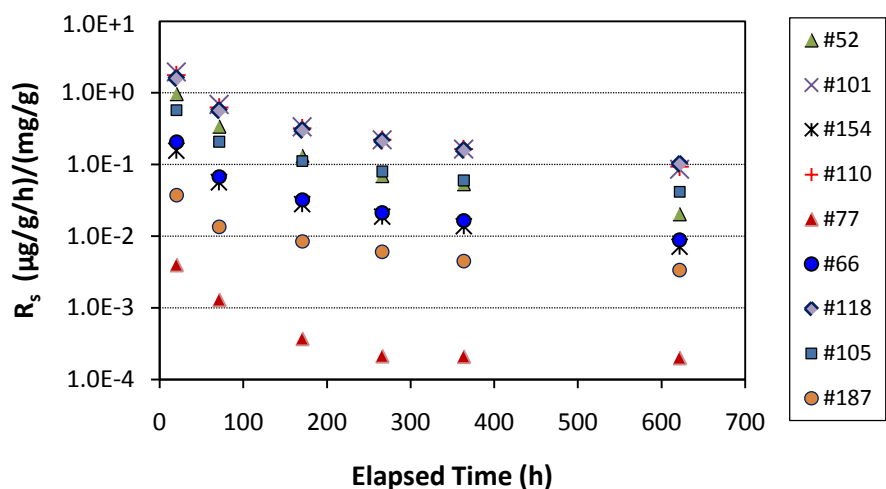


Figure 6.39. Normalized migration concentrations ( $C_s^*$ ) for dust in direct contact with the source (Test D-2; congener #77 was not detected in the air)

#### 6.3.3.4 Migration Rates

The time-averaged migration rate was calculated by dividing the experimentally determined migration concentration by the exposure time. As shown in Figure 6.40, all of the normalized migration rates decreased over time.



**Figure 6.40.** Time-averaged migration rates ( $R_s$ ) for house dust in direct contact with the source (Test D-2)

#### 6.3.3.5 Normalized Migration Rates

As shown in Figure 6.41, the normalized migration rates for different congeners had similar values, indicating that the volatility of the congeners had much less effect on dust/source partitioning than on dust/air partitioning. The greater difference in the late samples likely was caused by the “escape” of volatile congeners, as mentioned in Section 6.3.3.1. Table 6.7 compares four sets of normalized migration rates obtained from three tests, showing good repeatability.

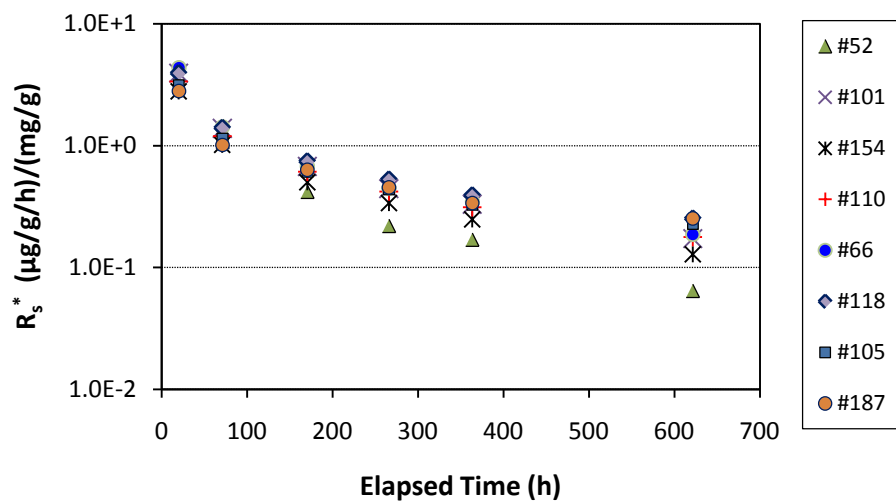


Figure 6.41. Normalized migration rates ( $R_s^*$ ) as a function of time for dust in direct contact with the source (Test D-2; congener #77 was not detected in the air)



**Table 6.7. Comparison of the normalized migration rates for dust samples in direct contact with the source from three chamber tests <sup>[a]</sup>**

Test ID	Aroclor 1254 in source panel (µg/g)	Normalized migration rate [(µg/g) <sub>dust</sub> /(mg/g) <sub>source</sub> ]							
		#52	#66	#101	#105	#110	#118	#154	#187
D-1	8380	46.2	120	105	140	100	140	130	125
D-1	4960	50.0	117	109	138	104	141	121	133
D-2	7710	59.0	124	119	119	113	142	89.1	--
D-3	2370	72.4	190	171	226	175	262	113	157
Mean		56.9	138	126	156	123	171	113	138
RSD		20.4%	25.5%	24.3%	30.6%	28.9%	35.4%	15.4%	12.2%

<sup>[a]</sup> Exposure durations: D-1 = 335 hours, D-2 = 364 hours, D-3 = 356 hours.

The effect of vapor pressure on the normalized migration rate was relatively small (Figure 6.42). As discussed previously, the smaller value for congener #52 in Figure 6.42 was most likely due to the re-emission (i.e., escape) from the dust as its concentration in the air decreased.

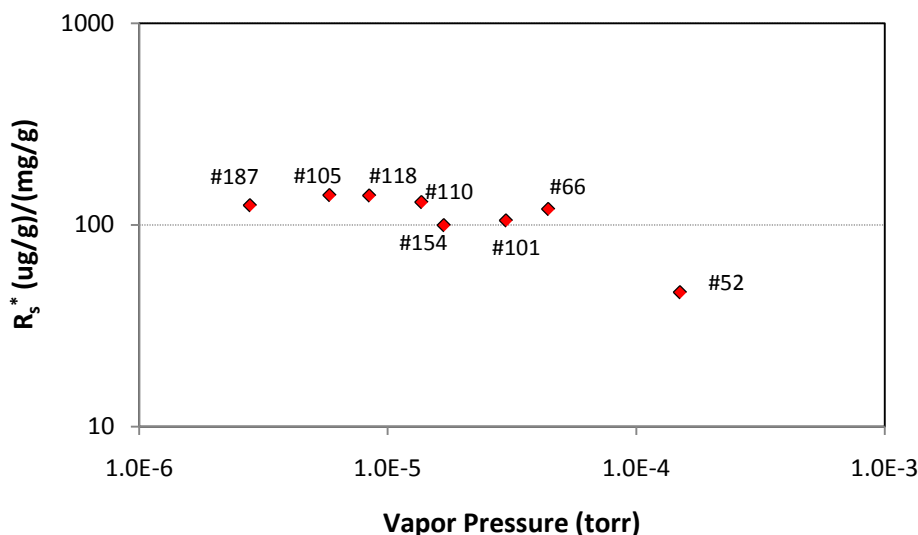


**Figure 6.42.** Normalized migration rate ( $R_s^*$ ) for dust/source partition as a function of vapor pressure (Test D-1;  $t = 335$  h)

#### 6.3.3.6 Congener Patterns in Dust in Direct Contact with the Source

There was some similarity in congener patterns between the source and the dust (Figure 6.43). The relative abundances of volatile congeners appeared higher in the dust collected from the PCB-free panels than in the dust collected from the PCB panels (Figure 6.44).

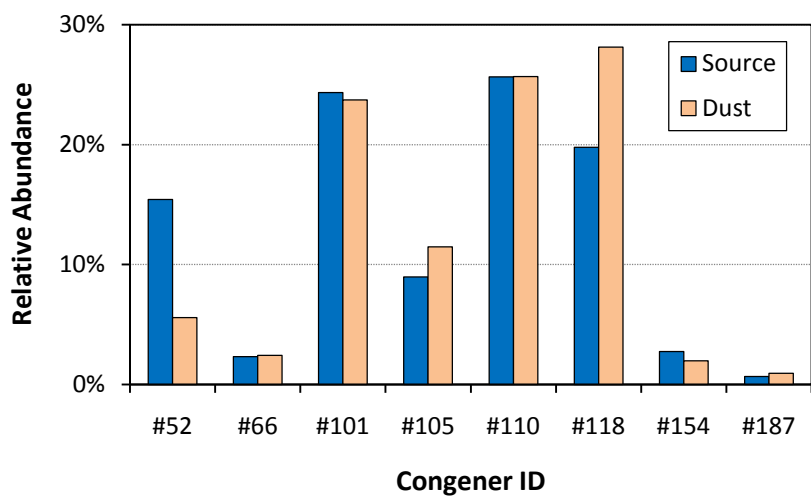


**Figure 6.43.** Comparison of congener patterns between the source and the dust in direct contact with the source (Test D-2;  $t = 622$  h)

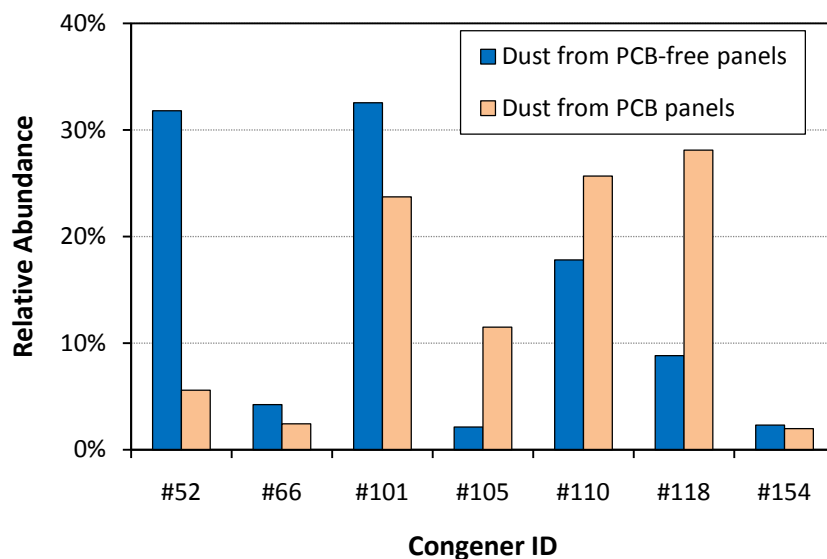


**Figure 6.44.** Comparison of congener patterns between the dust collected from PCB-free panels and the dust collected from the PCB panels (Test D-2; t = 622 h)

#### 6.3.4 Effect of Dust Loading

The effect of dust loading on PCB sorption from air was evaluated by applying different amounts of house dust on PCB-free test panels. The loading range was 0.24, 0.5, 1.0, and 2.0 g per panel, which are equivalent to 7.7, 15, 31, and 62 g/m<sup>2</sup>, respectively. As shown in Table 6.8, the effect of dust loading on PCB sorption from air was not significant in the loading range tested. Similar results were observed for the effect of dust loading on PCB migration due to direct contact with the source (Table 6.9).

**Table 6.8.** Effect of dust loading on the PCB transport due to dust/air partitioning <sup>[a]</sup>

Dust loading (g/m <sup>2</sup> )	Congener Sorption Concentrations in Dust (µg/g)						
	#52	#101	#154	#110	#66	#118	#105
7.71	0.756	0.753	<del>0.066</del>	0.386	<del>0.071</del>	0.176	<del>0.047</del>
15.4	0.518	0.503	<del>0.043</del>	0.251	<del>0.044</del>	0.114	<del>0.029</del>
30.8	0.756	0.763	<del>0.058</del>	0.402	0.085	0.197	<del>0.049</del>
61.7	0.754	0.536	0.039	0.263	0.060	0.125	0.030
Mean	0.696	0.639	0.052	0.326	0.065	0.153	0.039
RSD	17.0%	21.7%	24.7%	24.4%	26.4%	26.2%	28.8%

<sup>[a]</sup> Values in strikethrough font are below the PQL.

**Table 6.9. Effect of dust loading on the PCB transport due to dust/source partitioning <sup>[a]</sup>**

Dust loading ( $\mu\text{g}/\text{m}^2$ )	Congener Migration Concentrations in Dust ( $\mu\text{g}/\text{g}$ )						
	#52	#66	#101	#105	#110	#118	#154
7.71	15.2	<del>5.11</del>	49.6	<del>48.6</del>	49.0	<del>47.7</del>	<del>4.06</del>
15.4	18.7	<del>5.32</del>	54.7	<del>20.0</del>	53.3	<del>52.3</del>	<del>4.55</del>
30.8	19.4	6.01	59.9	<del>21.8</del>	59.6	57.5	<del>5.05</del>
61.7	17.1	5.18	53.0	19.2	52.2	49.1	4.29
Mean	17.6	5.40	54.3	19.9	53.5	51.7	4.49
RSD	10.8%	7.6%	7.9%	7.0%	8.3%	8.4%	9.4%

<sup>[a]</sup> Values in strikethrough font are below the PQL.

### 6.3.5 Effect of Surface Material on Dust/Source Partitioning

To compare the migration concentrations and rates due to direct contact with different types of source surfaces, house dust was loaded onto PCB-containing primer and caulk panels with the same loading ( $30.8 \text{ g}/\text{m}^2$ ), placed side-by-side in the test chamber, and removed from the chamber after 365.5 hours. The migration concentrations were normalized by the congener concentrations in the source. On average, the percent difference between primer and caulk panels was approximately 40% (Figure 6.45).

The dust was difficult to collect from the caulk panels because of the “sticky” surfaces and the finer dust tended to stay on the surface of the caulk panels. Under the same exposure conditions, the degree of sorption saturation (DSS) should be greater for smaller particles. The difference in DSS may have been a factor contributing to the difference shown in Figure 6.45.

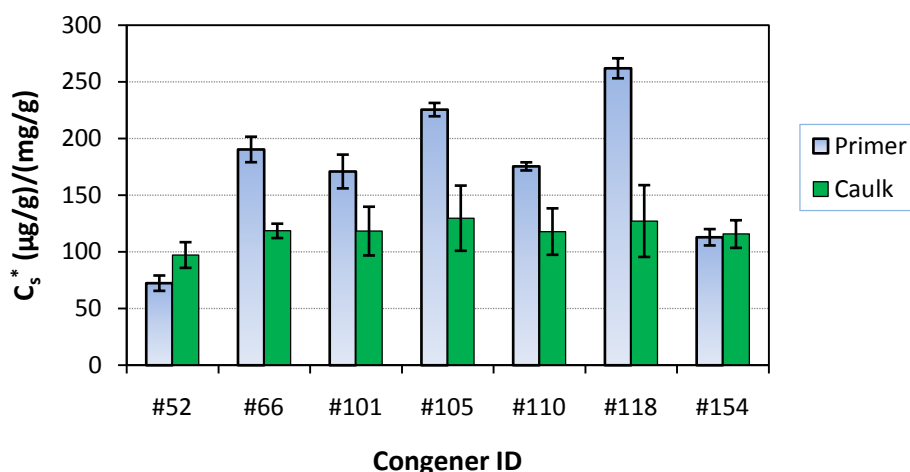


**Figure 6.45. Normalized migration concentration ( $C_s^*$ ) for dust in direct contact with PCB-containing primer and caulk panels in Test D-3 (The error bars represent  $\pm 1$  SD;  $n = 3$  for each data point)**

### 6.3.6 Comparison of Two Types of Dust

All dust data reported above were generated with the house dust. In Test D-4, two types of dust, the house dust and Arizona Test Dust, were compared side by side. Figure 6.46 compares the sorption concentrations in the dust samples collected from the PCB-free panels. Overall, the sorption concentration for Arizona Test Dust was 40% lower than for the house dust.

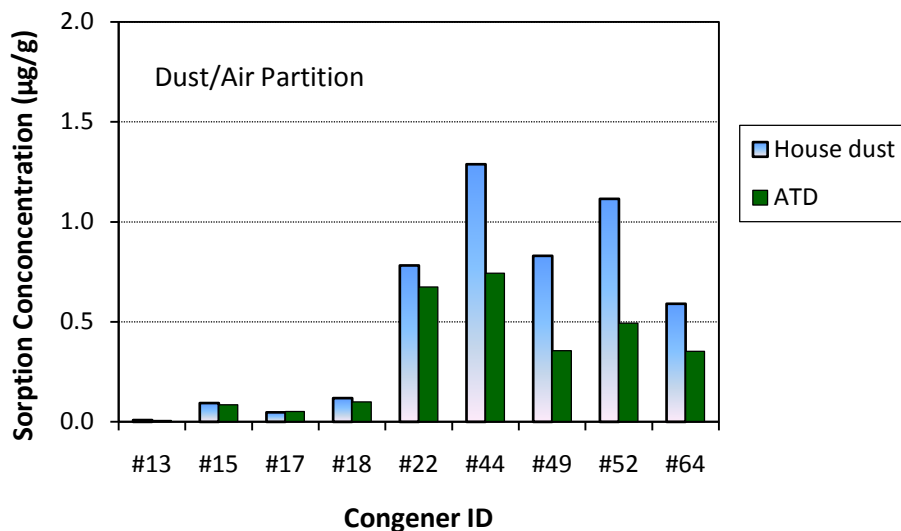


**Figure 6.46. Comparison of sorption concentrations between the house dust and Arizona Test Dust (t = 335 hours)**

An even greater difference was observed for the dust collected from the PCB panels (Figure 6.47). The migration concentrations differed by a factor of five in favor of the house dust.

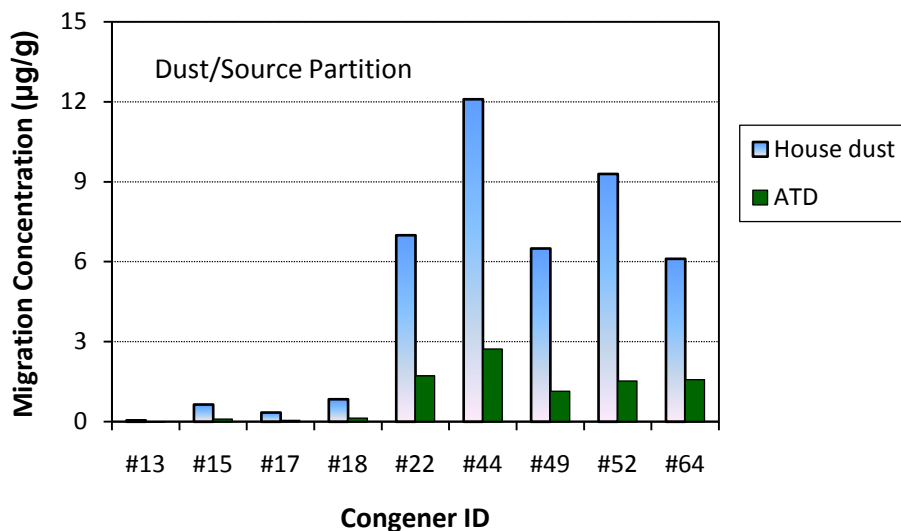


**Figure 6.47. Comparison of migration concentrations between the house dust and Arizona Test Dust (t = 335 hours)**

Under the same exposure conditions, the house dust can take up more PCBs than Arizona Test Dust and the difference is greater for dust/source partitioning than for dust/air partitioning. The particles of the Arizona Test Dust are much smaller in size and have much greater surface area than the particles of the house dust (Table 4.4 in Section 4.2.1). These features usually make pollutant transport easier, but the results indicated the opposite. The difference between the two types of dust was likely caused by the difference in their lipophilicity. The house dust contains 19.3% organic carbon as opposed to nearly no organic carbon for the ATD (Table 4.4). In general, organic compounds are more lipophilic than most inorganic compounds.

## 6.4 PCB Sorption in Test Chambers

### 6.4.1 Sorption by the Walls of the 44-mL Micro Chamber

The amount of a congener adsorbed by the interior walls of the microchamber as percentage of the total emission from the caulk sample was calculated by using Equation 6.13:

$$f_w = \frac{M_w}{M_{out} + M_w} \times 100\% \quad (6.13)$$

where  $f_w$  = percent sorption by the walls of the microchamber

$M_w$  = congener mass adsorbed by the walls of the chamber (µg)

$M_{out}$  = congener mass leaving the chamber during the emission test, from Equation 6.14 (µg)

$$M_{out} = C_a Q t \quad (6.14)$$

where  $M_{\text{out}}$  = congener mass leaving the chamber during the emission test ( $\mu\text{g}$ )

$C_a$  = average concentration of congener in the air ( $\mu\text{g}/\text{m}^3$ )

$Q$  = air change flow rate ( $\text{m}^3/\text{h}$ )

$t$  = test duration (h)

The results are presented in Tables 6.10 and 6.11. Overall, the sorption by the walls of the microchamber represented a small fraction of the total emissions and, thus, the effect of wall sorption on emissions testing was insignificant. Like other sink materials, the sorption by the walls of the microchamber favored less volatile congeners (Figure 6.48).

**Table 6.10. Amounts of PCB congeners adsorbed by the walls of the microchamber as determined by wipe sampling (units:  $\mu\text{g}$ )** <sup>[a] [b] [c]</sup>

Congener ID	Caulk CK-11a		Caulk CK-12	
	Before test	After test	Before test	After test
#17	ND	ND	ND	ND
#52	ND	ND	ND	$4.49 \times 10^{-2}$
#101	ND	<del><math>1.65 \times 10^{-2}</math></del>	ND	$2.10 \times 10^{-1}$
#154	ND	ND	ND	$6.82 \times 10^{-2}$
#110	ND	ND	ND	$5.66 \times 10^{-1}$
#77	ND	ND	ND	ND
#66	ND	ND	ND	$6.35 \times 10^{-2}$
#118	ND	<del><math>1.80 \times 10^{-3}</math></del>	ND	$5.52 \times 10^{-1}$
#105	ND	<del><math>4.89 \times 10^{-4}</math></del>	ND	$2.64 \times 10^{-1}$
#187	ND	<del><math>3.42 \times 10^{-4}</math></del>	ND	<del><math>1.90 \times 10^{-2}</math></del>

<sup>[a]</sup> Caulk samples CK-11 and CK-12 contained 9128 and 103000  $\mu\text{g}/\text{g}$  of Aroclor 1254, respectively (Guo et al., 2011).

<sup>[b]</sup> Values in strikethrough font are below the PQL.

<sup>[c]</sup> Test duration was 146 hours for both samples.

**Table 6.11. Amounts of PCB congeners adsorbed by the walls of the microchamber after the tests as a fraction of the total emissions <sup>[a]</sup>**

Congener ID	Caulk CK-11a			Caulk CK-12		
	M <sub>w</sub> (μg)	M <sub>out</sub> (μg) <sup>[b]</sup>	f <sub>w</sub>	M <sub>w</sub> (μg)	M <sub>out</sub> (μg) <sup>[b]</sup>	f <sub>w</sub>
#17	--	--	--	--	--	--
#52	--	--	--	4.49×10 <sup>-2</sup>	8.53×10 <sup>1</sup>	0.05%
#101	<del>1.65×10<sup>-2</sup></del>	1.92×10 <sup>-0</sup>	<del>0.85%</del>	2.10×10 <sup>-1</sup>	3.44×10 <sup>1</sup>	0.61%
#154	--	--	--	6.82×10 <sup>-2</sup>	3.39×10 <sup>0</sup>	1.97%
#110	--	--	--	5.66×10 <sup>-1</sup>	1.71×10 <sup>1</sup>	3.20%
#77	--	--	--	--	--	--
#66	--	--	--	6.35×10 <sup>-2</sup>	6.97×10 <sup>0</sup>	0.90%
#118	<del>1.80×10<sup>-3</sup></del>	5.12×10 <sup>-1</sup>	<del>0.35%</del>	5.52×10 <sup>-1</sup>	8.06×10 <sup>0</sup>	6.4%
#105	<del>4.89×10<sup>-4</sup></del>	1.33×10 <sup>-1</sup>	<del>0.37%</del>	2.64×10 <sup>-1</sup>	2.43×10 <sup>0</sup>	9.8%
#187	<del>3.42×10<sup>-4</sup></del>	6.92×10 <sup>-3</sup>	<del>4.7%</del>	<del>1.90×10<sup>-2</sup></del>	1.19×10 <sup>-1</sup>	<del>13.8%</del>

<sup>[a]</sup> Values in strikethrough are below the PQL.

<sup>[b]</sup> From Equation 6.14; data from Guo et al. (2011).

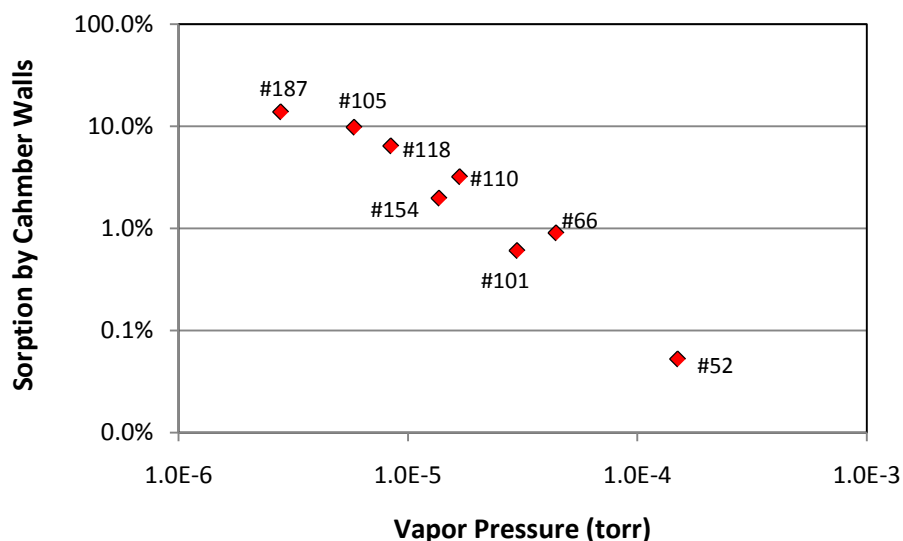


**Figure 6.48. Sorption by the walls of the microchamber as a function of vapor pressure of congeners**

#### 6.4.2 Sorption by the Walls of the 53-L Chamber

The sorption by the interior walls of the 53-L chamber was evaluated by conducting a sink test (See Figure 4.2) with an empty test chamber, and the percent sorption was calculated using Equation 6.15:



$$f_w = \frac{C_{in} - C_{out}}{C_{in}} \times 100\% \quad (6.15)$$

where  $f_w$  = percent sorption by the walls of the chamber

$C_{in}$  = concentration in the air at the inlet to the chamber ( $\mu\text{g}/\text{m}^3$ )

$C_{out}$  = concentration in the air at the outlet from the chamber ( $\mu\text{g}/\text{m}^3$ )

The results of duplicate tests (CS-1 and CS-2) are presented in Table 6.12.

**Table 6.12. Measured congener concentrations at the air inlet and outlet and percent sorption by the empty 53-L chamber <sup>[a]</sup>**

Test ID	Sampling point	Congener ID						
		#17	#52	#66	#101	#110	#118	#154
SC-1 <sup>[b]</sup>	Inlet ( $\mu\text{g}/\text{m}^3$ )	0.53	17.7	1.50	5.08	2.31	0.72	0.47
	Outlet ( $\mu\text{g}/\text{m}^3$ )	<del>0.35</del>	5.85	0.21	0.98	0.34	0.10	0.09
	Adsorbed	34.2%	66.9%	85.7%	80.7%	85.3%	86.8%	81.9%
SC-2 <sup>[c]</sup>	Inlet ( $\mu\text{g}/\text{m}^3$ )	0.37	14.9	0.75	5.30	2.50	0.76	0.50
	Outlet ( $\mu\text{g}/\text{m}^3$ )	0.23	4.90	0.15	0.87	0.28	0.07	0.07
	Adsorbed	38.7%	67.1%	79.4%	83.6%	88.9%	90.7%	85.8%

<sup>[a]</sup> Values in strikethrough are below the PQL.

<sup>[b]</sup> Air sampling started at 1.1 elapsed hours after the source was turned on.

<sup>[c]</sup> Air sampling started at 1.6 elapsed hours after the source was turned on.

The results in Table 6.12 show that the sorption by the walls of the 53-L chamber was too severe to test any sources that contain Aroclor 1254. For sources that contain Aroclor 1242, such as the light ballasts tested by Guo et al. (2011), the sorption was less severe but still significant. To estimate the chamber sorption for the major congeners in the emissions of Aroclor 1242, the two sets of data in Table 6.12 were combined to fit an exponential curve (Equation 6.16 and Figure 6.49):

$$f_w = 0.876 \times e^{-1560P} \times 100\% \quad (r^2 = 0.9995) \quad (6.16)$$

where  $f_w$  = percent sorption by the walls of the chamber

P = vapor pressure of the congener (torr)

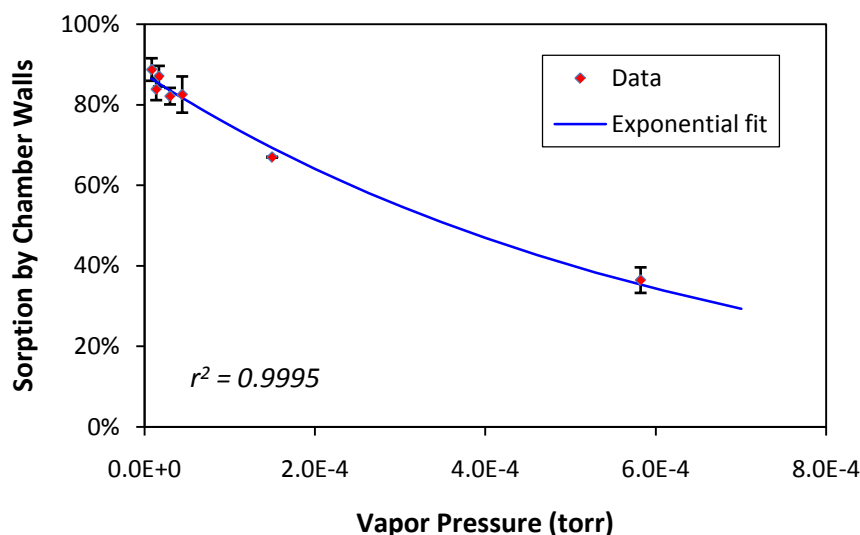


**Figure 6.49. Experimental results and exponential fit for sorption of PCB congeners by the interior walls of the 53-L chamber as a function of vapor pressure (error bar =  $\pm 1$  SD)**

The emissions data for the light ballasts showed that congener #18 was the most predominant congener in the emissions, followed by congeners #17 and #22 (Guo et al., 2011). By inserting the vapor pressures for these congeners into Equation 6.16, the sorption by the walls can be estimated. As shown in Table 6.13, the sorption by the walls may have caused underestimation of the PCB emission rates from light ballasts by over 30% for congener #18, the most predominant congener in the emissions.

**Table 6.13. Estimated congener sorption by the 53-L chamber for the three most predominant congeners in the emissions of Aroclor 1242**

Congener ID	Vapor Pressure (torr) <sup>[a]</sup>	Sorption by Chamber Walls (%)
#17	$5.82 \times 10^{-4}$	35%
#18	$6.38 \times 10^{-4}$	32%
#22	$1.97 \times 10^{-4}$	64%

<sup>[a]</sup> Data from Fischer et al. (1992), Method B.

Because the air sampling was started shortly after the start of the tests, the results presented in Tables 6.12 and 6.13 represent the worse-case scenario for the 53-mL chamber, i.e., when the sorption rates were the highest. The sorption should be less severe for longer test durations because the sorption rate decreases over time (See section 6.2.2.3).

To reduce the sink effect caused by the test chamber in future tests, smaller chambers are preferred, the chambers should be constructed of materials with small sorption capacity for PCBs, or the stainless steel walls should be coated with such materials. For example, a chamber made of or coated with PTFE may

perform better than one made of stainless steel because Cseh et al. (1989) have shown that PTFE does not adsorb PCBs significantly.

The effect of the sorption by chamber walls on sink testing is different from that on source testing. The results presented above are applicable only to source testing (i.e., emissions testing). The effect of wall sorption on sink testing depends on the selection of test methods (Section 3.1). For the conventional method, the sorption by chamber walls must be considered. For the microbalance method and the method used in this study, only the air concentration in the outlet matters.

## **7. Discussion**

### **7.1 The General Behavior of PCB Sinks**

The results of the sink tests presented in Section 6.2 demonstrate that the PCB flux between the air and the sink material can go in either direction (hence the term “reversible sink”). In the presence of a primary source, the sink material usually adsorbs PCBs from the air (i.e., negative emission rates). After the primary source is removed, the sink material becomes a re-emitting source. Such behavior helps explain the results of some remediation efforts in the field where major primary PCB sources had been removed but the PCB concentrations in the air remained higher than expected. Thus, control of potential re-emissions from sink materials after the primary sources are removed must be considered in the remediation plan. Understanding the behavior of reversible sinks is also important to exposure assessment. It is not recommended to estimate the total source strength in a building by summing all potential sources. Primary sources and PCB sinks should be evaluated separately.

### **7.2 The Significance of PCB Sinks as Secondary Sources**

The PCB sinks can affect indoor environmental quality and exposure in several ways including elevated air concentrations due to re-emissions, as a source for dermal exposure, and generation of PCB wastes. As described above, the contaminated interior surface materials may become re-emitting sources after the primary sources are removed. Although the PCB concentrations in the sink materials are much lower than in the primary sources, which is especially true for material/air partitioning, the exposed areas of the sink materials are often much larger than the primary sources. Thus, the effect of re-emissions from PCB sinks after removal of primary sources may not always be negligible. Materials containing 50 ppm or more PCBs are regulated by the Federal Toxic Substance Control Act (TSCA). Field measurements show that PCB accumulation in building materials can exceed the 50 ppm level (Weis et al., 2003; EH&E, 2012). Contaminated building materials are also potential sources for dermal exposure. Contaminated dust is a potential source for inhalation (if re-suspended) and ingestion exposure.

### **7.3 Comparison of Different Sink Materials**

Understanding the relationship between material type and sink strength is of practical importance because such knowledge may help environmental engineers identify the most important PCB sinks in a building. In this study, the experimentally determined sorption concentrations showed significant difference from material to material. For examples, a petroleum-based paint, a latex paint, and a certain type of carpet were among the strongest sinks, whereas solvent-free epoxy coating, certain types of flooring materials, and brick were among the weakest sinks (Figure 6.9 through 6.11). The authors cannot explain, however, why carpet A can adsorb three times more PCBs than carpet B and why the concrete can adsorb 25 times more than the brick.

To better understand the relationship between the properties of the material and its sink behavior, different types of experiments are needed. Cseh et al. (1989) studied the adsorption and desorption of PCBs by polymers in aqueous solutions and found that soft polymers tend to adsorb more PCBs than hard polymers. Similar screening methods can be developed for studying material/air partitioning for PCBs. In addition, determination of the key properties of the materials, such as lipophilicity and porosity, is equally important.

## 7.4 Ranking Building Materials as PCB Sinks

There are at least three ways by which building materials can be ranked for their sink strengths for PCBs: (1) using the experimentally determined normalized sorption concentrations ( $C_m^*$ ) presented in Section 6.2.2.2, (2) using the sorption capacity described above, or (3) using the sink sorption index (SSI). Although comparing the sorption concentrations is straightforward, their values are a function of time and the test method is difficult to standardize. The last two methods are discussed below

The sorption capacity is determined by two parameters, i.e., the concentration of the congener in the air ( $C_a$ ) and the material/air partition coefficient for the congener and the material ( $K_{ma}$ ). With the roughly estimated material/air partition coefficients presented in Table 6.5, the sorption capacity can be calculated from Equations 2.1 or 2.3. In Table 6.5, the rough estimates of the material/air partition coefficients for congener 52 for the 20 materials ranged from  $2.65 \times 10^6$  to  $2.54 \times 10^7$ . Thus, if the concentration in air is  $1 \mu\text{g}/\text{m}^3$ , the sorption capacity will range from  $2.65 \times 10^6$  to  $2.54 \times 10^7 \mu\text{g}/\text{m}^3$ . A more useful tool for ranking the sink materials is described in Section 7.2, below. A major drawback of this method is that the sorption capacity is applicable only to the equilibrium conditions.

The sink sorption index (SSI) uses two parameters, i.e., the partition and diffusion coefficients ( $K_{ma}$  and  $D_m$ ). A previous study showed that, for a given sink material, the products of the partition and diffusion coefficients,  $K_{ma} \times D_m$ , for the individual constituents of the same class of chemicals have the same order of magnitude (Xu et al., 2008), whereas the partition and diffusion coefficient data presented in Table 6.5 show that the products of  $K_{ma} \times D_m$  for different materials cover a range of almost four orders of magnitude. Thus,  $K_{ma} \times D_m$  can be used to compare the sink strengths of different materials. For simplicity, the sink sorption index (SSI) is defined by Equation 7.1:

$$SSI = -\log(K_{ma} D_m) \quad (7.1)$$

This definition is easy to understand because of its similarity to the definition of pH (Equation 7.2):

$$pH = -\log[H^+] \quad (7.2)$$

The result of Equation 7.2 is that stronger acids have lower pH values. Analogously, stronger sinks have smaller SSI values. Table 6.5 lists the SSIs for the sink materials tested and Figure 7.1 shows the correlation between SSI and the experimentally determined normalized sorption concentrations for congener #52.

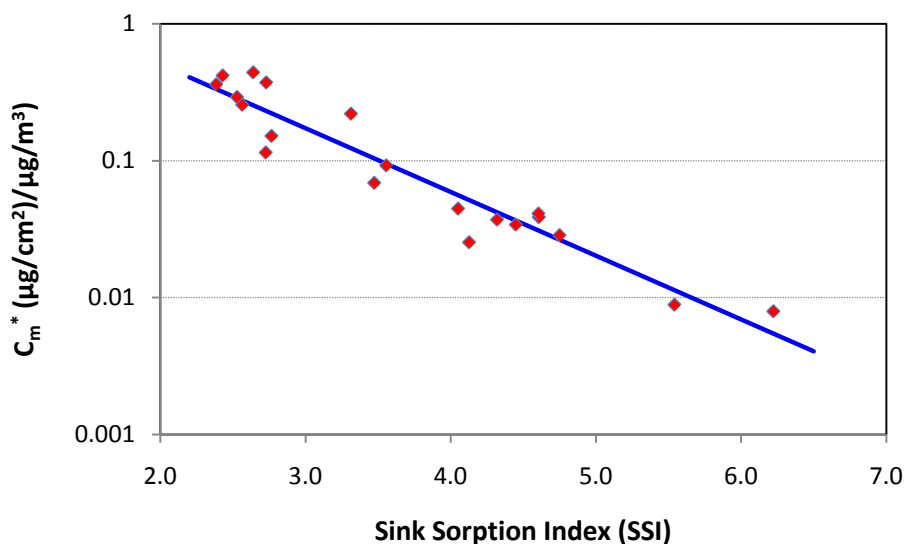


**Figure 7.1. Correlation between SSI and experimentally determined normalized sorption concentrations ( $C_m^*$ ) for congener #52 ( $t = 269$  h for data from Test S-2 and  $t = 240$  h for data from Test S-3)**

## 7.5 Similarity of Congener Patterns between the Primary Sources and PCB Sinks

Other researchers have observed that the congener pattern for a sink material often looks similar to the pattern for the primary source (Garbriio et al., 2000). The same observation was made in this study. This similarity, if proven to be accurate, will make it difficult, if not impossible, to differentiate between primary sources and PCB sinks solely based on congener patterns. Thus, understanding the congener patterns for PCB sinks is of both practical and theoretical importance.

The similarity in congener patterns between the primary sources and PCB sinks can be explained by the combined effect of two factors: (1) the emissions from the primary source favor the volatile congeners, and (2) the sorption by the PCB sink favors the less volatile congeners. These two factors offset each other. As a result, the congener pattern for the PCB sink is often similar, but not identical, to the congener pattern for the primary source.

For demonstration purposes, simulations were made by using a PCB-containing caulk as the primary source, and concrete and brick as the PCB sinks. The congener emissions from the caulk were calculated by the method presented in Part 1 of this report series (Guo et al., 2011). The partition coefficients presented in Table 6.5 were used to calculate the sorption capacities for concrete and brick. Key parameters are presented in Table 7.1, and details of the calculations are provided in Appendix D. Figures 7.2 and 7.3 compare the congener patterns of the primary sources and PCB sinks. Some similarity in congener patterns can be seen in the two cases.

**Table 7.1. Parameters used to model the congener patterns in concrete and brick as PCB sinks**

Parameter Category	Parameter	Value	Notes
Building	Room volume	300 m <sup>3</sup>	
	Air change rate	1 h <sup>-1</sup>	
Primary source	Source type	Caulk	
	PCB content	100000 µg/g	Aroclor 1254
	Exposed area	0.2 m <sup>2</sup>	
	Congeners modeled	Top 25 in Aroclor 1254	[a]
PCB sink — concrete	Material/air partition coefficient ( $K_{ma}$ ) for #52	$2.11 \times 10^7$ [b]	From Table 6.5
	Index $\alpha$ in Eq. 6.9	0.544 [b]	From Table 6.5
PCB sink — brick	Material/air partition coefficient ( $K_{ma}$ ) for #52	$2.65 \times 10^6$	From Table 6.5
	Index $\alpha$ in Eq. 6.9	1.07	From Table 6.5

[a] Frame et al. (1996).

[b] Average of three estimates.

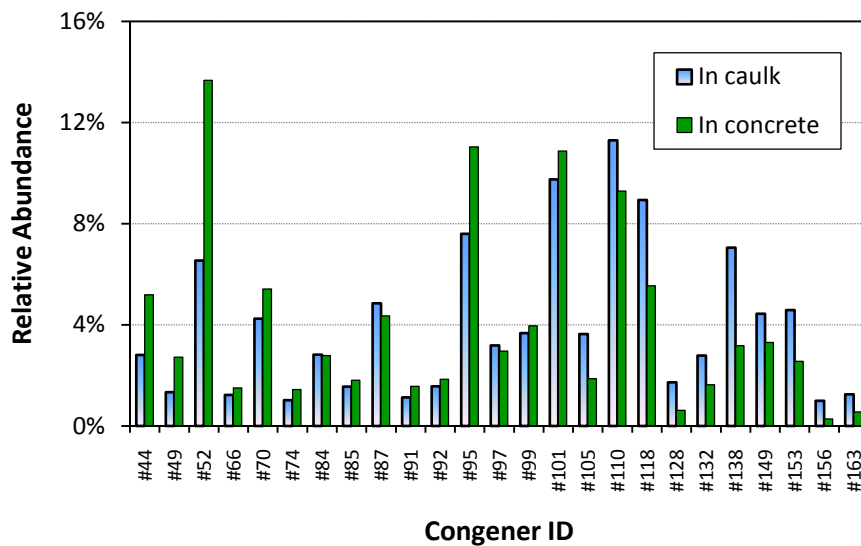


**Figure 7.2. Comparison of congener patterns of the primary source (caulk) and the PCB sink (concrete)**

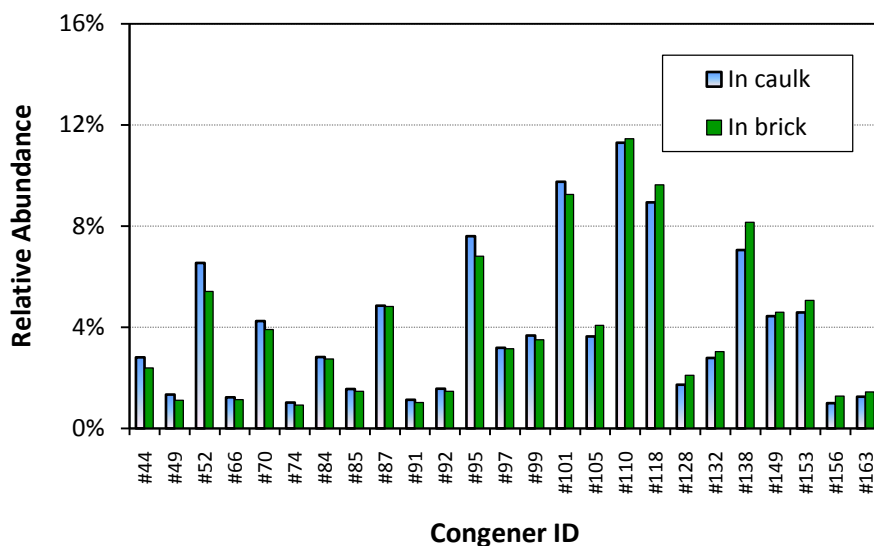


**Figure 7.3. Comparison of congener patterns of the primary source (caulk) and the PCB sink (brick)**

As a practical matter, it may be important to differentiate between the primary sources and PCB sinks. Although the similarity of congener patterns makes such differentiation difficult, there are still ways to determine whether a PCB source is primary or secondary because the distributions of PCBs in these sources are different. For instance, for a PCB sink due to material/air partitioning, the PCBs are concentrated in a thin layer of the material below the exposed surface (See Section 7.6.2 below). On the other hand, the PCB distribution in a primary source is often nearly uniform. Thus, if a core sample is taken perpendicular to the exposed surface and the PCB concentrations at different depths are determined, one should be able to determine whether the source is primary or secondary. This method does not work for coating materials, however, because the material is too thin.

## 7.6 Effects of Temperature and Relative Humidity on Sorption by Sink Materials

This study did not investigate the effects of temperature and relative humidity on the behavior of PCB sinks. Given the potential importance of this topic to the remediation efforts, information that is available in the literature is presented in Appendix E.

## 7.7 Predicting Congener Concentrations in the Sink Material

The sorption of PCB congeners by a sink material can be predicted by using either the DSS models or the dynamic sink models. The following demonstration predicts the concentrations of congeners #118 and #156 in concrete by using the DSS model proposed by Crank (1975) (i.e., Equation 2.6).

The calculation includes three steps: (1) estimation of the partition and diffusion coefficients for the two congeners by using the data in Table 6.5, (2) calculating the degree of sorption saturation (DSS) by using Equation 2.6, and (3) calculating the sorption concentrations by using Equation 2.5. The assumed exposure conditions are as follows:



- Average air concentration for congener #118:  $0.05 \mu\text{g}/\text{m}^3$
- Average air concentration for congener #156:  $0.01 \mu\text{g}/\text{m}^3$
- Exposure duration: 40 years.

The congeners in the concrete were also assumed to be concentrated in a 1-cm-thick layer near the exposed surface (i.e., material thickness = 1 cm with one side exposed). The step-by-step calculations are presented in Appendix F.

The predicted DSSs are presented in Figure 7.4, and the congener concentrations in the material are presented in Figure 7.5. After four decades of exposure, the concrete is still not saturated even within 1-cm depth.

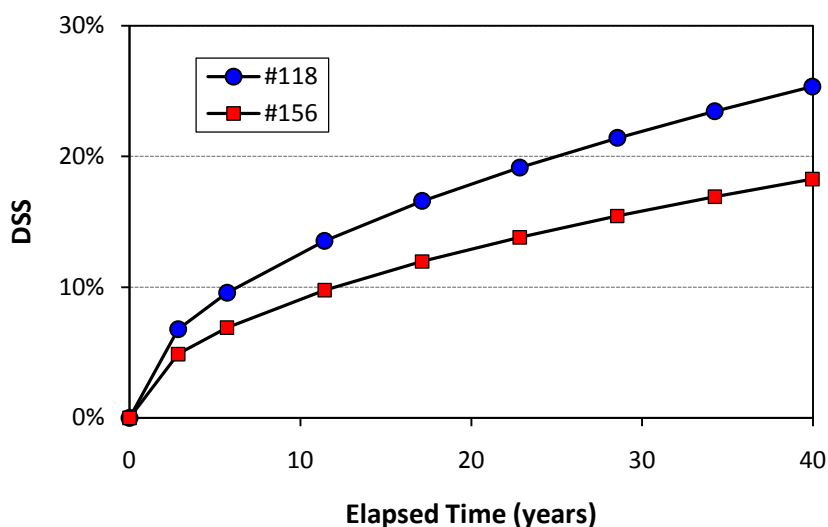


**Figure 7.4. Predicted DSS for congeners #118 and #156 in concrete**

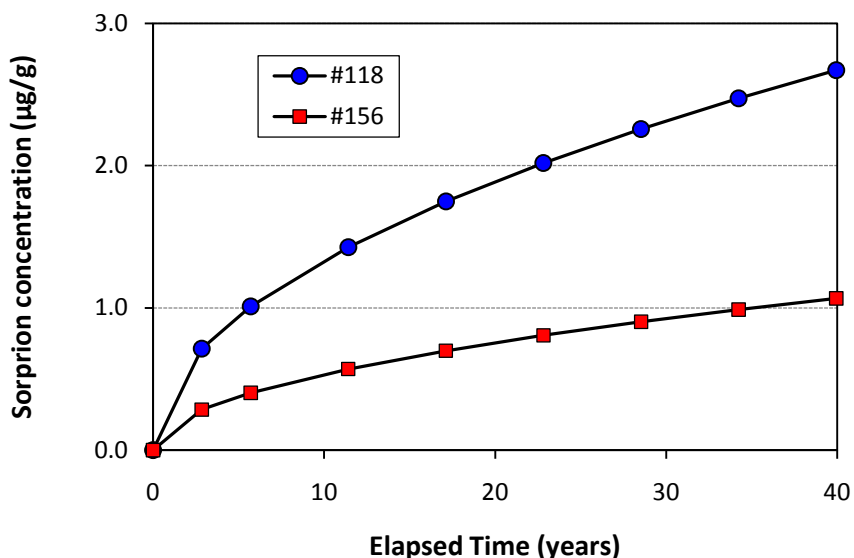


**Figure 7.5. Predicted concentrations for congeners #118 and #156 in concrete.**

The DSS model does not predict the concentration profiles in the sink material as a function of depth. To predict the distribution of congeners in the sink material, dynamic sink models, which are computationally intensive, must be used (See Section 7.6, below.)

## 7.8 Using the Dynamic Sink Models

### 7.8.1 Predicting the Concentrations in Air after Removal of the Primary Source

Dynamic sink models can be used to predict the concentrations in the air due to the re-emissions from a sink material as a secondary source after the primary source is removed. In the demonstration below, the model (Equations 2.16 through 2.19) developed by Little and Hodgson (1996) was used to predict the re-emission of congener #52 from concrete walls in a room. A MATLAB version of the simulation program was obtained from the developer of the model. The assumed conditions are presented in Table 7.2. The predicted concentrations in room air are shown in Figure 7.6. The results should be considered semi-quantitative because of the uncertainties in the partition and diffusion coefficients and because of the highly simplified exposure scenario (i.e., constant concentration in air for 40 years).

**Table 7.2. Input parameters for predicting the re-emission of congener #52 from concrete walls after the primary source is removed**

Parameter Category	Parameter	Value	Notes
Building	Volume	300 m <sup>3</sup>	
	Air change rate	1 h <sup>-1</sup>	
Sink material (concrete walls)	Area	400 m <sup>2</sup>	
	Thickness	1 cm	
	Material/air partition coefficient for #52	$2.11 \times 10^7$	From Table 6.5
	Diffusion coefficient for #52	$2.98 \times 10^{-11}$ m <sup>2</sup> /h	From Table 6.5
Exposure scenario	Concentration in air	0.5 µg/m <sup>3</sup>	[a]
	Exposure duration	40 years	

<sup>[a]</sup> This is  $C_{in}$  in Equation 2.16, the concentration in the air due to the emissions from the primary sources.

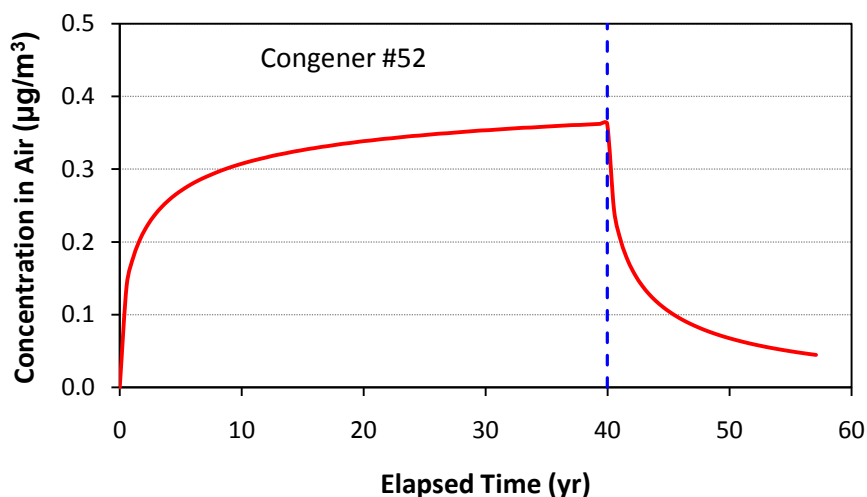


**Figure 7.6. Re-emission of congener #52 from concrete walls after the primary source was removed at 40 years elapse**

### 7.8.2 Predicting the PCB Distribution in the Sink Material

The dynamic sink models can also be used to predict the distribution of the PCB congeners in the sink material. The results can be used to determine the level of contamination as a function of the depth of the material. In the demonstration below, the parameters in Table 7.3 were used except the concentration in air was 0.1 µg/m<sup>3</sup>. The sink model developed by Little and Hodgson (1996) was used for the calculations (See Equations 2.16 through 2.19.) The simulation results are presented in Figure 7.7.

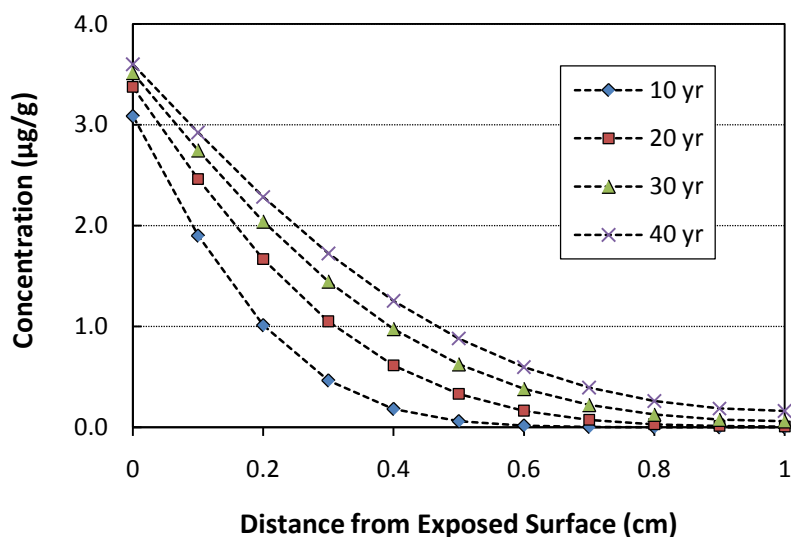


**Figure 7.7 Predicted distribution of congener #52 in the 1-cm-thick layer of concrete**

## 7.9 Rough Estimation of the Material/Source Partition Coefficients for House Dust

The experimental results with the house dust showed that the migration concentrations of PCB congeners in the house dust that was in direct contact with the source were relatively stable over time (Figure 6.38). Thus, for a given congener, the ratio between its concentration in the dust and its concentration in the source can provide a rough estimate of the material/source partition coefficient (i.e.,  $K_{12}$  in Equation 2.21). Using the data from Test D-2, the estimated  $K_{12}$  values ranged from 0.04 to 0.16 (Table 7.3). These values are indicative of the sink strength of the house dust being in the middle or lower-middle range. That is, the house dust tested is a modest sink for PCBs.

**Table 7.3. Roughly estimated dust/source partition coefficients for the house dust collected from PCB-containing primer panels**

	Congener ID							
	#52	#66	#101	#105	#110	#118	#154	#187
In dust (µg/g) <sup>[a]</sup>	12.6	5.50	53.6	25.9	58.0	63.5	4.46	2.10
In primer (µg/g)	316	47.6	498	183	525	405	<del>56.0</del>	<del>13.41</del>
$K_{12}$	0.04	0.12	0.11	0.14	0.11	0.16	0.08	0.16

<sup>[a]</sup> Collected from test panels coated with a primer that contained known amounts of PCBs.

## 7.10 Study Limitations

In this report, methods, data, and tools are presented that should help decision makers, environmental engineers, researchers, and the general public better understand the PCB sinks in PCB-contaminated

buildings. However, since a single study cannot address all the important questions that must be answered, this study represents only the beginning in the effort to fill an important data gap in PCB sorption by sink materials and the re-emission of the PCBs from these materials. The scope of this study was necessarily limited. Some specific research limitations are discussed below.

This study was limited only to laboratory testing. This study complements and supplements an ongoing field study conducted by EPA.

Because of time constraints, this study tested only a small number of sink materials (20 building and furniture materials and two types of dust). The number of tests conducted was also rather small. There are many types of building and furniture materials, and there are many brands and varieties of each type, all of which have different physical and chemical properties. Thus, care should be taken when applying the test results to seemingly similar materials in real-world situations.

Three mass transfer mechanisms have been identified that are responsible for pollutant transport from indoor sources to sink materials and dust: (1) material/air partitioning, (2) material/material partitioning, and (3) particle formation due to weathering of the source or mechanical forces such as abrasion. This study focused on the first mechanism. The second mechanism was evaluated for settled dust only; PCB transport between two adjacent building materials was not studied. The third mechanism was not evaluated.

The material/air partition coefficient and solid-phase diffusion coefficient are two key parameters for characterizing sink materials. The values presented in this study are rough estimates. More accurate estimation requires that they be determined independently. The DSS model used to estimate these parameters (see Section 2 and Appendix C) are more suitable for porous materials than for non-porous and impenetrable materials such as uncoated metal sheets. For the latter, the Langmuir model may work better.

In this study, a new sink test method was developed that is suitable for PCBs and other chemicals with low volatilities. This new method has higher sensitivity, allows multiple materials to be tested in a single test chamber, and minimizes the effect of sorption by the walls of the test chamber. However, there are improvements that could be made to the method. For example, designs of future chambers should allow the sample “buttons” to be removed without opening the chamber lid. Developing a repeatable, constant source for different mixtures of PCB congeners also would be beneficial.

## 8. Conclusions

A new experimental method was developed for testing the sorption and subsequent re-emission of PCBs from building materials. This method has higher sensitivity than the existing methods, allows multiple materials to be tested at the same time, and minimizes the sink effect of chamber walls. [See Sections 3.14, 4.1.2, and 4.13]

Twenty building materials and furniture were tested as PCB sinks. The experimentally-determined sorption concentrations for 20 materials differed by as much as a factor of 50, indicating that the sink strengths vary significantly from material to material. The test results can help identify the most important PCB sinks (i.e., re-emitting sinks or secondary sources) in buildings. [See Section 6.2.2.1]

Understanding the behavior of the PCB sinks is important to environmental engineers because the re-emissions from the sink materials may reduced the effectiveness of primary source removal. Both experimental results and mass transfer models show that, in the presence of a primary source, the sorption concentration increases over time, but the sorption rate decreases over time. PCB sorption on sink materials is a reversible process. In the presence of a primary source, the sink materials do not emit PCBs into the air. Rather, it adsorbs PCBs from the air. Only after the primary source is removed, can the sink materials become a re-emitting source. Although the PCB concentrations in the sink materials are usually much lower than in the primary sources, the PCB sinks often have much greater surface areas and, thus, may cause elevated concentrations in room air due to re-emissions after removal of primary sources. Therefore, a remediation plan must consider the potential effect of PCB sinks as secondary sources on indoor air quality. [See Sections 6.2.2, 6.2.3, and 7.1]

The material/air partition coefficient and solid-phase diffusion coefficient are two key parameters that can be used to describe the properties of PCB sinks. The roughly estimated material/air partition coefficient for congener #52 (i.e., the reference congener) ranged from  $2.65 \times 10^6$  to  $3.33 \times 10^7$  (dimensionless) and diffusion coefficients ranged from  $7.08 \times 10^{-14}$  to  $3.63 \times 10^{-10}$  ( $\text{m}^2/\text{h}$ ). The partition and diffusion coefficients for other congeners can be calculated by using Equations 6.9 and 6.10 and data in Table 6.5. When both the partition and diffusion coefficients are known for a given material, its sink strength can be described by its sink sorption index (SSI), which can be used to rank sink materials. [See Sections 6.2.4 and 7.4]

Both theoretical calculations and experimental observations confirmed that PCB sorption by the sink materials favored the less volatile congeners if the congener concentrations in the air were the same. However, because the PCB emissions from the primary sources favor the more volatile congeners (Guo et al., 2011), these two factors partially or nearly totally cancel, resulting in similar congener patterns in the primary sources and PCB sinks. Such similarity makes it difficult to differentiate between primary sources and PCB sinks based on their congener patterns. [See Section 7.5]

Several mass-transfer based sink models are available and can be used to better understand the behavior of PCB sinks in contaminated buildings. Most of them require two key parameters, i.e., material/air partition coefficient and solid-phase diffusion coefficient. New experimental methods are needed to determine these two parameters more accurately. In addition, the applicability of these models to multiple sink materials in a room should be evaluated. [See Sections 6.2.4 and Appendix C]

Settled dust is a special sink for indoor PCBs. Because of its very large surface area-to-volume ratio, settled dust can adsorb PCBs faster than building materials either from air or by direct contact with a primary source. Experimental results show that dust can adsorb more PCBs through direct contact with a source than from indoor air. Because of the possibility of re-suspension, settled dust is a potential source for inhalation exposure. [See Section 6.3]

The interior walls of environmental chambers can also adsorb PCBs, causing reduced concentrations in the air outlet. Test results showed that sorption by the 44-mL microchamber that the authors used to test caulk samples was insignificant. The walls of the 53-L chamber that was used to test the emissions from light ballasts adsorbed significant quantities of PCBs. For congener #18, which is the most abundant congener in the emissions from Aroclor 1242, the sorption by the walls of the chamber was estimated to cause more than 30% underestimation of the emission rate. Future testing of PCB sources should consider the use of smaller chambers or the use of chambers made of, or coated with, the materials that are weak sinks for PCBs. [See Section 6.4]

This study was limited to laboratory testing and the scope of the study was limited. [See Section 7.10]

## **Acknowledgments**

The authors thank Drs. John Little and Zhe Liu of Virginia Polytechnic Institute and State University for providing the MATLAB code for a sorption model; Jacqueline McQueen of EPA's Office of Science Policy for assistance in communications and technical consultation; Mark Strynar of EPA's National Exposure Research Laboratory (NERL) for providing the house dust sample; Robert Willis of EPA's NERL for providing scanning electron microscope images of dust samples; Russell Logan and Corey Mocka of ARCADIS for laboratory support; Robert Wright of EPA's National Risk Management Research Laboratory and Joan Bursey of EPA's National Homeland Security Research Center for QA support.



## References

(Website accessibilities were last verified on August 15, 2011)

- An, Y., Zhang, J.S. and Shaw, C.Y. (1997). Sink effect study for common building materials - a literature review & research plan. NRC-CNRC Report No. IRC-IR-681.  
<http://www.nrc-cnrc.gc.ca/obj/irc/doc/pubs/ir/ir681/ir681.pdf>
- ASHRAE (1997). *ASHRAE Handbook of Fundamentals*, American Society of Heating, Refrigeration and Air-conditioning Engineers, Atlanta, GA.
- ASTM (2006). ASTM D6661-01. Standard practice for field collection of organic compounds from surfaces using wipe sampling. ASTM International, West Conshohocken, PA.
- ASTM (2010). ASTM D5116-10. Standard guide for small-scale environmental chamber determinations of organic emissions from indoor materials/products. ASTM International, West Conshohocken, PA.
- Bent, S., Rachor-Ebbinghaus, R., and Schmidt, C. (2000). Decontamination of highly polychlorinated biphenyl contaminated indoor areas by complete removal of primary and secondary sources. *Gesundheitswesen*, 62: 86-92 (in German with English abstract).
- Bodalal A., Zhang J. S. and Plett, E. G. (2000). A method for measuring internal diffusion and equilibrium partition coefficients of volatile organic compounds for building materials. *Building and Environment*, 35: 101-110.
- Bodalal, A., Zhang, J. S., Plett, E. G., and Shaw, C.Y. (2001). Correlations between the internal diffusion and equilibrium partition coefficients of volatile organic compounds (VOCs) in building materials and the VOC properties, *ASHRAE Transactions*, 107: 789–800.
- Clausen, P. A., Hansen, V., Gunnarsen, L., Afshari, A., and Wolkoff, P. (2004). Emission of di-2-ethylhexyl phthalate from PVC flooring into air and uptake in dust: emission and sorption experiments in FLEC and CLIMPAQ. *Environmental Science and Technology*, 38: 2531-2537.
- Coghlan, K. M., Chang, M. P., Jessup, D. S., Fragala, M. A., McCrillis, K., and Lockhart, T. M. (2002). Characterization of polychlorinated biphenyls in building materials and exposures in the indoor environment. *Proceedings: Indoor Air 2002*, pp 147-152.
- Cox, S. S., Zhao, D., and Little, J. C. (2001). Measuring partition and diffusion coefficients for volatile organic compounds in vinyl flooring. *Atmospheric Environment*, 35: 3823–3830.
- Crank, J. (1975). *The Mathematics of Diffusion*, 2<sup>nd</sup> ed., Clarendon Press, Oxford, England, ch 4, p 48.
- Cseh, T., Sanschagrin, S., Hawari, J., and Samson, R. (1989). Adsorption-desorption characteristics of polychlorinated biphenyls on various polymers commonly found in laboratories. *Applied and Environmental Microbiology*, 55(12): 3150-3154.

DeBortoli, M., Knoppel, H., Columbo, A., and Kefalopoulos, S. (1996). Attempting to characterize the sink effect in a small stainless steel test chamber. *ASTM STP1287*, pp 305-318.

Deng, Q., Yang, Y., and Zhang, J. S. (2009). Study on a new correlation between diffusion coefficient and temperature in porous building materials. *Atmospheric Environment*, 43: 2080–2083.

Deng, Q., Yang, X., and Zhang, J. S. (2010). New indices to evaluate volatile organic compound sorption capacity of building materials (RP-1321., *HVAC&R Research*, 16: 95-105.

EH&E (2012). Literature review of mitigation methods for PCBs in buildings, EPA/600/R-12/034, prepared for U.S. EPA by Environmental Health & Engineering, Inc.

Evans, W. C. (1996). Linear systems, compartment modeling, estimability issues in IAQ studies, in *Characterizing Sources of Indoor Air Pollution and Related Sink Effect*, ASTM STP 1287, Tichenor, B. A. Ed., American Society for Testing and Materials, pp 239-262.

Fischer, R. C., Wittlinger, R., and Ballschmiter, K. (1992). Retention-index based vapor pressure estimation for polychlorobiphenyls (PCBs) by gas chromatography. *Fresenius' Journal of Analytical Chemistry*, 342(4): 421-425.

Frame, G. M., Cochran, J. W., and Bøwadt, S. S. (1996). Complete PCB congener distributions for 17 Aroclor mixtures determined by 3 HGC systems optimized for comprehensive, quantitative, congener-specific analysis. *Journal of High Resolution Chromatography*, 19(12): 657-668.

Franzblau, A., Zwica, L., Knutson, K., Chen, Q., Lee, S. Y., Hong, B., Adriaems, P., Demond, A., Garabrant, D., Gillespie, B., Lepkowski, J., Luksemburg, W., Maier, M., and Towey, T. (2009). An investigation of homes with high concentrations of PCDDs, PCDFs, and/or dioxin-like PCBs in house dust, *Journal of Occupational and Environmental Hygiene*, 6(3): 188-99.

Gabrio, T., Piechotowski, I., Wallenhorst, T., Klett, M., Cott, L., Friebe, P., Link, B., and Schwenk, M. (2000). PCB-blood levels in teachers, working in PCB-contaminated schools. *Chemosphere*, 40: 1055-1062.

Guo, Z. (2002). Review of indoor emission source models – Part 2. Parameter estimation. *Environmental Pollution*, 120: 551-564.

Guo, Z., Liu, X., Krebs, K. A., Stinson, R. A., Nardin, J. A., Pope, R. H., and Roache, N. F. (2011). *Laboratory study of polychlorinated biphenyl (PCB) contamination and mitigation in buildings – part 1. emissions from selected primary sources*, EPA/600/R-11/156, U.S. EPA, Office of Research and Development, National Risk Management Research Laboratory, 127 pp.

Haghighat, F., Lee, C.-S., and Ghaly, W. S. (2002). Measurement of diffusion coefficients of VOCs for building materials: review and development of a calculation procedure. *Indoor Air*, 12: 81-91.

Hansson, P. and Stymne, H. (2000). VOC diffusion and adsorption properties of indoor materials – consequences for indoor air quality, in: *Proceedings of Healthy Building 2000*, International Society of Indoor Air Quality and Climate, Vol. 4, 151-156.

Harrad, S., Goosey, E., Desborough, J., Abdallah, M. A.-E., Roosens, L., and Covaci, A. (2010). Dust from UK primary school classrooms and daycare centers: the significance of dust as a pathway of exposure of young UK children to brominated flame retardants and polychlorinated biphenyls. *Environmental Science & Technology*, 44: 4198-4202.

Heinzow, B., Mohr, S., Ostendorp, G., Kerst, M., and Körner, W. (2007). PCB and dioxin-like PCBs in indoor air of public buildings contaminated with different PCB sources--deriving toxicity equivalent concentrations from standard PCB congeners. *Chemosphere*, 67(9): 1746-53.

Hellman, S. J., Lindroos, O., Palukka, T., Priha, E., Rantio, T., and Tuhkanen, T. (2008). PCB contamination in indoor buildings, in *Air Pollution XVI*, Brebbia, C.A ,ed., WIT Press, Southampton, UK, 672 pp.

Herrick, R. F., McClean, M. D., Meeker, J. D., Baxter, L. K., and Weymouth, G. A. (2004). An unrecognized source of PCB contamination in schools and other buildings. *Environmental Health Perspectives*, 112(10): 1051-1053.

Hover, C., Banasik, M., Harbison, R. D., Hardy, M., Price, D. J., and Stedeford, T. (2009). Occurrence of five classes of chemicals in indoor dust: An evaluation of the human health risks. *Science of the Total Environment*, 407: 5194-5196.

Huang, H., Haghighat, F., Blondeau, P. (2006). Volatile organic compound (VOC) adsorption on material: influence of gas phase concentration, relative humidity and VOC type, *Indoor Air*, 16(3): 236–247.

Hwang, H. M., Park, E. K., Young, T. M., and Hammock, B. D. (2008). Occurrence of endocrine-disrupting chemicals in indoor dust. *Science of the Total Environment*, 404: 26-35.

Kofoed-Sørensen, V., Vibenholt, A., Wolkoff, P., and Clausen, P. A. (2011). Emission and uptake of gas phase di(2ethylhexyl)phthalate by floor dust, in *Proceedings: Indoor Air 2011*, manuscript a499 2, the 12<sup>th</sup> International Conference on Indoor Air Quality and Climate, June 5-10, Austin, Texas.

Kohler, M., Tremp, J., Zennegg, M., Seiler, C. Minder-Kohler, S., Beck, M., Lienemann, P., Wegmann, L., and Schmid, P. (2005). Joint sealants: an overlooked diffuse source of polychlorinated biphenyls in buildings. *Environmental Science & Technology*, 39: 1967-1973.

Köppl, B. and Piloty, M. (1993). PCB in sealants: experience and results of procedures in Berlin and decontamination of a school. II. Follow-up of PCB decontamination and evaluation of individual decontamination steps. *Gesundheitswesen*, 55: 629-634 (in German with English abstract).

Kumar, D. and Little, J. C. (2003). Characterizing the source/sink behavior of double-layer building materials. *Atmospheric Environment*, 37: 5529–5537.

Kuusisto, S., Lindroos, O., Rantio, T., Priha, E., and Tuhkanen, T. (2007). PCB contaminated dust on indoor surfaces – Health risks and acceptable surface concentrations in residential and occupational settings. *Chemosphere*, 67: 1194-1201.

Lee, C. S., Haghighat, F., and Ghaly, W. S. (2005). A study on VOC source and sink behavior in porous building materials - analytical model development and assessment. *Indoor Air*, 15: 183-96.

Little, J.C. and Hodgson, A.T. (1996). A strategy for characterizing homogeneous, diffusion-controlled, indoor sources and sinks, in *Characterizing Sources of Indoor Air Pollution and Related Sink Effects*, ASTM STP 1287, Tichenor, B. A., ed., American Society for Testing and Materials, 294-304.

Meininghaus, R., Gunnarsen, L., and Knudsen, H.N. (2000). Diffusion and sorption of volatile organic compounds in building materials-impact on indoor air quality. *Environmental Science & Technology*, 34: 3101-3108.

NERL, 2010. *A Research Study to Investigate PCBs in School Buildings*, EPA 600R-10/074, National Exposure Research Laboratory. <http://www.epa.gov/pcbsincaulk/research-plan.pdf>

Pizer, S. M. and Wallace, V. L. (1983). *To Compute Numerically*, Little, Brown & Company, Toronto, Canada, 366 pp.

Roosens, L., Abdallah, M. A.- E., Harrad, S., Neels, H., and Covaci, A. (2010). Current exposure to persistent polychlorinated biphenyls (PCBs) and dichlorodiphenyldichloroethylene (p,p'-DDE) of Belgian students from food and dust. *Environmental Science & Technology*, 44: 2870-2875.

Rudel, R. A., Liesel, M., Seryak, L. M., and Brody, J. B. (2008). PCB-containing wood floor finish is a likely source of elevated PCBs in residents' blood, household air and dust: a case study of exposure. *Environmental Health*, 7, 8 pp (electronic publication: <http://www.ehjournal.net/content/pdf/1476-069X-7-2.pdf>).

Schripp, T., Fauck, C., and Salthammer, T. (2010). Chamber studies on mass-transfer of di(2-ethylhexyl)phthalate (DEHP) and di-n-butylphthalate (DnBP) from emission sources into house dust. *Atmospheric Environment*, 44: 2840-2845.

Schwarzenbach, R.P., Gschwend, P. M., and Imboden, D. M. (2003). *Environmental Organic Chemistry*, 2<sup>nd</sup> Edition, John Wiley & Sons, Hoboken, NJ, 1311 pp.

Tan, J., Cheng, S. M., Loganath, A., Chong, Y. S., and Obbard, J. P. (2007). Selected organochlorine pesticide and polychlorinated biphenyl residues in house dust in Singapore. *Chemosphere*, 68: 1675-1682.

Tichenor, B. A., Guo, Z., Dunn, J. E., Sparks, L. E., and Mason, M. A. (1991). The interaction of vapor phase organic compounds with indoor sinks. *Indoor Air*, 1: 23-35.

Tiffonnet, A.L., Blondeau, P., Amiri, O. and Allard, F. (2000). Assessment of contaminant diffusivities in building materials from porosity tests, in: *Proceedings of Healthy Building*, Espoo, Finland, Vol. 4, pp 199-203.

Tue, N. M., Suzuki, G., Takahashi, S., Isobe, T., Trang, P. T. K., Viet, P. H., and Tanabe, S. (2010). Evaluation of dioxin-like activities in settled house dust from Vietnamese E-waste recycling sites: relevance

of polychlorinated/brominated dibenzo-*p*-dioxin/furans and dioxin-like PCBs. *Environmental Science & Technology*, 44: 9195-9200.

U.S. EPA (2007). EPA Method 8082A, Polychlorinated biphenyls (PCBs) by gas chromatography. <http://www.epa.gov/waste/hazard/testmethods/sw846/pdfs/8082a.pdf>

U.S. EPA (2008a), EPA Method 1668B, Chlorinated biphenyl congeners in water, soil, sediment, biosolids and tissue by high resolution gas chromatography/high resolution mass spectrometry (HRGC/HRMS). <http://epa.gov/waterscience/methods/method/files/1668.pdf>

U.S. EPA (2008b). Test methods for evaluating solid waste, physical/chemical methods, in EPA publication SW-846, U.S. EPA, Government Printing Office: Washington, D.C.

U.S. EPA (2010). PCBs in Caulk – QA. <http://www.epa.gov/pcbsincaulk/caulk-faqs.pdf>

Vorhees, D. J., Cullen, A. C., and Altshul, L. M. (1999). Polychlorinated biphenyls in house dust and yard soil near a Superfund site. *Environmental Science & Technology*, 33: 2151-2156.

Webster, T. F., Harrad, S., Millette, J. R., Holbrook, R. D., Davis, J. M., Stapleton, H. M., Allen, J. G., McClean, M. D., Ibarra, C., Abdallah, M. A.-E., and Covaci, A. (2009). Identifying transfer mechanisms and sources of decabromodiphenyl ether (BDE 209) in indoor environments using environmental forensic microscopy. *Environmental Science & Technology*, 43: 3067-3072.

Weis, N., Köhler, M., and Zorn, C. (2003). Highly PCB-contaminated schools due to PCB-containing roughcast, in: *Proceedings of Healthy Building 2003*, International Society of Indoor Air Quality and Climate, pp 283-288.

Weschler, C. J. and Nazaroff, W. W. (2008). Semivolatile organic compounds in indoor environments, *Atmospheric Environment*, 42: 9018-9040.

Wilson, N. K., Chuang, J. C., and Lyu, C. (2001). Levels of persistent organic pollutants in several child day care centers. *Journal of Exposure Analysis and Environmental Epidemiology*, 11: 449-458.

Won, D. Y., Corsi, R. L., Rynes, M. (2001). Sorptive interactions between VOCs and indoor materials, *Indoor Air*, 11(4): 246-256.

Xu, J., Zhang, J., Grunewald, J., Guo, B., Zhao, Z., and Plagge, R. (2008). A dual-chamber experimental method for determining the transport properties of building materials, *Indoor Air 2008 Proceedings*, Paper ID: 232. International Society of Indoor Air Quality and Climate, Santa Cruz, CA.

Yang, X. and Chen, Q. (2001). A coupled airflow and source/sink model for simulating indoor VOC exposures. *Indoor Air*, 11: 257-269.

Yang, X., Zhang, J. S., and Deng, Q. (2010). *Modeling VOC sorption of building materials and its impact on indoor air quality - phase II (second phase of RP-1097)*, ASHRAE RP-1321, American Society of

Heating, Refrigerating and Air-Conditioning Engineers.  
<http://rp.ashrae.biz/page/ASHRAE-D-RP-1321-20100428.pdf>

Zhang, J., Chen, Q., and Zhang, J. (2001). *Modeling VOC sorption of building materials and its impact on indoor air quality*, ASHRAE RP-1097 Phase I, American Society of Heating, Refrigerating and Air-Conditioning Engineers. <http://rp.ashrae.biz/page/rp-1097.pdf>

Zhang, J. S., Zhang, J. S., Chen, Q., and Yang, X. (2002). A critical review on studies of volatile organic compound (VOC) sorption on building materials. *ASHRAE Transactions*, 108: 162-174.

Zhang, Y. P., Luo, X. X., Wang, X. K., Qian, K., Zhao, R. Y. (2007). Influence of temperature on formaldehyde emission parameters of dry building materials, *Atmospheric Environment*, 41: 3203-3216.

Zhao, D. Y., Cox, S. S., and Little, J. C. (1999). Source/sink characterization of diffusion-controlled building materials, *Indoor Air 99: Proceedings of the Eighth International Conference on Indoor Air Quality and Climate*, Vol. 1. pp. 408–413.

## Appendix A. Characterization of the Caulk Sample Used as the PCB Source for the Sink Tests

As described in Section 4.1.3.1, a PCB-containing caulk sample was used as the PCB source for the sink tests. This sample contained 103000 µg/g of Aroclor 1254. The content of the target congeners in this caulk sample is presented in Table A.1. The emissions data are presented in Table A.2. The congener concentrations in the air of the test chamber as a function of time are shown in Figures A.1 (in normal scale) and A.2 (in semi-log scale). All the data presented below were from Part 1 of this report series (Guo et al., 2011).

**Table A.1 Content of the target congeners in the caulk sample<sup>[a][b]</sup>**

Congener ID	Content (µg/g)
#17	<del>25.8</del>
#52	3142
#66	1156
#77	<del>6.92</del>
#101	6423
#105	2653
#110	7085
#118	6470
#154	<del>33.9</del>
#187	186

<sup>[a]</sup> Caulk sample ID: CK-12 (Guo et al., 2011).

<sup>[b]</sup> Values in strikethrough font are below the PQL.

**Table A.2 Concentrations of the target congeners in air of the chamber during the emission test<sup>[a]</sup>**

Congener ID	Elapsed Time (h)				
	8.79	80.5	105	129	154
#17	0.74	0.68	0.66	0.69	0.69
#52	22.1	21.4	22.7	22.3	20.5
#66	1.71	1.84	1.85	1.98	1.52
#77	<del>0.00</del>	<del>0.01</del>	<del>0.01</del>	<del>0.01</del>	<del>0.01</del>
#101	8.47	8.83	9.36	8.91	8.35
#110	3.80	4.24	4.70	4.66	4.46
#118	1.88	1.97	2.17	2.14	2.13
#105	0.45	0.60	0.63	0.68	0.74
#154	0.76	0.84	0.86	0.91	0.95
#187	<del>0.02</del>	<del>0.03</del>	<del>0.03</del>	<del>0.03</del>	<del>0.04</del>

<sup>[a]</sup> Concentration units: (µg/m<sup>3</sup>); values in strikethrough font are below the PQL.

<sup>[b]</sup> Test conditions: chamber volume = 44 mL; exposed area = 6.45 cm<sup>2</sup>; air flow rate = 447 mL/min; temperature = 21.2 °C; sample ID = CK-12.

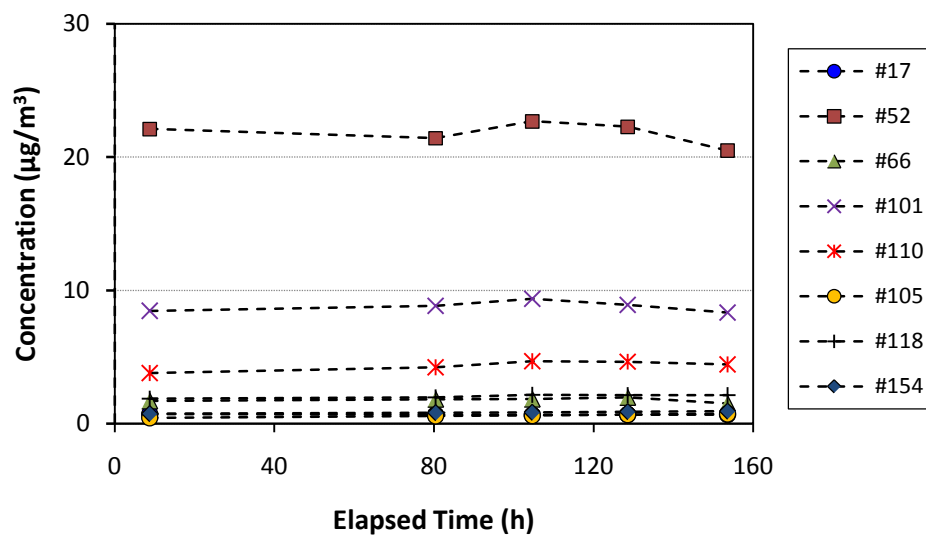


Figure A.1 Congener concentrations in the air of the test chamber as a function of time (in normal scale)

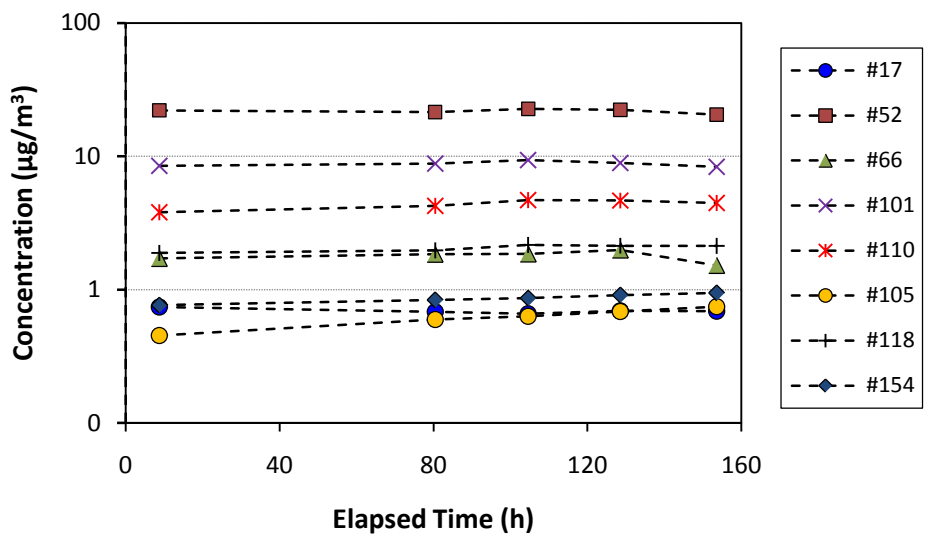


Figure A.2 Congener concentrations in the air of the test chamber as a function of time (in semi-log scale)



## Appendix B. Sample Dimensions and Weights in Sink Tests S-2, S-3, and S-4

**Table B.1. Dimensions and weights of test specimens in sink test S-2**

No	Material Name	Exposed area (cm <sup>2</sup> )	Volume (cm <sup>3</sup> )	Thickness <sup>[a]</sup> (cm)	Weight (g)
1	Concrete	20.1	5.21	2.59	9.38
		20.3	5.30	2.61	9.31
3	Ceiling Tile	6.72	9.37	1.39	0.31
8	Oil-based paint	4.14	0.21	0.05	0.16
9	Latex paint, high-gloss	4.17	0.21	0.05	0.17
		4.33	0.22	0.05	0.16
11	Epoxy coating, polyamide	4.19	0.21	0.05	0.20
12	Epoxy coating, solvent free	4.16	0.21	0.05	0.21
13	Carpet, residential <sup>[b]</sup>	5.38	3.13	0.58	1.22
15	Vinyl flooring B, no pad	5.80	5.50	0.95	0.64
16	Oak flooring, pre-finished	7.63	11.9	1.56	0.82
17	Laminate flooring	5.44	5.65	1.04	0.40

<sup>[a]</sup> For bulky materials such as concrete, the effective material thickness = sample volume divided by exposed area.

<sup>[b]</sup> Fleecy material; the exposed area was based on the physical dimension of the sample.

**Table B.2. Dimensions and weights of test specimens in sink test S-3**

No	Material Name	Exposed area (cm <sup>2</sup> )	Volume (cm <sup>3</sup> )	Thickness (cm)	Weight (g)
1	Concrete	7.02	1.48	0.21	2.07
2	Brick	16.2	3.72	0.23	8.24
		17.1	4.28	0.25	9.01
4	GB conventional	2.86	0.16	0.06	0.09
5	GB paperless	2.80	0.13	0.05	0.09
6	GB conventional (core)	8.25	1.39	0.17	1.12
7	GB paperless (core)	8.50	1.44	0.17	1.34
10	Latex paint, eggshell	3.20	0.14	0.04	0.10
14	Carpet, commercial <sup>[b]</sup>	9.84	2.01	0.20	0.77
18	Painted metal	3.40	0.24	0.07	1.67
19	Medium density fiberboard	8.03	1.39	0.17	1.47
20	Plastic laminate countertop	3.80	0.28	0.07	0.45

<sup>[a]</sup> For bulky materials such as concrete, the effective material thickness = sample volume divided by exposed area.

<sup>[b]</sup> Fleecy material; the exposed area was based on the physical dimension of the sample.

**Table B.3. Dimensions and volumes of concrete buttons in sink test S-4**

Button No	Exposed area (cm <sup>2</sup> )	Volume (cm <sup>3</sup> )	Thickness (cm)	Weight (g)
1	5.22	0.84	0.161	1.44
2	5.56	0.94	0.169	1.51

**Table B.4. Dimensions and weights of concrete panels in sink test S-4**

Tile No.	Exposed area (cm <sup>2</sup> )	Volume (cm <sup>3</sup> )	Thickness (cm)	Weight (g)
1	523	216	0.93	486
2	519	204	0.88	466
3	519	205	0.88	457
4	515	201	0.87	473
5	520	202	0.86	467
6	517	187	0.80	416
Sum	3114	1215	--	2764

## Appendix C. Method for Rough Estimation of the Partition and Diffusion Coefficients for Building Materials

### C.1 Purpose

This Appendix describes the method for rough estimation of the partition and diffusion coefficients for sink materials by applying the DSS model (Deng et al., 2010) to the experimentally determined sorption concentrations. The intended use is for modelers and others who are interested in estimating parameters for sink models.

### C.2 Model

The model developed by Deng et al. (2010) was used for estimating the partition and diffusion coefficients for building materials. The model consists of three equations (2.7 through 2.9 in Section 2.2.2), which can be generalized as:

$$DSS = \frac{M(t)}{M_{\infty}} = f(N^*, \Theta, F_{om}) \quad (C.1)$$

or

$$M(t) = M_{\infty} DSS = f(N^*, \Theta, F_{om}) \quad (C.2)$$

where DSS = degree of sorption saturation (dimensionless)

M(t) = amount of pollutant adsorbed by the sink material at time t (μg)

M<sub>∞</sub> = sorption capacity in mass units, from Equation C.3 below (μg)

N\* = dimensionless air change rate, from Equation 2.10

Θ = dimensionless mass capacity, from Equation 2.11

F<sub>om</sub> = Fourier number for mass transfer, from Equation 2.12

f(N\*, Θ, F<sub>om</sub>) = one of the three correlations (i.e., Equations 2.7, 2.8 and 2.9)

$$M_{\infty} = C_a K_{ma} A \delta \quad (C.3)$$

where C<sub>a</sub> = concentration in air (μg/m<sup>3</sup>)

K<sub>ma</sub> = material/air partition coefficient (dimensionless)

A = exposed area of the sink material (m<sup>2</sup>)

δ = thickness of the sink material (m)

According to the definitions of  $M_{\infty}$ ,  $N^*$ ,  $\Theta$ , and  $F_{om}$ , Equation C.2 also can be expressed as

$$M(t) = f(K_{ma}, D_m, C_a, A, \delta, V, N, t) \quad (C.4)$$

where  $K_{ma}$  = material/air partition coefficient (dimensionless)

$D_m$  = diffusion coefficient ( $m^2/h$ )

$C_a$  = concentration in air ( $\mu g/m^3$ )

$A$  = exposed area of the sink material ( $m^2$ )

$\delta$  = thickness of sink material (m)

$V$  = volume of the chamber ( $m^3$ )

$N$  = air change rate ( $h^{-1}$ )

$t$  = time (h)

Because  $M(t)$ ,  $C_a$ ,  $A$ ,  $\delta$ ,  $V$ ,  $N$ , and  $t$  can be determined experimentally,  $K_{ma}$  and  $D_m$  become the only unknown parameters in Equation C.4.

### C.3 Data-fitting Software

The data-fitting software MicroMath Scientist 2.0 (MicroMath, Saint Louis, MO) was used for the nonlinear regression.

### C.4 Data-fitting Method

#### *C.4.1 Estimating the Partition and Diffusion Coefficients for Individual Congeners*

Several test runs were conducted to estimate the partition and diffusion coefficients ( $K_{ma}$  and  $D_m$ ) from computer generated data for PCB content in the sink material as a function of time (See Figure 3.3). Estimating both parameters from a single data set was unsuccessful because of the inability to obtain unique parameter estimates from the data. Non-linear regression requires the user provide initial estimates (i.e., starting values) to start the function evaluation by the computer program. Depending on the starting values the user chooses, the program may give different results. This problem is fairly common for estimating sink parameters (DeBortoli et al., 1996; An et al., 1997; Zhang et al., 2001; Haghghat et al., 2002). Evans (1996) provided an excellent explanation of the nature of the problem in mathematical terms.

#### *C.4.2 Estimating the Partition and Diffusion Coefficients Based on the Experimental Data for Multiple Congeners*

More test runs were conducted to apply the model to multiple data sets in an attempt to reduce the number of parameters to be estimated on a per-data-set basis. Instead of estimating the partition and diffusion coefficients for each individual congener, these coefficients were estimated by using the following correlations. Several studies have demonstrated that, within each class of chemicals, the following

correlations exist for partition coefficient  $K_{ma}$  (Equation C.5) and diffusion coefficient  $D_m$  (Equation C.6) (Zhao et al, 1999; Bodalal et al., 2001; Cox et al., 2001; Guo, 2002):

$$\frac{K_{ma0}}{K_{mai}} = \left( \frac{P_i}{P_0} \right)^\alpha \quad (C.5)$$

where  $K_{ma0}$  = material/air partition coefficient for the reference constituent in the class (dimensionless)

$K_{mai}$  = material/air partition coefficient for constituent i in the class (dimensionless)

$P_i$  = vapor pressure for constituent i (torr)

$P_0$  = vapor pressure for the reference constituent (torr)

$\alpha$  = an empirical value depending on the properties of the chemical class and the sink material

$$\frac{D_{m0}}{D_{mi}} = \left( \frac{m_i}{m_0} \right)^\beta \quad (C.6)$$

where  $D_{m0}$  = diffusion coefficient for the reference constituent in the class ( $m^2/h$ )

$D_{mi}$  = diffusion coefficient for constituent i in the class ( $m^2/h$ )

$m_i$  = molecular weight for constituent i (g/mol)

$m_0$  = molecular weight for the reference constituent (g/mol)

$\beta$  = an empirical value depending on the properties of the chemical class and the sink material

With these correlations, only four parameters are needed to calculate the partition and diffusion coefficients for any chemicals in the class, i.e.,  $K_{ma0}$ ,  $D_{m0}$ ,  $\alpha$ , and  $\beta$ . If four sets of  $M(t)$  data (i.e., data for four different congeners for the same sink material) are used for the nonlinear regression, the number of parameters to be estimated is reduced to one per data set.

Test runs showed that estimating four parameters with four sets of data was still unstable. To further reduce the number of unknowns, index  $\beta$  was fixed at 6.5, which is the average of existing  $\beta$  values for non-wood products (Guo, 2002). Thus, the parameters to be estimated were  $K_{ma0}$ ,  $D_{m0}$ , and  $\alpha$ .

Selection of the reference constituent is arbitrary. In this study, congener #52 was selected because of its high concentrations in the air and sink materials.

## C.5 Input Data

Input data needed for the nonlinear regression are summarized in Table C.1.

**Table C.1 Input data needed for estimating  $K_{ma0}$ ,  $D_{m0}$ , and  $\alpha$  by non-linear regression**

Parameter Category	Name	Symbol	Data Source	Note
Independent variable	Time	t	Measured	
Dependent variables	Amount of congener adsorbed	M(t)	Measured	[a]
Constants — chamber	Volume of chamber	V	Measured	
	Air change rate	N	Measured	
	Air concentration	$C_a$	Measured	
Constants – sink material	Exposed area	A	Measured	
	Thickness	$\delta$	Measured	
Constants – congener properties	Vapor pressure	P	Literature	[b]
	Molecular weight	m	Literature	
	Index in Eq. C.6	$\beta$	Literature	[c]

<sup>[a]</sup> Data for four congeners for each sink material; from sink Tests S-2 and S-3.

<sup>[b]</sup> Data from Fischer et al. (1992), Method B.

<sup>[c]</sup>  $\beta = 6.5$ , an average of available data for other classes of chemical and nonwood products (Guo, 2002)

## C.6 Parameters to Be Estimated

Three parameters are to be estimated:

- Partition coefficient for the reference congener (i.e., #52)
- Diffusion coefficient for the reference congener (i.e., #52)
- Index  $\alpha$  in Equation C.5.

## C.7 Parameter Estimation Procedure

- Step 1: Run MicroMath Scientist 2.0 and open the model file
- Step 2: Enter input parameters (See Table C.1, above)
- Step 3: Set the starting values for  $K_{ma0}$  and  $D_{m0}$  that are smaller than their expected values (e.g.,  $K_{ma0} = 5 \times 10^6$  and  $D_{m0} = 1 \times 10^{-11}$ )
- Step 4: Set the starting values for  $\alpha = 0.8$
- Step 5: Save and compile the model file
- Step 6: Import the four sets of sorption data [ M(t) vs. t ] into the spreadsheet within MicroMath Scientist 2.0

- Step 7: Perform nonlinear regression to obtain one set of estimates for  $K_{ma0}$ ,  $D_{m0}$ , and  $\alpha$
- Step 8: Adjust the starting values for  $K_{ma0}$  and  $D_{m0}$  so that they are greater than the estimated values
- Step 9: Perform nonlinear regression to obtain the second set of estimates for  $K_{ma0}$ ,  $D_{m0}$ , and  $\alpha$
- Step 10: Adjust the starting values for  $K_{ma0}$  and  $D_{m0}$  so that they are between the two estimated values obtained
- Step 11: Perform nonlinear regression to obtain the third set of estimates for  $K_{ma0}$ ,  $D_{m0}$ , and  $\alpha$
- Step 12: Calculate and report the mean and standard deviation for  $K_{ma0}$ ,  $D_{m0}$ , and  $\alpha$  based on the three sets of estimates.

## C.8 Results

The estimated material/air partition coefficients, diffusion coefficients, and index  $\alpha$  for 20 sink materials are presented in Table 6.5.

## C.9 Method Limitations

The procedure described above does not solve the fundamental problem described in Section C.4.1 above; rather, the procedure above only reduces the uncertainty to a certain extent. Thus, the results should be treated as rough estimates. To solve the fundamental problem, the partition and diffusion coefficients should be determined independently.

The sink models based on the solid-air partition and solid-phase diffusion may work well for porous materials but may not work well for impenetrable materials such as uncoated metal sheets. The Langmuir sink models may work better for the latter.

## Appendix D. Congener Patterns in Primary Sources and Sink Materials

### D.1 Purpose

In this appendix, examples are used to explain why the congener patterns in primary sources and sink materials are similar.

### D.2 Approach

Caulk containing Aroclor 1254 was used as a primary source in an imagined room. An empirical emission model developed in Part 1 (Guo et al., 2011) was used to calculate the concentrations of PCB congeners in the air. The material/air partition coefficients obtained from this study were used to calculate the sorption capacity of the sink materials. Twenty-five of the most abundant congeners in Aroclor 1254 were used to calculate the congener patterns. The entire calculation process included the following steps:

- Define the primary source
- Calculate the emission rates of the 25 congeners by using the empirical model developed in Part 1
- Calculate the congener concentrations in room air by using a simple box model
- Calculate the sorption capacity by using the air concentration from the previous step and the material/air partition coefficients estimated in Section 6.5 of this report
- Compare the relative abundances for the 25 congeners in the primary sources and sink material.

### D.3 Calculations

#### *D.3.1 Defining the Primary Source*

Assume that a caulk contains 100,000  $\mu\text{g/g}$  of Aroclor 1254. The concentrations of the 25 most abundant congeners in the Aroclor and the vapor pressure of the congeners are listed in Table D.1.



**Table D.1 Content of top 25 congeners in the primary source and their vapor pressures**

<b>Congener ID</b>	<b>Content in Aroclor 1254 (wt %) <sup>[a]</sup></b>	<b>Content in Caulk (µg/g)</b>	<b>Vapor Pressure (torr) <sup>[b]</sup></b>
#44	2.31	2310	9.75E-05
#49	1.10	1100	1.22E-04
#52	5.38	5380	1.29E-04
#66	1.01	1010	3.80E-05
#70	3.49	3490	4.13E-05
#74	0.84	840	5.19E-05
#84	2.32	2320	2.28E-05
#85	1.28	1280	3.31E-05
#87	3.99	3990	1.83E-05
#91	0.93	930	5.00E-05
#92	1.29	1290	3.44E-05
#95	6.25	6250	5.58E-05
#97	2.62	2620	1.99E-05
#99	3.02	3020	2.81E-05
#101	8.02	8020	3.03E-05
#105	2.99	2990	5.08E-06
#110	9.29	9290	1.50E-05
#118	7.35	7350	7.80E-06
#128	1.42	1420	2.19E-06
#132	2.29	2290	6.81E-06
#138	5.80	5800	3.72E-06
#149	3.65	3650	1.19E-05
#153	3.77	3770	6.10E-06
#156	0.82	820	1.20E-06
#163	1.03	1030	3.69E-06

<sup>[a]</sup> From Frame et al. (1996)

<sup>[b]</sup> From Fischer et al. (1992), Method B.

### D.3.2 Calculating the Emission Factors for Congeners from Caulk

The emission factor for PCB-containing caulk can be calculated from Equations D.1 and D.2 (Guo et al., 2011):

$$\ln N_{Ei} = 14.02 + 0.976 \ln P_i \quad (D.1)$$

$$E_i = N_{Ei} \frac{x_i}{1000} \quad (D.2)$$

where  $N_{Ei}$  = normalized emission factor ( $\mu\text{g}/\text{m}^2/\text{h}$ )

$P_i$  = vapor pressure for congener i (torr)

$E_i$  = emission factor for congener i ( $\mu\text{g}/\text{m}^2/\text{h}$ )

$x_i$  = congener content in the source ( $\mu\text{g}/\text{g}$ )

Using the data in Table D.1, the emission rate for each congener can be calculated.

### D.3.3 Calculating the Congener Concentrations in Room Air

The following environmental conditions were assumed:

- Room volume (V)                       $300 \text{ m}^3$
- Air change rate (N)                       $1 \text{ h}^{-1}$
- Surface area of caulk (A)               $0.2 \text{ m}^2$

Then, the steady-state concentrations of the congeners can be calculated from Equation D.3:

$$C_{ai} = \frac{A E_i}{V N} \quad (D.3)$$

where  $C_{ai}$  = the concentration of congener i in air ( $\mu\text{g}/\text{m}^3$ )

$E_i$  = emission factor for congener i ( $\mu\text{g}/\text{m}^2/\text{h}$ )

### D.3.4 Calculating the Sorption Capacities for the Sink Material

The sorption capacities for different congeners are calculated from Equation D.4:

$$C_{m\infty} = C_a K_{ma} \quad (D.4)$$

where  $C_{m\infty}$  = sorption capacity ( $\mu\text{g}/\text{m}^3$ )

$C_a$  = congener concentration in air ( $\mu\text{g}/\text{m}^3$ )

$K_{ma}$  = material/air partition coefficient (dimensionless)

The partition coefficients for different congeners are calculated from Equation D.5:

$$K_{mai} = K_{ma0} \left( \frac{P_0}{P_i} \right)^\alpha \quad (\text{D.5})$$

where  $K_{mai}$  = material/air partition coefficient for congener i (dimensionless)

$K_{ma0}$  = material/air partition coefficient for the reference congener (i.e., congener #52) (dimensionless)

$P_0$  = vapor pressure for the reference congener (i.e., congener #52) (torr)

$P_i$  = vapor pressure for congener i (torr)

In this demonstration, the data for concrete and brick were used (Table D.3):

**Table D.3 Parameters used for estimating the partition coefficients for different congeners** <sup>[a]</sup>

Material	$K_{ma0}$	$\alpha$
Concrete	$2.11 \times 10^7$	0.544
Brick	$2.65 \times 10^6$	1.07

<sup>[a]</sup> Data from Table 6.5.

#### D.3.5 Calculating the Relative Abundances (RA)

The relative abundances for congeners in the primary sources and sink materials were calculated from Equations D.6 and D.7, respectively.

$$RA_{ip} = \frac{x_i}{\sum_{j=1}^{25} x_j} \quad (\text{D.6})$$

where  $RA_{ip}$  = relative abundance for congener i in the primary source (fraction)

$x_i$  = concentration of congener i in the primary source ( $\mu\text{g}/\text{g}$ )

$x_j$  = concentration of congener j in the primary source ( $\mu\text{g}/\text{g}$ )

$$RA_{is} = \frac{C_{mi}}{\sum_{j=1}^{25} C_{mj}} \quad (\text{D.7})$$

where  $RA_{is}$  = relative abundance for congener i in the sink material (fraction)

$C_{mi}$  = sorption capacity for congener i ( $\mu\text{g}/\text{m}^3$ )

$C_{mj}$  = sorption capacity for congener j ( $\mu\text{g}/\text{m}^3$ ).

### **D.3 Results**

The calculated results are shown in Tables D.8 and D.9, in which  $N_E$  = normalized emission factor,  $E$  = emission factor,  $C_a$  = concentration in air,  $K_{ma}$  = material/air partition coefficient, and  $C_{m\infty}$  = sorption capacity. Comparison of congener patterns are shown in Figures 7.2 and 7.3.

**Table D.8. Calculated sorption capacities for top 25 congeners in Aroclor 1254 for concrete**

<b>Congener ID</b>	<b>N<sub>E</sub> (µg/m<sup>2</sup>/h)</b>	<b>E (µg/m<sup>2</sup>/h)</b>	<b>C<sub>a</sub> (µg/m<sup>3</sup>)</b>	<b>K<sub>ma</sub> (—)</b>	<b>C<sub>m∞</sub> (µg/m<sup>3</sup>)</b>
#44	149	345	0.230	2.46E+07	5.66E+06
#49	185	204	0.136	2.18E+07	2.97E+06
#52	197	1059	0.706	2.11E+07	1.49E+07
#66	59.6	60.1	0.0401	4.11E+07	1.65E+06
#70	64.6	225	0.150	3.93E+07	5.90E+06
#74	80.7	67.8	0.0452	3.47E+07	1.57E+06
#84	36.1	83.7	0.0558	5.43E+07	3.03E+06
#85	52.0	66.6	0.0444	4.43E+07	1.97E+06
#87	29.1	116	0.0775	6.12E+07	4.74E+06
#91	77.8	72.4	0.0482	3.54E+07	1.71E+06
#92	53.9	69.6	0.0464	4.34E+07	2.01E+06
#95	86.7	542	0.361	3.33E+07	1.20E+07
#97	31.6	82.8	0.0552	5.85E+07	3.23E+06
#99	44.4	134	0.0893	4.84E+07	4.32E+06
#101	47.7	382	0.255	4.65E+07	1.19E+07
#105	8.35	25.0	0.0167	1.23E+08	2.04E+06
#110	24.0	223	0.148	6.82E+07	1.01E+07
#118	12.7	93.3	0.0622	9.73E+07	6.05E+06
#128	3.67	5.21	0.0035	1.94E+08	6.75E+05
#132	11.1	25.4	0.0170	1.05E+08	1.78E+06
#138	6.17	35.8	0.0238	1.45E+08	3.47E+06
#149	19.1	69.9	0.0466	7.73E+07	3.60E+06
#153	9.98	37.6	0.0251	1.11E+08	2.79E+06
#156	2.04	1.67	0.0011	2.70E+08	3.00E+05
#163	6.11	6.30	0.0042	1.46E+08	6.13E+05

**Table D.9. Calculated sorption capacity for top 25 congeners in Aroclor 1254 for brick**

<b>Congener ID</b>	<b>N<sub>E</sub> (µg/m<sup>2</sup>/h)</b>	<b>E (µg/m<sup>2</sup>/h)</b>	<b>C<sub>a</sub> (µg/m<sup>3</sup>)</b>	<b>K<sub>ma</sub> (—)</b>	<b>C<sub>m∞</sub> (µg/m<sup>3</sup>)</b>
#44	149	345	0.230	3.59E+06	8.25E+05
#49	185	204	0.136	2.83E+06	3.85E+05
#52	197	1059	0.706	2.65E+06	1.87E+06
#66	59.6	60.1	0.0401	9.83E+06	3.94E+05
#70	64.6	225	0.150	8.99E+06	1.35E+06
#74	80.7	67.8	0.0452	7.05E+06	3.18E+05
#84	36.1	83.7	0.0558	1.70E+07	9.50E+05
#85	52.0	66.6	0.0444	1.14E+07	5.06E+05
#87	29.1	116	0.0775	2.15E+07	1.67E+06
#91	77.8	72.4	0.0482	7.33E+06	3.54E+05
#92	53.9	69.6	0.0464	1.10E+07	5.08E+05
#95	86.7	542	0.361	6.51E+06	2.35E+06
#97	31.6	82.8	0.0552	1.97E+07	1.09E+06
#99	44.4	134	0.0893	1.36E+07	1.21E+06
#101	47.7	382	0.255	1.25E+07	3.20E+06
#105	8.35	25.0	0.0167	8.47E+07	1.41E+06
#110	24.0	223	0.148	2.67E+07	3.96E+06
#118	12.7	93.3	0.0622	5.35E+07	3.33E+06
#128	3.67	5.21	0.0035	2.09E+08	7.25E+05
#132	11.1	25.4	0.0170	6.19E+07	1.05E+06
#138	6.17	35.8	0.0238	1.18E+08	2.82E+06
#149	19.1	69.9	0.0466	3.41E+07	1.59E+06
#153	9.98	37.6	0.0251	6.97E+07	1.75E+06
#156	2.04	1.67	0.0011	3.98E+08	4.43E+05
#163	6.11	6.30	0.0042	1.19E+08	5.00E+05

## Appendix E. Effects of Temperature and Relative Humidity on Sink Behavior

### E.1 Purpose

This study did not evaluate the effects of temperature and relative humidity on the behavior of reversible sinks. This Appendix summarizes some of the most recent information that is available in the literature.

### E.2 Effect of Temperature

#### E.2.1 Models

Equations E.1 and E.2 represent generalized statements of the effects of temperature on the material/air partition coefficient and the diffusion coefficient for the sink material (Zhang, et al., 2007; Deng et al., 2009; Yang et al., 2010):

$$K_{ma} = a_1 T^{0.5} e^{a_2/T} \quad (\text{E.1})$$

$$D_m = b_1 T^{1.25} e^{b_2/T} \quad (\text{E.2})$$

where  $K_{ma}$  = material/air partition coefficient (dimensionless)

$D_m$  = diffusion coefficient in the sink material ( $\text{m}^2/\text{s}$ )

$T$  = temperature (K)

$a_1, a_2, b_1, b_2$  = constants specific to a given adsorbent and adsorbate pair.

#### E.2.2 Parameters

There are no data for the constants in Equations E.1 and E.2 for PCBs. To understand the general trends of the temperature effect, the constants for 1,2-dichlorobenzene found in the literature were used (Table E.1).

**Table E.1. Values for the constants in Equations 7.3 and 7.4 for 1,2-dichlorobenzene with ceiling tile and carpet** <sup>[a][b]</sup>

Constant	Ceiling tile	Carpet
$a_1$	0.0041	$6.00 \times 10^{-5}$
$a_2$	2234	4187.9
$b_1$	$1.00 \times 10^{-11}$	6.0917
$b_2$	-694.22	-9353.2

<sup>[a]</sup> From Yang, et al. (2010).

<sup>[b]</sup> The values in the table are for  $K_{ma}$  in (dimensionless) and  $D_m$  in ( $\text{m}^2/\text{s}$ ).

### E.2.3 Results

As shown in Figures E.1 and E.2, as the temperature increases, the partition coefficient decreases and the diffusion coefficient increases. The smaller the partition coefficient becomes, the smaller the sorption capacity is (Equation 2.1). Thus, elevated temperature may “drive off” PCBs from the PCB sinks because of its reduced sorption capacity. A greater diffusivity means that the PCB molecules migrate more easily in the sink material. Thus, elevated temperature accelerates the homogenization process for PCBs in the sink material. In controlling re-emissions, temperature may have a more important effect on the partition coefficient than on the diffusion coefficient.

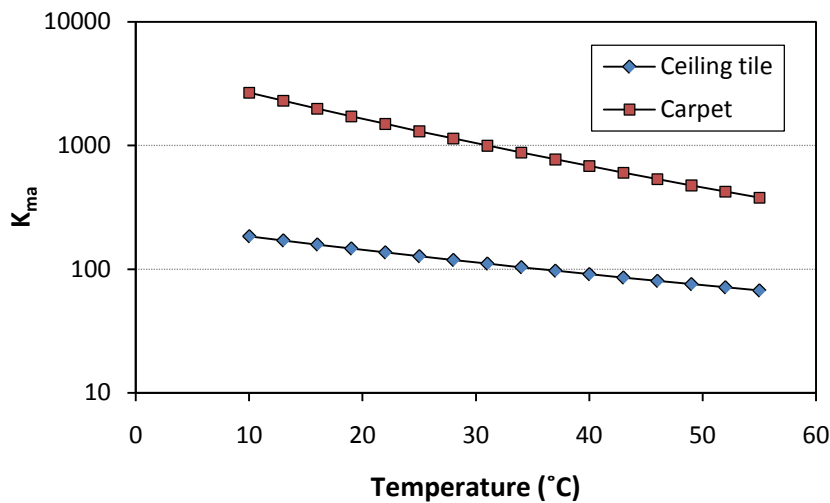


**Figure E.1.** Effect of temperature on the partition coefficients for 1,2-dichlorobenzene with ceiling tile and carpet (according to data from Yang, et al., 2010)

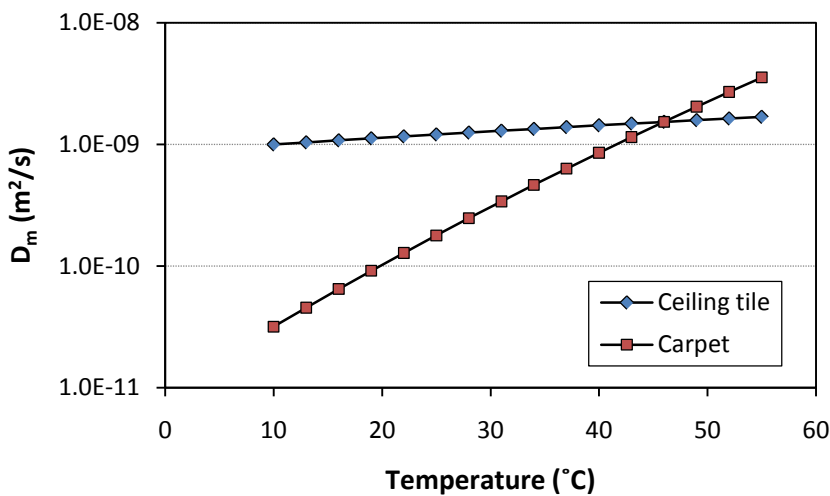


**Figure E.2.** Effect of temperature on the diffusion coefficients for 1,2-dichlorobenzene with ceiling tile and carpet (according to data from Yang, et al., 2010)



### **E.3 Effect of Relative Humidity**

Several studies (e.g., Won et al., 2001; Huang, et al., 2002; Yang, et al., 2010) have shown that the effect of relative humidity on the sorption of non-polar, hydrophobic chemicals is rather small. Recently, Yang and his co-workers (Yang, et al, 2010) studied the sorption of six non-polar compounds (ethylbenzene, 1,2-dichlorobenzene, decane, undecane, dodecane, and benzaldehyde) by a carpet and ceiling tile at 25%, 50% and 80% relative humidity. They concluded that the effect of relative humidity on the sorption of these chemicals is insignificant in the range of typical indoor relative humidity level (i.e., <80%).

## Appendix F. Predicting Sorption Concentrations for Sink Materials

### F.1 Purpose

This appendix supplements Section 7.5 by describing the step-by-step procedure for predicting the sorption concentrations for sink materials by using the DSS models and roughly estimated partition and diffusion coefficients for sink materials.

### F.2 Conditions

#### F.2.1 Congeners

In this demonstration, two dioxin-like congeners, i.e., #118 and #156, were used as examples. Congener #156 was not a target compound in this study, but it has been measured in indoor air by other researchers (e.g., Heinzow et al., 2007). The hypothetical exposure conditions were as follows:

- Exposure duration 40 years
- Average air concentration for #118  $0.05 \mu\text{g}/\text{m}^3$
- Average air concentration for #156  $0.01 \mu\text{g}/\text{m}^3$

#### F.2.2 Sink Material

Concrete was selected as the sink material. The congener distribution inside the substrate was assumed to be concentrated within 1 cm from the exposed surface.

#### F.2.3 Other Input Parameters

The vapor pressure and molecular weight of the congeners are listed in Table F.1. Congener #52 is listed because it is the reference congener for estimating the partition and diffusion coefficients for concrete (See Table 6.5.)

**Table F.1 Vapor pressure and molecular weight for congeners #52, #118, and #156**

Congener ID	Vapor Pressure <sup>[a]</sup> (torr)	Molecular Weight (g/mol)
#52	$1.50 \times 10^{-4}$	292.0
#118	$8.42 \times 10^{-6}$	326.5
#156	$1.20 \times 10^{-6}$	361.0

<sup>[a]</sup> From Fischer et al. (1992), Method B.

Parameters needed to calculate the partition and diffusion coefficients for concrete were from Table 6.5 (average of three sets of estimates):

$$K_{ma0} = 2.11 \times 10^7$$

$$\alpha = 0.544$$

$$D_{m0} = 2.98 \times 10^{-11} \text{ m}^2/\text{h}$$

$$\beta = 6.5$$

### F.3 Model

Either of the two DSS models shown in Section 2.2.2 would work. In this demonstration, Equation F.1 (i.e., Equation 2.6 in the main body of this report) was used because it required fewer input parameters than the other model.

$$DSS = 1 - \sum_{n=0}^{\infty} \left\{ \frac{8}{(2n+1)^2 \pi^2} \exp \left[ \frac{-D_m (2n+1)^2 \pi^2 t}{4 \delta^2} \right] \right\} \quad (\text{F.1})$$

where  $D_m$  = diffusion coefficient of the pollutant in the sink material ( $\text{m}^2/\text{h}$ )

$\delta$  = thickness of the sink material if only one side is exposed to air; or one half of the thickness of the material if both sides are exposed (m)

$t$  = time (h)

### F.4 Calculations

The calculations involved three steps: (1) calculate the partition and diffusion coefficients for congeners #118 and #156, (2) calculate the degree of sorption saturation (DSS) by using the Equation F.1, and (3) calculate the concentration of congeners #118 and #156 in the concrete layer by using Equation 2.3.

#### F.4.1 Calculating the Partition and Diffusion Coefficients for Congeners #118 and #156

The material/air partition coefficient and diffusion coefficient are estimated from equations F.3 and F.4 (i.e., Equations 6.9 and 6.10 in the main body):

$$\frac{K_{ma0}}{K_{mai}} = \left( \frac{P_i}{P_0} \right)^\alpha \quad (\text{F.3})$$

where  $K_{ma0}$  = material/air partition coefficient for the reference congener (dimensionless)

$K_{mai}$  = material/air partition coefficient for congener i (dimensionless)

$P_i$  = vapor pressure for congener i (torr)

$P_0$  = vapor pressure for the reference congener (torr)

$\alpha$  = an empirical value specific to the sink material

$$\frac{D_{m0}}{D_{mi}} = \left( \frac{m_i}{m_0} \right)^\beta \quad (\text{F.4})$$

where  $D_{m0}$  = diffusion coefficient for the reference congener ( $\text{m}^2/\text{h}$ )

$D_{mi}$  = diffusion coefficient for congener i ( $\text{m}^2/\text{h}$ )

$m_0$  = molecular weight for the reference congener ( $\text{g/mol}$ )

$m_i$  = molecular weight for congener i ( $\text{g/mol}$ )

$\beta$  = an empirical value specific to the sink material.

Using the data in Table F.1, the following results in Table F.2 were obtained.

**Table F.2 Calculated partition and diffusion coefficients for congeners #118 and #156**

<b>Congener ID</b>	<b>Partition Coefficient (<math>\rightarrow</math>)</b>	<b>Diffusion Coefficient (<math>\text{m}^2/\text{h}</math>)</b>
#118	$1.01 \times 10^8$	$1.44 \times 10^{-11}$
#156	$2.92 \times 10^8$	$7.50 \times 10^{-12}$

#### *F.4.2 Calculating the DSS*

The DSS model (Equation F.1) was implemented in a spreadsheet. This model required only three parameters:  $D_m$ ,  $\delta$ , and  $t$ . Using the data in Table F.2 and a material thickness of 1 cm, the DSS was calculated (Figure F.1). It is somewhat surprising that, after four decades, the sink material is still not saturated. Note that DSS is a function of material thickness. If a thicker layer of concrete is considered, the DSS is even lower.

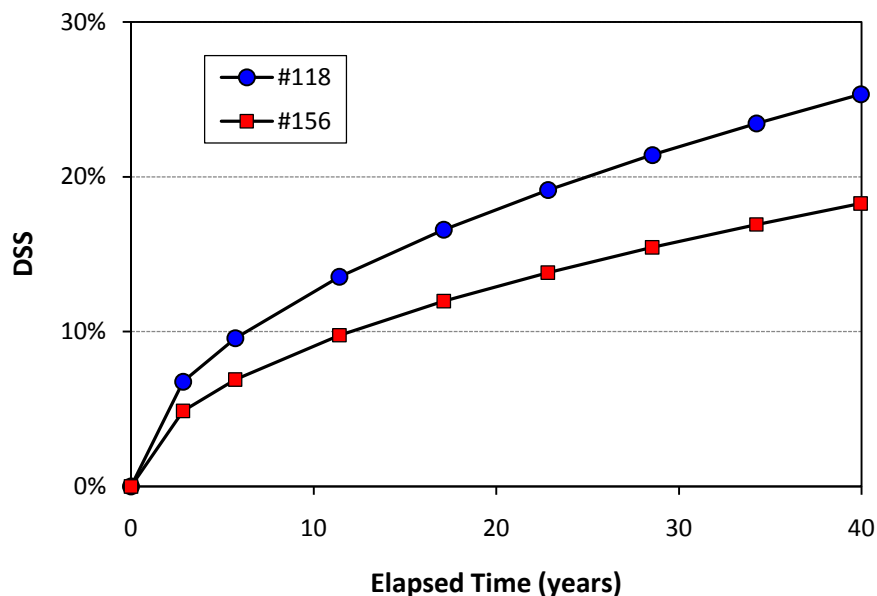


**Figure F.1. Calculated DSS for congeners #118 and #156 in concrete after 40-years of exposure**

#### *F.4.3 Calculating the Sorption Concentration*

The amount of congener that entered the sink material at time  $t$ ,  $M(t)$ , was calculated from Equation F.5 (i.e., Equation 2.5 in the main body):

$$DSS = \frac{M(t)}{M_{\infty}} = \frac{M(t)}{C_{m\infty} A \delta} \quad (F.5)$$

where  $M(t)$  = amount of congener that entered the sink material at time  $t$  ( $\mu\text{g}$ )

$M_{\infty}$  = maximum amount of pollutant the sink material can adsorb from air ( $\mu\text{g}$ )

$C_{m\infty}$  = sorption capacity ( $\mu\text{g}/\text{m}^3$ )

$A$  = exposed surface area of the sink material ( $\text{m}^2$ )

$\delta$  = thickness of the sink material (m).

Sorption capacity ( $C_{m\infty}$ ) was calculated by using Equation F.6 (i.e., Equation 2.1 in the main body):

$$K_{ma} = \frac{C_{m\infty}}{C_a} \quad (F.6)$$

where  $K_{ma}$  = material/air partition coefficient (dimensionless)

$C_a$  = concentration of the congener in air ( $\mu\text{g}/\text{m}^3$ )

Substituting air concentration data in Section F.2.1 and partition coefficient data in Table F.2 into Equation F.6, the sorption capacity ( $C_{m\infty}$ ) was obtained. Then,  $M(t)$  was calculated by using Equation F.5. In Figure F.2, the results were converted to the mass unit ( $\mu\text{g/g}$ ) by using Equation 2.2 in the main body, assuming the density of concrete was  $2 \text{ g/cm}^3$ .

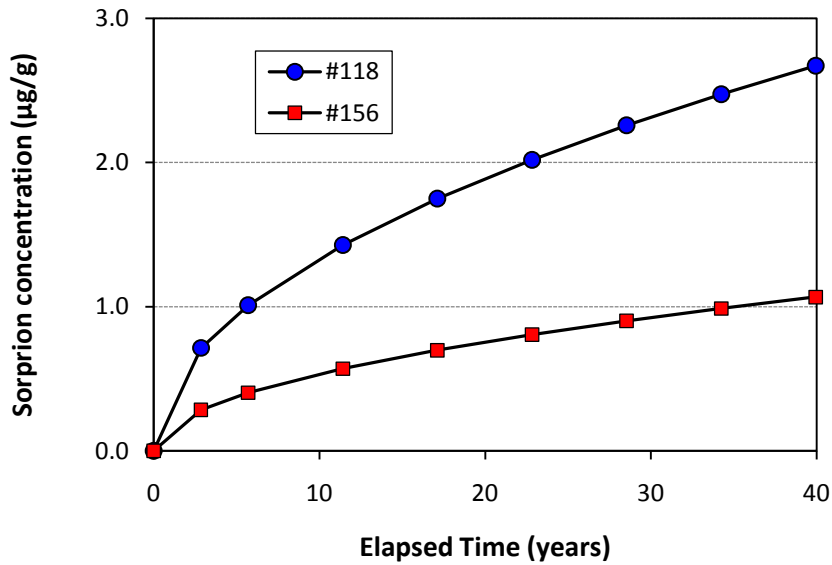


**Figure F.2. Predicted sorption concentrations for congeners #118 and #156**